An International Journal

Nature and Science

ISSN 1545-0740

Volume 5 - Number 4 (Cumulated No. 17), December 1, 2007

Marsland Press, Michigan, The United States

Nature and Science

The ***Nature and Science*** is an international journal with a purpose to enhance our natural and scientific knowledge dissemination in the world under the free publication principle. Any valuable papers that describe natural phenomena and existence or any reports that convey scientific research and pursuit are welcome, including both natural and social sciences. Papers submitted could be reviews, objective descriptions, research reports, opinions/debates, news, letters, and other types of writings that are nature and science related. The Authors are responsible to the contents of their articles.

Introductions to Authors

1. General Information

(1) Goals: As an international journal published both in print and on internet, *Nature and Science* is dedicated to the dissemination of fundamental knowledge in all areas of nature and science. The main purpose of *Nature and Science* is to enhance our knowledge spreading in the world under the free publication principle. It publishes full-length papers (original contributions), reviews, rapid communications, and any debates and opinions in all the fields of nature and science.

(2) What to Do: *Nature and Science* provides a place for discussion of scientific news, research, theory, philosophy, profession and technology - that will drive scientific progress. Research reports and regular manuscripts that contain new and significant information of general interest are welcome.

(3) Who: All people are welcome to submit manuscripts in any fields of nature and science.

(4) Distributions: Web version of the journal is freely opened to the world, without any payment or registration. The journal will be distributed to the selected libraries and institutions for free. For the subscription of other readers please contact with: editor@americanscience.org or americansciencej@gmail.com or editor@sciencepub.net.

(5) Advertisements: The price will be calculated as US$400/page, i.e. US$200/a half page, US$100/a quarter page, etc. Any size of the advertisement is welcome.

2. Manuscripts Submission

(1) Submission Methods: Electronic submission through email is encouraged and hard copies plus an IBM formatted computer diskette would also be accepted.

(2) Software: The Microsoft Word file will be preferred.

(3) Font: Normal, Times New Roman, 10 pt, single space.

(5) Manuscript: Don't use "Footnote" or "Header and Footer".

(6) Cover Page: Put detail information of authors and a short title in the cover page.

(7) Title: Use Title Case in the title and subtitles, e.g. "**Debt and Agency Costs".**

(8) Figures and Tables: Use full word of figure and table, e.g. **"Figure 1.** Annul Income of Different Groups**", Table 1. Annual Increase of Investment".**

(9) References: Cite references by "last name, year", e.g. "(Smith, 2003)". References should include all the authors' last names and initials, title, journal, year, volume, issue, and pages etc.

Reference Examples:

Journal Article: Hacker J, Hentschel U, Dobrindt U. Prokaryotic chromosomes and disease. Science 2003;301(34):790-3.

Book: Berkowitz BA, Katzung BG. Basic and clinical evaluation of new drugs. In: Katzung BG, ed. Basic and clinical pharmacology. Appleton & Lance Publisher. Norwalk, Connecticut, USA. 1995:60-9.

(10) Submission Address: editor@sciencepub.net, Marsland Company, P.O. Box 21126, Lansing, Michigan 48909, The United States, 517-980-4106.

(11) Reviewers: Authors are encouraged to suggest 2-8 competent reviewers with their name and email.

2. Manuscript Preparation

Each manuscript is suggested to include the following components but authors can do their own ways:

(1) Title page: including the complete article title; each author's full name; institution(s) with which each author is affiliated, with city, state/province, zip code, and country; and the name, complete mailing address, telephone number, facsimile number (if available), and e-mail address for all correspondence.

(2) Abstract: including Background, Materials and Methods, Results, and Discussions.

(3) Keywords.

(4) Introduction.

(**5) Materials and Methods**.

(**6) Results**.

(**7) Discussions**.

(**8) References**.

(**9) Acknowledgments**.

Journal Address:

Marsland Press
P.O. Box 21126
Lansing, Michigan 48909
The United States
Telephone: (517) 349-2362
Email: editor@sciencepub.net,
naturesciencej@gmail.com
Websites: http://www.sciencepub.org

Nature and Science

ISSN: 1545-0740

Volume 5 - Number 4 (Cumulated No. 17), December 1, 2007

Cover Page, Introduction, Contents, Call for Papers, All in one file

Contents

Marsland Press, P.O. Box 21126, Lansing, Michigan 48909, The United States
Edmondson Intercultural Enterprises, P.O. Box 1324, East Lansing, Michigan 48826, The United States
(347) 789-4323

http://www.sciencepub.org editor@sciencepub.net

Effects Of Containers And Storage Conditions On Bacteriological Quality Of Borehole Water

*[1]Eniola K. I. T., [1]Obafemi, D. Y., [1]Awe, S. F., [1]Yusuf I. I. [2]Falaiye, O. A. and [3]Olowe, A.O.

kennyeniola@yahoo.com
Eniola K.I.T.: Environmental and Public Health Research (EPHR) Laboratory, Department of Microbiology, University of Ilorin, P.M.B. 1515, Ilorin, Kwara,. kennyeniola@yahoo.com,
Obafemi, D. Y. Environmental and Public Health Research (EPHR) Laboratory, Department of Microbiology, University of Ilorin. P.M.B. 1515, Ilorin, Kwara, giftarose2000@yahoo.com
Awe, S. F., Environmental and Public Health Research (EPHR) Laboratory, Department of Microbiology, University of Ilorin. P.M.B. 1515, Ilorin, Kwara, asflor5@yahoo.com
Yusuf I. I.: Environmental and Public Health Research (EPHR) Laboratory, Department of Microbiology, University of Ilorin. P.M.B. 1515, Ilorin, Kwara, ephr_lab@yahoo.co.uk
Falaiye, O. A.: Baseline Surface Radiation Network (BSRN) Station, Department of Physics, University of Ilorin, P.M.B. 1515, Ilorin, Kwara,
Olowe, A.O.: Department of Medical Microbiology and Parasitology, Ladoke Akintola University of Technology, College of Health Sciences. P.M.B. 4400, Osogbo.Osun State Email: olowekunle@yahoo.com

ABSTRACT: Water from a borehole was collected into tap-fitted plastic buckets of different colours. A set of the buckets were stored indoor while duplicate were stored outdoor. The atmospheric conditions as indicated by sky condition, relative humidity, total radiation and aerosol optical depth were monitored during the storage period. The effects of colour of the container and storage conditions on the bacteriological quality of the stored water were studied by examining physicochemical (pH, temperature and total suspended solids) and bacteriological parameters (total bacterial count and total coliform count) indicative of water quality during the storage period. The atmosphere was generally cloudy with high relative humidity, while total radiation and aerosol optical depth were low; hence temperatures indoor and outdoor were not significantly different. The total suspended solid content and total heterotrophic bacterial counts declined with storage; decrease in bacterial counts was more pronounced in the transparent buckets stored outdoor. Eight bacterial species: *Bacillus subtilis, Citrobacter diversus, Enterobacter aerogenes, Klebsiella pneumonia, Micrococcus luteus, Proteus vulgaris, Pseudomonas aeruginosa* and *Staphylococcus aureus* were isolated; three of them survived the indoor and outdoor storage. [Nature and Science. 2007;5(4):1-6].

Keywords: borehole, radiation, aerosol optical depth, sky condition, relative humidity

INTRODUCTION

The supply of water in terms of quality, quantity, when and where it is needed continues to generate concerns. It plays a significant role in socio-economic development of human populations (Micheal, 1998). The erratic supply of piped water has occasioned the sourcing of water from underground sources. Groundwater sources: wells, boreholes and springs; that are properly located produce water of very good quality (Gerald *et al.,* 1992). However, it must not be taken for granted that groundwater will always meet the WHO standards for drinking water. Rogbesan *et al.* (2002) reported heavy bacterial load in water from some boreholes in Ilorin, Nigeria.

The erratic nature of piped water supply has made water storage a common practice among individuals and households, especially in areas where there is pressure on available water source. Maggy *et al.* (2003) indicated that the duration of storage affected the microbiological quality of stored ground water. Similarly, Olayemi *et al.* (2005) and Eniola *et al*. (2006) highlighted the importance of a few days of indoor storage in improving the physical and microbiological quality of water. In many communities in Nigeria, it is common to pump ground water into overhead storage-tanks. The most common household reservoirs are plastic tanks, usually of different colours, placed outdoor.

The outdoor location of the water tanks exposes them to solar radiation. In addition to generating heat, many forms of radiations are harmful to microorganisms. Low levels of ionizing radiations will produce mutations and may indirectly result in death, whereas higher levels are directly lethal. Even visible light, when present in sufficient intensity can damage or kill microbial cells (Prescott *et al.,* 1999). The amount of radiation available is affected by aerosol optical depth and cloud parameters (Sekiguchi *et al*.,

2003). Climatic condition is affected by scattering or adsorption of radiation by aerosols, scattering of shortwaves, adsorption of solar and longwave radiations (King *et al*., 1999; Penner, *et al*., 2002; Takemura *et al*., 2002).

This study is an investigation of the effect the colour of container and condition of storage (indoor and outdoor) on the bacteriological quality of borehole water. Atmospheric conditions (the relative humidity, aerosol optical depth, total radiation sky condition and temperature) as well as physicochemical (pH, temperature, and total suspended solids) and bacteriological (total bacterial and total coliform counts) parameters indicative of water quality were examined at interval of four days.

MATERIALS AND METHODS

Sample collection and Storage.

Water was obtained from a borehole within the main campus of University of Ilorin, Ilorin into disinfected tap-fitted coloured (Green, red and transparent) plastic buckets as described by WHO (1997). A set of buckets of the three colours was stored indoor in the Environmental and Public Health Research (EPHR) laboratory of the Department of Microbiology, University of Ilorin. A duplicate set of the buckets was stored outdoor at the Baseline Surface Radiation Network (BSRN) station in the Department of Physics, University of Ilorin. The water samples were stored for 12 days and samples taken for analysis at an interval of 4 days.

Atmospheric condition, Physicochemical and Bacteriological Parameters.

The temperature and relative humidity were monitored by HMP45C temperature and relative humidity probe at the BSRN station, Ilorin Nigeria (8^o 28'N, 4^o 38'E to 8^o 31'N, 4^o 40'E). The sky condition was taken by the Synoptic observation. The aerosol optical depth and radiation were taken using Microtops II Sun photometer. The pH and total suspended solid content were determined as described by American Society for Test and Measurement Standards (1988). The total heterotrophic bacterial counts were determined by Standard plate Count (SPC) method employing the pour plate technique (APHA, 1990). The total coliform count was determined as Most Probable Number (MPN) using the multiple tube fermentation test (Olutiola *et al.,* 1991). The isolates were characterized on the basis of colonial morphology, cellular characters, staining reactions and biochemical tests (Olutiola *et al.,* 1991). They were subsequently identified using Cowan and Steel's Manual for the identification of Medical Bacteria (Barrow and Feltham, 1995).

RESULTS

Table 1 shows the atmospheric conditions during the storage period. The relative humidity ranged between 81.08 and 85.08, total radiation ranged from 156 to 196 Wm^{-2}. Variations in pH and temperature of the water samples during storage are shown in Tables 2 and 3. The pH ranged between 6.54 and 7.90, while the temperature ranged between 23.5 and 29^OC. The total suspended solids contents varied from 1.40 x 10^{-2} to 1.73 x 10^{-2} g/ml (Table 4). Total heterotrophic bacterial (THB) count ranged between 5 x 10^2 and 64 x 10^2 cfu/ml (Figure 1). The total coliform count of the borehole water was zero prior to storage. A total of eight (8) bacterial species: *Bacillus subtilis, Citrobacter diversus, Enterobacter aerogenes, Klebsiella pneumonia, Micrococcus luteus, Proteus vulgaris, Pseudomonas aeruginosa* and *Staphylococcus aureus* were encountered (Table 3). Their successions in the water samples during the storage period are shown in Table 4. Three of them survived the 12 days of indoor and outdoor storage.

Table 1. Atmospheric Condition during Storage Period

Storage period (Days)	Atmospheric Condition				
	Relative humidity (%)	Sky condition	Aerosol Optical depth	Total Radiation (Wm^{-2})	Temperature (^oC)
0	85.08	Cloudy	0.55	190	33
4	81.87	Cloudy	0.56	156	34
8	81.08	Cloudy	0.55	196	31
12	83. 84	Cloudy	0.63	190	32

Table 2. Variations in pH of water samples during storage

Storage period (Days)	pH					
	Green Bucket		Purple Bucket		Transparent Bucket	
	Indoor	Outdoor	Indoor	Outdoor	Indoor	Outdoor
0	6.54	6.54	6.54	6.54	6.54	6.54
4	6.60	6.82	6.61	6.81	6.60	6.81
8	7.30	7.40	7.20	7.60	7.00	6.80
12	7.40	7.80	7.80	7.90	7.80	7.90

Table 3. Variations in Temperature of water samples during storage

Storage period (Days)	Temperature					
	Green Bucket		Purple Bucket		Transparent Bucket	
	Indoor	Outdoor	Indoor	Outdoor	Indoor	Outdoor
0	29.0	29.0	29.0	29.0	29.0	29.0
4	25.0	28.0	25.5	28.8	25.4	28.0
8	24.3	26.0	24.5	26.1	24.0	26.0
12	23.5	24.0	23.5	24.0	23.8	24.5

Table 4. Succession of Bacteria in water samples during storage

Bacterial Isolates	Occurrence of Bacterial Isolate																							
	Green Bucket								Purple Bucket								Transparent Bucket							
	Indoor				Outdoor				Indoor				Outdoor				Indoor				Outdoor			
	0	4	8	12	0	4	8	12	0	4	8	12	0	4	8	12	0	4	8	12	0	4	8	12
Bacillus subtilis	+	+	-	-	+	-	-	-	+	+	-	-	+	-	-	-	+	+	-	-	+	-	-	-
Citrobacter freundii	+	+	+	+	+	+	+	+	+	+	+	+	+	+	+	+	+	+	+	+	+	+	+	+
Enterobacter aerogenes	+	+	+	-	+	+	+	-	+	+	+	-	+	+	+	-	+	+	+	-	+	+	-	-
Klebsiella pneumonia	+	+	+	-	+	+	-	-	+	+	+	-	+	+	-	-	+	+	+	-	+	-	-	-
Micrococcus luteus	+	+	-	-	+	+	-	-	+	+	-	-	+	+	-	-	+	+	-	-	+	-	-	-
Proteus vulgaris	+	+	+	+	+	+	+	+	+	+	+	+	+	+	+	+	+	+	+	+	+	+	+	+
Pseudomonas aeruginosa	+	+	+	+	+	+	+	+	+	+	+	+	+	+	+	+	+	+	+	+	+	+	+	+
Staphylococcus aureus	+	-	-	-	+	-	-	-	+	-	-	-	+	-	-	-	+	-	-	-	+	-	-	-

Key: +: Present; -: Absent

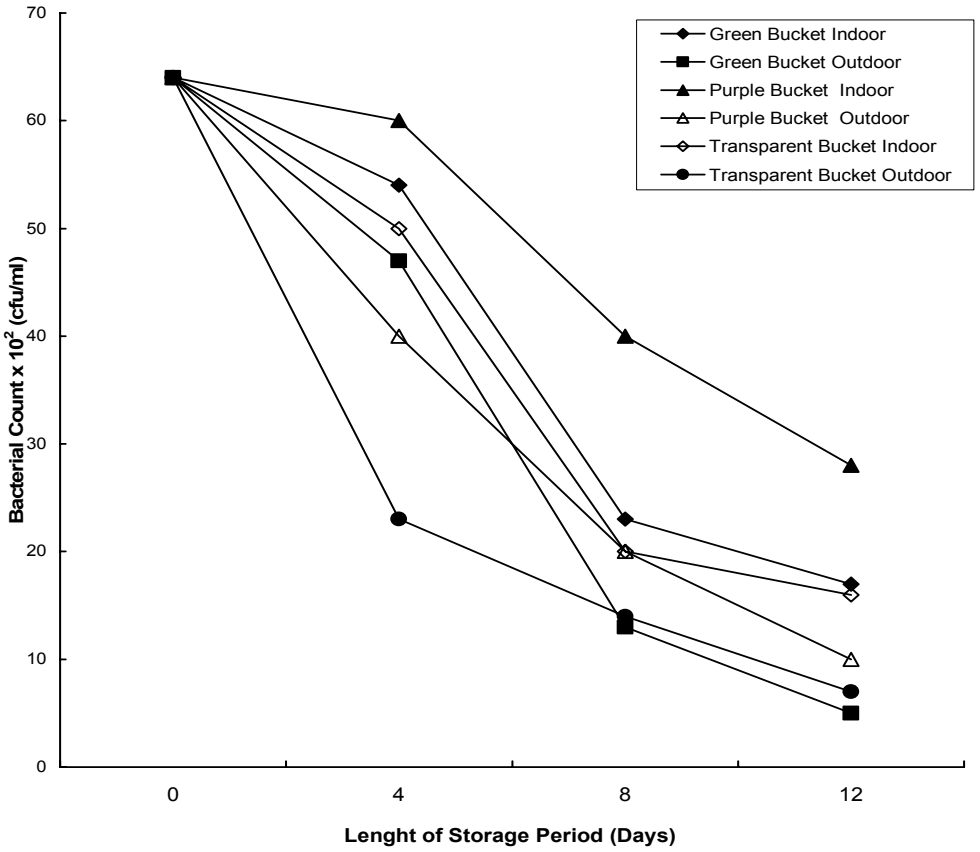

Figure 1. Variation in Total Bacterial Count during Storage.

DISCUSSION

The cloudy nature of the atmosphere during the storage period suggests possible absorption of radiation; the low aerosol optical depth suggests low scattering of radiation; hence more radiation is likely to reach the earth. The high relative humidity and cloud cover will result in high temperature due to retention of longwave radiations by water vapour (Penner *et al*., 2002; Takemura *et al*., 2002). The resultant effect is that there is no significant temperature gradient between indoor and outdoor conditions. This is further reflected in the temperature of the stored water samples (Table 2). Statistical analysis indicates a strong positive correlation between the relative humidity and temperature of the samples (r= 0.8647).

The pHs falls within the range that would favour bacterial proliferation (Atlas, 1995). The observed increases in pH during storage could be due to the activities of the resident flora and or their death, which results in the release of inorganic substances such as ammonia (Rogbesan *et al.,* 2002). The progressive reduction in suspended solid content is similar to the observations of Olayemi *et al*. (2005) and Eniola *et al*. (2006). It has been attributed to gravitational pull, which causes suspended materials to settle out of the water over time. It is likely that if the time of storage is increased, all suspended materials present in the water could settle out under gravitational pull. This is probably the basis for the influence of storage on bacteriological quality of water as observed by Maggy *et al*. (2003).

The zero total coliform count shows the borehole is free of fecal contamination, contrary to the observation by Rogbesan *et al.* (2002) that water from this borehole contained coliforms exceeding the WHO (2004) standard required of untreated drinking water. This is suggestive of an improvement in the handling of the borehole and its catchment. The presence of *Citrobacter freundii, Proteus vulgaris* and *Pseudomonas aeruginosa* in the water however shows it is not fit for consumption. *Pseudomonas aeruginosa* is an opportunistic pathogen. Members of the genus *Proteus* and *Citrobacter* are common

causes of bladder, kidney and other body infections (Stanier *et al.,* 1987).The WHO (1996) standard requires that water intended for drinking should be free of pathogens and bacterial indicative of faecal contaminaation.

The reduction in population of total bacteria as the day of storage increased in similar to the observation by Payment *et al* (1985). Decline in the bacterial population can be attributed to death of the resident bacteria during the storage period due to depletion of nutrients (Olayemi *et al.,* 2005). Reduction in the bacterial load was more prominent in buckets stored outdoor. This is attributable to direct radiation from sunlight on the buckets outside. Among those outdoor, penetration by radiations would be more pronounced in the transparent bucket. Sedimentation of suspended material in the water due to gravitational force could also contribute to the decline in bacterial populations (Salle, 1973; Eniola *et al.*, 2006). It is possible in such a situation that the organisms remain in the biofilm produced. The survival of *Citrobacter freundii, Proteus vulgaris* and *Pseudomonas aeruginosa* after 12 days of storage portends some dangers to consumers of the water due to their pathogenic nature (Stanier, *et al*., 1987).

This study buttress that storage is valuable as a preliminary accessory stage of treatment but it cannot be relied on as a sole measure of purification. The colour of the bucket and fluctuation in light and radiation are also importance. There was no significant difference in effect of the different colour of buckets. This is attributable to cloud cover that creates a uniform temperature condition. In conclusion, outdoor storage of water in light coloured container was found to be desirable. It is therefore recommended that borehole water could be stored outdoors in light coloured container for about 10 to 14 days.

Correspondence to:
Eniola K. I. T.
Environmental and Public Health Research (EPHR) Laboratory
Department of Microbiology
University of Ilorin
P.M.B. 1515, Ilorin, Kwara,
kennyeniola@yahoo.com,

Received: 11/8/2007

REFERENCES

1. American Public Health Association (APHA). Standard Method for the Examination of Wastewater (16th edition). Washington, D.C. 1985
2. American Society for Test and Measurements (ASTM) Annual book of American Society for Test and Measurements Standards (Water). 1985 11.01
3. Atlas, R. Microorganisms in our World (6th edition). Mosby Publisher. 1995.
4. Barrow, G.I. and Feltham, R.K.A. Cowan and Steel's Manual for the identification of Medical Bacteria. 3rd Edition, Cambridge University Press. 1995.
5. Eniola, K.I.T., Olayemi, A.B., Awe, S., Adegoke, A., Osanoto, I.B., Abolade, G.O. and Kayode-Isola, T.M. Effect of Storage on Bacteriological Quality of Well Water. *African Journal of Clinical and Experimental Microbiology*. 2006; 7(1): 27- 32.
6. Gerald, J.T., Case, L.C. and B. R. Funke. Microbiology – An Introduction. *Soil and Water Microbiology* (4th edition). The Benjamin/Cummings publishing Co. Inc., Redwood City, California. 1992; 672-683.
7. King, M. D., Kaufman, Y. J., Tanre, D. and T. Nakajima). Remote sensing of trophospheric aerosols from space: past, present and future. *Bulletin of the American Meteorological Society*. 1999; 80 (11): 2229- 2259.
8. Maggy, N., Momba, B. and T. L. Notshe. Operational Paper: The Microbiological quality of groundwater derived drinking water after long storage in household containers in a rural community of South Africa. *Journal Water SRT- Aqua*. 2003; 52: 67- 77.
9. Micheal, O. K. The Impact of Industrial growth on groundwater quality and availability: a case study of Ikeja Industrial area. *In Current issues in Nigeria Environment* (Osuntokun, A. Ed.) Davidson Press. Ibadan. 1998
10. Olayemi, A.B., Awe, S., Eniola, K.I.T., Osanoto, I.B., Adegoke, A., Abolade, G.O. Effect of Storage on Bacteriological Quality of Borehole Water. African *Journal of Clinical and Experimental Microbiology*. 2005; 6(3): 213- 218

11. Park, K. Environment and Health. *Park's Textbook of Preventive and social Medicine* (16th edition). M/S Babarsidas Bhanot Publishers, India. 2001; 483-500.
12. Payment, P., Trudel, M. and R. Plante. Correlation Analysis of Virus density with Bacterial Data From Seven Drinking Water Treatment Plants in Canada. *Applied and Environmental Microbiology*. 1985; 49: 1418-1427.
13. Penner, J. E., Zhang, S.Y., Chin, M., Chuang, C. C., Feichter, J., Feng, Y. Geogdzhayev, I. V., Ginoux, P,. Herzog, M., Higurashi, A., Koch, D., Land C., Lohmann, U., Mishchenko, M., Nakajima, T., PItari, G. Soden, B., Tengen, I., and L. Stowe. A comparison of model- and satellite- derived aerosol optical depth and reflectivity. *Journal of the Atmospheric Sciences.* 2002; 59: 441- 460.
14. Prescott, L.M., Harley, J.P. and D.A. Klein, Water. *Microbiology* (4th edition). McGraw-Hill Co. Inc., NewYork. 1999; 876-882.
15. Rogbesan, A.A., Eniola, K.I.T. and A.B. Olayemi, Bacteriological Examination of some Boreholes within University of Ilorin (PS). *Nigeria Journal of Pure and Applied Science*. 2002; 17: 1223-1226.
16. Salle, A. J. Bacteriology of Water. *Fundamental Principle of Bacteriology* (7th edition). McGraw-Hill. 1973; 689- 710.
17. Sekiguchi, M., Nakajima, T., Suzuki, K., Kawamoto, K, Higurashi, A., Rosenfeld, D. Sano, I. and S. Mukai. A study of the direct and indirect effects of aerosols using global satellite data set of aerosol and cloud parameters. Journ*al of Geophysical Research* 2003; 108(D22, 4699): AAC 4 -1 – AAC 4 - 14.
18. Stanier, R.Y., Ingram, J.L., Wheelis, M.L. and Painter, P.R. Bacteria. *General Microbiology* (5th edition). Prentice-Hall, New Jersey. 1987; 447-448, 641-642.
19. Takemura, T., Nakajima, T., Dubovik, O. Holben, B. N. and S. Kinne Single-scattering albedo and radiative forcing of various aerosol species with a global three dimensional model. *Journal of Climate*. 2002; 15 (4). 333- 352.
20. WHO: World Health Organization Guidelines for Drinking Water Quality (2nd Edition). 2. Health Criteria and Supporting Information. Geneva, Switzerland. 1996
21. WHO: World Health Organization Guidelines for Drinking Water Quality (2nd Edition). 3. Surveillance and Control of community supplies. Geneva, Switzerland. 1997
22. WHO: World Health Organization World Health Organization guidelines for drinking water quality (3rd Edition) 1, Recommendation. Geneva, Switerland. 2004.

Structural stability of Dystric Nitisol in Relation to Some Edaphic Properties under Selected Land Uses

G.E. Osuji E.U. Onweremadu

Department of Soil Science and Technology, Federal University of Technology PMB 1526 Owerri, Nigeria
E-mail: uzomaonweremadu@yahoo.com

Abstract: We conducted this study before the rains in 2005 to assess the aggregate stability of soils of a toposequence as affected by soil properties under six land uses, namely cassava cultivation polluted with crude oil (CP), rubber plantation (RP), non polluted cassava cultivation (NCP), forest (F), oil palm plantation (OPP) and bare fallow (BF).Target soil sampling technique was used to collect soil samples based on physiography and land use. Routine laboratory analyes were conducted on soil samples and data generated were analyzed using simple mean (descriptive statistic) and correlation coefficient (inferential statistic). Results show differences in selected soil properties due to land use. Total porosity, organic matter (OM) water stable aggregates and mean weight diameter of soil peds varied due to land use and topography. Mean weight diameter increased with declining slope gradients while aggregates were more stable under CP, F, BF and RP. Mean weight diameter had significant relationship with OM (r=0.52), total nitrogen (r =0.51), exchangeable Ca (r =0.39), exchangeable Na (r = 0.34), pH(r =0.32), and exchangeable H (r =-0.21) at 1% level of probability. [Nature and Science. 2007;5(4):7-13].

Keywords: Land use, Nitisols, pedality, physiography, tropical soils.

Introduction

Aggregate stability of a soil has a great influence on crop performance, soil erosion, runoff and transport of contaminants from farmlands to water bodies (Rasiah and Kay, 1994). A good soil structure is important in sustaining long term crop production on agricultural soils (Eneje *et al., 2005)* because it influences water status, workability resistance to erosion, nutrient availability, crop growth and development (Piccolo and Mbagwu, 1999). Aggregate stability is one of such measures used in determining structural suitability of soils for agricultural and non-agricultural uses.

Aggregate stability of soils is influenced by quality and quantity of organic matter (Piccolo, 1996; Spaccini *et al., 2001;* Adesodum *et al., 2004),* cations content (Dexter and Chan, 1991; Levy and Torrento, 1995), soil texture (Boix-Fayos *et al.*,1992). These were classified into biotic and abiotic factors (Brady and Weil, 1999). In addition to these, anthropogenic activities influence aggregate stability. Spaccini e*t al.* (2001) observed that cultivation reduced aggregate stability and increased proportions of the small size aggregate relative to forest soils. Labile pool of organic matter which enhances aggregate stability is highly affected by land use (Cambardella and Elliott, 1992). Mbagwu and Auerswald (1999) reported that forest, bush fallows, mulched and minimum-tilled plots had higher percolation stability when compared with paddy rice fields, unmulched, and continuously cropped plots. Eynard e*t al.*(2004) reported high water stable aggregates in grassland than cultivated soils.

There is a death of information on the relationship between aggregate stability and land use types in soils of the Southeastern Nigeria. 5cantiness of soil information as it pertains aggregate stability could be responsible for the increasing spate of soil structural breakdown and development of a variety of rills and gullies on a once beautiful landscape, leading to soil loss, displacement of homes loss of
farmlands, poor nutrient reserve and declining yield of crops. The major objective of this study was to investigate the relationship between aggregate stability and soil properties while relating these to land use types.

MATERIALS AND METHODS

Study Area: The study was conducted before rains in 2005 in six sites of Owerri Agricultural Zone lying between latitudes 5^{o} 25' and 5^{o} 45' N and longitudes 6^{o} 45' and 7^{o}05'E. Soils are derived from Coastal Plain Sands (Benin formation) of the Miocene-Oligocene geologic era. Earlier, soils of the area were classified as Dystric Nitisols (Onweremadu, 2006).

The area has a lowland geomorphology. Mean annual rainfall is about 2400mm while mean annual temperature ranges from 26-29^{o}C. Rainforest vegetation predominates in the area. Farming is a major socio-economic activity of the area.

Field studies: Target soil survey sampling technique was used with emphasis on land use and topography. Soil samples were collected at a depth of O-15cm with an auger from six sites. The six sites include Asaa, Obitti, Ihiagwa, Eziobodo, Etekwuru and Emebiam, all in Imo State. Six land use practices used were used and include cassava cultivation polluted with crude oil (CP), cassava cultivation not polluted with crude oil (NCP), forest (F), oil palm plantation (OP), rubber plantation (RP) and bare fallow (BF). All these land uses were of the same topography (0-1%; 3% and 5%). A total of nine bulk samples were collected from each study site with 3 samples from each slope gradient. Nine core samples were also collected from each land use type. The composite soil samples were air-dried and sieved through 4.76mm sieve for water stable aggregate analysis and the remaining soil particles were passed through 2-mm sieve for soil characterization. Core samples were used for bulk density and total porosity determinations.

Laboratory Analyses: Particle size distribution was determined by Bouyoucos hydrometer method (Gee and Or, 2002) while bulk density was measured by core method (Grossman and Reinsch, 2002). Soil aggregate stability was estimated by wet-sieving techniques (Kemper and Rosenau, 1986). Mean weight diameter (MWD) was computed as:

$$MWD = \sum_{i=1}^{n} XiWi$$

Where MWD = mean weight diameter of water –stable aggregates
Xi = Mean diameter of each size fraction (MM)
Wi = Mean Proportion of the total sample weight in the corresponding size fraction.

Soil pH was determined potentiometrically in soil-water ratio of 1:2.5 as described by Hendershot e*t al.* (1993). Soil organic carbon was measured by wet digestion (Nelson and Sommers, 1996) while total nitrogen was estimated by microkjeldahl method (Bremner, 1996). Exchangeable acidity and exchangeable bases determined by potassium chloride extraction method (Juo, 1981). Available phosphorus was measured by Olsen method (Emteryd, 1989). Soil cation exchange capacity was estimated by a method described by Rhoades (1982).

Calculations: Exchangeable Sodium Percentage (ESP) was computed as

$$ESP = \frac{\text{Exchangeable Sodium (meq/100g)}}{\text{Cation exchange capacity (meg/100g)}} \times 100\%$$

Sodium Adsorption Ratio (SAR) was calculated as follows:

$$SAR = \frac{\text{Exchangeable Sodium}}{\sqrt{\frac{(\text{Exchangeable Calcum} + \text{Magnesium})}{2}}}$$

Statistics: Results were subjected to mean of values. Correlations and multiple regression analyses were also conducted to relate changes in aggregate stability (MWD) and soil properties using SPSS(1999).

Results

Soil properties: Selected properties of soils studied are shown in Table 1.Coarse sand predominated over other size fractions irrespective of land use. While percent silt was low in line with Igwe *et al.* (1995), textural class ranged from sand to sandy loam. Also low clay content was observed in studied soils.Forest and oil palm plantation soils had the lowest bulk density value of 1.29 g/cm3 with highest value recorded in soils under cassava cultivation polluted with crude oil (CP) and this corresponded to high and low total porosity values for the former and latter land uses, respectively. Organic fractions were highest in soils under CP and rubber plantations (RP) and least in soils under cassava cultivation non polluted (NCP) and bare fallow (BF). Available phosphorus was highest in RP and least in oil palm plantation (OP). Highest value of base saturation (BSat) was found in soils under RP while least value was recorded in forest soils. Soils under NCP and CP recorded highest exchangeable sodium percentage (ESP) and sodium adsorption ratio (SAR). Soils were generally strongly acidic irrespective of land use type with soils under forest exhibiting highest value of exchangeable aluminium (1.1 meg/100g soil).

An introduction of slope factor gave differences in some soil properties (Table 2). Average coarse sand content decreased with slope decrease irrespective of land use and this contrasted with the trend in fine sand and clay distribution Total porosity and organic matter increased downslope irrespective of land use

type. Conversely bulk density decreased downslope, ranging from 1.47 to 1.24 g/cm3 (mean values). Highest bulk density values were recorded in RP, CP and NCP in all the physiographic positions.

Aggregate Stability: Aggregate stability varied among physiographic position (Table 3). Highest percentage of water-stable aggregates were recorded in the less than 0.25 mm diameter water-stable aggregates at each slope type. The 4-2 mm water-stable aggregates increased in the downslope direction for all the land use types. Organic matter (OM) increased downslope with RP having highest mean OM at the bottomslope. Very sharp increased in OM occurred in CP from 5 to 3 % slope gradient while BF exhibited the least OM increased.

Mean weight diameter (MWD) increased with declining slope gradient, having 0.41 mm (5% slope), 0. 54 mm (3%) and 0.66 mm (0-1%). Aggregates were most stable in CP, jointly followed by F and OP, then BF, RP and NCP in a decreasing order. The NCP followed the general trend of decreasing upslope as in other treatments but values not as comparable with others. Surprisingly; BF did not show least stability despite its exposure to climatic and anthropogenic forces.

Relationship between Aggregate Stability and Soil Properties: Results of correlation analysis between aggregate stability (MWD) and some soil properties are shown in Table 4. There were very significant (P =0.01) positive relationship between OC, pH T.N., exchangeable calcium and exchangeable and sodium MWD while exchangeable hydrogen related very significantly (P-0.01) but negatively related with the aggregate stability index. However, exchangeable potassium has a significant (P=0.05) with MWD while exchangeable magnesium, total exchangeable acidity, BD, ESP and SAR showed no significant relationship with MWD. Of the variables assessed organic fractions (OC and TN) had the best relationship with MWD. These results show consistency with the studies of Rachman *et al*. (2003) which reported greater aggregate stability as OM increased in long-term cropping systems.

TABLE 1. Selected properties of soils studied (0-15 cm)

Properties	Unit	CP	RP	NCP	F	OP	BF
CS	%	55	49	70	76	63	62
Fs	%	28	28	17	16	24	18
Silt	%	7	12	2	1	7	9
Clay	%	10	11	11	7	6	11
TC		LS	SL	Ls	S	L	SL
BD	g/cm3	1.53	1.43	1.36	1.29	1.29	1.36
TP	%	42	46	48	51	51	52
$pH_{(1:2.5/H20)}$		4.8	4.7	4.8	1.4	4.7	4.5
OC	%	2.2	2.2	1.1	1.7	1.9	1.7
TN	%	0.20	0.20	0.10	0.16	0.18	0.11
Av.P	ppm	8.1	26.6	9.5	10.2	7.6	7.9
Ca^{2+}	meq/100g	0.8	1.8	0.4	0.6	1.6	0.8
Mg^{2+}	meq/100g	0.5	0.6	0.6	0.5	0.9	0.5
K^{+}	meq/100g	0.1	0.2	0.1	0.1	0.1	0.1
N^{a+}	meq/100g	0.8	0.7	0.7	0.6	0.5	0.6
H+	meq/100g	0.2	0.2	0.3	0.3	0.2	0.2
AI^{3+}	meq/100g	0.7	0.5	0.8	1.1	0.2	0.8
CEC	meq/100g	4.9	5.6	3.8	5.2	5.9	4.5
Bsat	%	44	59	47	34	50	44
ESP	%	16	12	18	11	8	13
SAR		3.2	2.4	3.3	2.8	1.5	2.4

CP = Cassava cultivation polluted with crude oil
RP = rubber plantation, NCP = Cassava Cultivation not polluted, F = forest, OP = oil palm plantation, BF = Bare Fallow, LS = Loamy Sand, S = sand,
SL = sandy loamy
CS = Coarse sand, FS = fine sand, TC =textural class,
BD = Bulk density, TP = total porosity, OC = organic carbon,
TN = Total nitrogen, AVP = available phosphorus, CEC = cation
Exchange capacity, BSat = base saturation, ESP = exchangeable
Sodium percentage, SAR = sodium absorption ratio.

Table 2. Properties of soils under 6 land uses in relation to slope (0-15cm)

Land use	CS (%)	FS (%)	Silt (%)	Clay (%)	TP (%)	BD (%)	OM (%)
5 % slope							
CP	54.5	30.0	6.5	9	41	1.56	2.0
RP	55.5	29.0	7.5	8	38	1.64	1.8
NCP	72.5	15.0	2.5	10	43	1.50	1.5
F	75.0	18.5	0.5	6	48	1.38	3.1
OP	67.0	21.5	6.5	5	47	1.40	1.9
BF	65.5	14.0	12.5	8	49	1.35	1.8
Mean	65.0	21.3	6.0	7.6	44.3	1.47	2.0
3% Slope							
CP	54.0	29.5	6.5	10	42	1.53	4.5
RP	55.0	28.5	7.5	9	42	1.54	2.7
NCP	70.0	16.5	2.5	11	50	1.32	2.0
F	76.0	15.5	1.5	7	52	1.25	2.6
OP	64.0	23.5	7.5	5	52	1.26	3.7
BF	60.5	20.0	8.5	11	49	1.24	1.9
Mean	60.8	22.2	5.6	8.3	48.0	1.35	2.9
0 –1% slope							
CP	56.5	25.0	7.5	11	43	1.52	4.8
RP	38.0	25.5	20.5	16	58	1.12	6.6
NCP	67.0	18.5	5.2	12	52	1.25	2.2
F	76.5	13.0	2.5	8	53	1.24	2.8
OP	57.0	26.5	8.5	8	54	1.22	4.0
BF	58.5	23.0	6.5	14	58	1.10	2.2
Mean	58.9	22.2	8.4	11.5	53.0	1.24	3.8

CS = Coarse sand, FS = fine sand, TP = Total porosity,
BD = Bulk density, OM = organic matter

Table 3. Structural stability of studied soils

Land Use	Water-stable aggregates (mm) 4-2	2-1	1-0.5	0.5-0.25	<0.25	MWD(mm)	OM
CP	11.2	10.9	16.9	19.7	32.9	0.75	1.9
RP	2.1	1.1	4.8	21.3	69.8	0.28	1.8
NCP	1.3	2.1	8.1	20.5	64.0	0.29	1.5
F	3.5	4.9	13.2	24.9	50.8	0.44	3.1
OF	1.6	1.4	5.1	34.1	55.3	0.31	1.9
BF	4.1	3.5	9.7	27.5	53.7	0.42	1.8
Mean	3.96	4.00	9.63	24.66	54.91	0.41	2.0
3 % Slope							
CP	13.2	13.2	11.5	14.0	46.9	0.79	4.5
RP	4.6	5.2	12.9	23.7	50.1	0.47	2.7
NCP	2.2	2.5	8.6	27.5	58.2	0.35	2.0
F	4.8	10.8	17.3	25.4	39.1	0.58	2.6
OP	8.7	6.6	9.2	23.8	49.2	0.58	3.7
BF	6.0	4.3	10.5	29.1	48.2	0.49	1.9
Mean	6.58	7.10	11.66	23.91	48.61	0.54	2.9
0 – 1% Slope							
CP	16.3	17.5	17.8	17.6	26.9	0.99	4.8
RP	11.1	12.1	12.1	6.8	46.7	0.69	6.6
NCP	2.3	2.9	6.8	31.9	55.3	0.35	2.2

F	6.3	12.1	15.7	23.5	39.7	0.63	2.8
OP	9.7	12.5	20.8	15.9	38.7	0.74	4.0
BF	5.3	8.5	13.6	21.1	39.7	0.55	2.2
Mean	8.50	10.93	14.46	19.46	41.16	0.66	3.7

MWD = Mean weight diameter

Table 4. Relationship between MWD and some soil properties (N=90)

Variable	r	r^2	Level of Significance
OC	0.52	0.270	* *
pH(water)	0.32	0.100	* *
TN	0.51	0.260	* *
Ca^{2+}	0.39	0.150	* *
Mg^{2+}	-0.03	0.001	NS
K^{+}	0.22	0.050	* *
N^{a+}	-0.34	0.110	* *
BSat	0.34	0.110	* *
H	-0.21	0.040	* *
TEA	-0.13	0.010	NS
BD	-0.07	0.005	NS
SAR	0.05	0.003	NS
ESP	0.13	0.02	NS

MWD = Mean weight diameter, OC = organic carbon, TN = total nitrogen, TEA= exchangeable acidity, BSat = base saturation, BD =bulk density, SAR = sodium Adsorption Ratio ** Significant at P = 0.01, * Significant at P = 0.05 NS = not significant, r =correlation coefficient, r^2 = coefficient of Determination.

Discussion

Sandiness, acidity and low organic matter content of soils could be attributed to a combination of influences from parent materials climate, land use type and land use history. The presence of Coastal Plain Sands as a parent material resulted in the formation of sand-sized fractions with little clay content and clayiness affects aggregate stability (Kay and Angers, 1999). It implies that the predominance of sand-sized particles promotes aggregate instability, and this is characteristic of studied soils of the study site. Instability of aggregates is worsened by high rainfall duration, amount and intensity which heighten erosivity of these disaggregated soils. Also, low content of organic matter in these soils especially those on 5% slope enhances disaggregation of macroaggregates. It has been reported that a positive relationship exists between organic matter and aggregate stability (Spaccini *et al.* 2001; Adesodum *et al.,* 2004). Despite a good value of OC recorded in CP, it still has the highest value of bulk density (1.53 g/cm^3), and this is attributable to effect of cultivation and crude oil pollution of these soils. Foth (1984) reported that crude oil spillage increases bulk density due to aggregate disintegration as tillage operations break down aggregates, reduce structural stability while increasing bulk density (Eynard *et al.,* 2004). In Southern Brazil, Viera *et al.*(2002) reported changes in bulk density resulting from cultivation.

Exchangeable calcium strongly correlated with MWD (r =0.39; p = 0.01, N = 90) possibly due to the ability of the basic cation to promote flocculation of soil colloids (Curlin *et al.,* 1994; Dontsova and Norton, 2002). Exchangeable potassuim had the same effect while Na^{+} significantly decreased as MWD increased (r = 0.34; P =0.01). Earlier, Dontsova *et al.* (2004) reported that exchangeable cations significantly influence soil-water relations and this may have affected structural stability. Exchangeable Na and Mg enhance dispersion and clay swelling in the soil exchange complex. Cationic hydrogen had a significant negative correlation (r = -0.21; p = 0.01) with MWD, which could be attributed to its preponderance after intensive leaching of basic cations in the tropical rainforest agroecology. In the same study, values of exchangeable Na were low and exhibited insignificant relationship with ESP and SAR, suggesting that exchangeable sodium is not a principal factor influencing MWD and consequent erodibility of soils of the study area.

Conclusions

The study revealed that properties of soils varied due to land use practices. Rubber plantation and CP soils exhibited highest BD values while RP and CP soils were high in OM. While BD decreased downslope, OM increased towards 0-1% slope. Structural stability of aggregates also varied with land use, with CP showing highest MWD in all the physiographic positions. However,in all land use types, MWD was very strongly related with OC and TN. There is a great need to use other aggregate stability indices in soils of the study site for increased knowledge and for purposes of comparisons.

Correspondence to:
Dr. Emmanuel Uzoma Onweremadu
Soils Survey and Environmental Management Unit
Department of Soil Science and Technology
Federal University of Technology, PMB 1526
Owerri, Nigeria.
E-mail: uzomaonweremadu@yahoo.com

REFERENCES

1. Adesodun JK, Mbagwu JSC, Oti N. Distribution of carbohydrate pools within water-stable aggregates of an Ultisol in Southern Nigeria' International Agrophysics 2001; 18:103-109.
2. Boix-Fayos C, Calvo-Cases A, Imeson AC, Soriano-Soto MD. Influence of soil properties on the aggregation of some Mediterranean soils and the use of aggregate size and stability as land degradation indications. CATENA 2001; 44:47-67.
3. Brady NC, Weil RR. The nature and properties of soils. 12th edition, Macmillian Ltd, New York.
4. Bremner JM. Nitrogen total. In:Sparks DL(Ed). Methods of Soil analysis, Part 3, Chemical methods, 2nd edition, ASA and SSSA Book series No.5 Madison WI 1996; 1085-1121.
5. Cambardella CA, Elliott ET. Particulate soil organic matter changes across a grassland cultivation sequence. Soil Science Society of America Journal 1992; 56:777-783.
6. Curtin D, Steppuhn H, Selles F. Effects of Magnesium on cation selectivity and structural stability of sodic soil 1994; 58:730-737.
7. Dextor Ar, Chan KY. Soils mechanical properties as influenced by exchangeable cations. Journal of Soil Science 1991; 42: 219-226.
8. Dontsova KM, Norton LD, Johnston CT, Bigham JM. Influence of exchangeable actions on water adsorption by soil clays. Soil Science Society of America Journal 2004; 68:1218-1227.
9. Dontsova KM, Norton LD. Clay dispersion, infiltration and erosion as influenced by exchangeable Ca and Mg. Soil Science 2002, 167:184-193.
10. Emteryd O. Chemical and physical analysis of inorganic nutrients in plats, soils water and air. Sterial No Uppsala, Swedish University Agricultural Science.
11. Eneje RC, Ogbonna CV, Nuga BO. Saturated hydraulic conductivity, water stable aggregates and soils organic matter in a sandy –loamy soil in Ikwuano LGA of Abia State. AgroScience 2005;34-37.
12. Eynard A, Schumacher TE, Lindstrom MJ Malo DD. Aggregate sizes and stability in cultivated South Dakota Prairie Ustolls and Usterts. Soil Science Society of America Journal 2004; 68:1360-1365.
13. Gee GW, Or D. Particle size analysis. In: Dane JH, Topp GC(Eds.). Methods of soil analysis, Part 4, Physical methods. Soil Science Society America Book series No. 5 ASA and SSSA, Madison, WI. 2002, 255-293.
14. Greenland DJ, Wild A, Adams D. Organic matter dynamics in soils of the tropics from myth to complexity. In: Lal R, Sanchez Pa (Eds.) Myths and science of soils of the tropics. Proceedings of an International Symposium. SSSA special Publication No. 29Madison WI 1992; 17-33.
15. Grossman RB, Reinsch TG. Bulk density and linear extensibility. In: Dane JH, Topp GC (Eds). Methods of soil analysis, part 4, physical methods, Soil Science Society of America Book Series No. 5 ASA and SSSA Madison, WI 2002; 201-228.
16. Hendershot WH, Lalande H, Duquette M. Soil reaction and exchangeable acidity. In: Carter MR (Ed.). Soil sampling and methods of analysis. Canadian Society of Soil Science, Lew Publishers, London 1993; 141-145
17. Igwe CA, Akamigbo FOR, Mbagwu JSC. Physical properties of soil of Southeastern Nigeria and the role of some aggregating agents in their stability. Soil Science 1995; 160:431-441.
18. Juo ASR. Selected methods for soil an plant analysis, 11TA. Manual series No. 1 11TA Ibadan 1981.

19. Kay BD, Angers DA. Soil structure. IN: Summer ME (Ed.) Handbook of Soil Science, CRC Press New York 1999; 229-269.
20. Levy GJ, Torrento JR. Clay dispersion and macroaggregate stability as affected by exchangeable potassium and sodium. Soil Science 1995; 160:352-358.
21. Mbagwu JSC, Auerswald K. Relationship of percolation stability of soil aggregates to pand use, selected properties, structural indices and simulated rainfall erosion. Soil and Tillage Research 1999; 50:197-206.
22. Nelson DW, Sommers LE. Total carbon, organic carbon and organic matter. In: Sparks DL (Ed.). Methods of soil amalysis, part 3 chemical methods, 2nd edition, ASA and SSSA Book series No. 5, Madison WI 1996; 960-1010.
23. Onweremadu, E.U. Application of geographic information systems on soil and soil-related environmental problems in southeastern Nigeria. A PhD Thesis of the University of Nigeria , Nsukka, Nigeria 2006; 330.
24. Piccola A. Humus and soil conservation. In: Piccola A (Ed.) Humic substances in terrestrical ecosystem. Elsevier, Amsterdam 1996;225-264.
25. Piccola A, Mbagwu JSC. Role of Gydrophobic components of soil organic matter on soil aggregate stability. Soil Science Society of America Journal 1999; 63: 1801-1810.
26. Rasiah V, Kay BD. Characterizing changes in aggregate stability subsequent to introduction of forages. Soil Science Society of America Journal 1994; 58: 935-942
27. Rhoades JD. Cation exchange capacity. In: Page, A.L; Miller, R.H., Keeney DR (Eds.). Methods of soil analysis, part 2, America Soiety of Agronomy, Madison WI 1982, 149-158.
28. Spaccini R, Zena A, Igwe CA, Mbagwu JSC, Picolla A. Carbohydrate in waterstable aggregates and particle size fractions in forested and cultivated soils in two contrasting tropical ecosystems. Biogeochemistry 2001; 53:1-22.
29. SPSS INC. SYSTAT 9 statistics I.SPSS Inc. Chicago, IL, 1999.
30. Rachman A, Anderson SH, Gantzer, CJ, Thompson AL. Influence of long-term cropping system on soil physical properties related to soil erodibility. Soil Science Society of America Journal 2003; 67:637-644.
31. Viera SR, Mbagwu JSC, Castro OM, De Alves MC, Dechen SCF, De Maria JC. Changes in some physical properties of a typic Haplorthox in Southern Brazil under no-tillage crop rotation systems. AgroScience 2002;1-12.

Serum Trace elements Profile in the Nigerian with Onchocerca volvulus Infection

[1]Nmorsi OPG, [2]Ukwandu NCD, and [1]Owhojedo O.

1. Tropical Research Unit, Department of Zoology, Ambrose Alli University, Ekpoma. Nigeria.
2. Department of Medical Microbiology, College of Medicine, Ambrose Alli University, Ekpoma. Nigeria.
nmorsiopg@yahoo.com

ABSTRACT: The serum trace element namely copper, selenium and zinc among Nigerians with microfiladermia and 4 clinical manifestations of onchocerciasis were investigated. The prevalence of the clinical presentations were onchocercal dermatitis 48 (48.9%), leopard skin 40 (40.8%), onchocercal nodules 40 (40.8%) and hanging groin 9 (9.2%). The relationship between prevalence of onchocercal dermatitis, onchocercal nodules and hanging groin and microfilarial load were positively correlated (r= 0.81, r = 0.12 and r = 0.51) respectively. Leopard skin had negative correlation with the microfilarial load (r= -0.64). The mean serum trace elements of the infected volunteers were copper 670.3±28.6 ng/ml, selenium 59.0±5.9 ng/ml and zinc 400.3±12.4 ng/ml. The differences between the mean concentration of copper of infected volunteers and their control was statistically significant (χ^2 = 20.3, p>0.05). The differences between mean concentration of selenium and zinc of the control and infected volunteers were statistically not significant (χ^2 =1.61, p<0.05) (χ^2=0.64, p<0.05) respectively. The relationship between the serum copper, selenium and zinc and the microfilarial load were negatively correlated (r =-0.93, r =-0.94 and r =-0.84) respectively. The depleted mean serum trace elements in the infected volunteers than their control subjects implicated the deficiency of copper, selenuim and zinc in the pathogenesis of onchocerciasis and the need to incorporated dietary trace element supplements in management of onchocerciasis. [Nature and Science. 2007;5(4):14-17].

INTRODUCTION

The pathogenesis of onchocerciasis is mainly due to the effects of microfilariae which manifests by different clinical presentations mainly in chronic phase. The chronicity of this infection includes lichenification such as leopard skin and other skin pathology (Nmorsi *et al*., 2007).

Nutrition plays a major role in maintaining health and micronutrients are known to influence the disease progression in man (Hussey and Clement 1996). Zinc which is one of the essential trace elements and indeed a member of one of the major subgroups of micronutrient has attained prominence in human nutrition and health (Hambridge, 2000). Zinc deficiency depresses the ability of the body to respond to infection, affecting both cell-mediated immune and humoral responses (Shankar and Prasad 1998; Ibs and Rink, 2003). The established role of selenium in human is its antioxidant activity. Low plasma selenium is found in varied clinical disorders and excessive chronic selenium intake causes skin pathology (Lockitch, 1989). Several bacteria known to be human pathogens die when placed in copper alloy surfaces. Copper continues to play a vital role as we age by keeping our hair and skin in good condition while repairing and maintaining connective tissues in our organs (Michels *et al*., 2005). Deficiencies of some trace elements such as copper and zinc have been associated with higher worm burden. The possibility is emerging that there may be optimum trace element in the diet above which or below which a parasite is advantaged. Moreover, there is some specific data to suggest that specific trace elements may be directly toxic to parasites (Koski and Scott, 2003).

There is paucity or no information on the relationship between trace elements and parasites especially *O. volvlulus* in this part of globe despite the demonstrable relevance of trace elements in pathogenesis of parasitic infections. We therefore investigated the serum trace elements profile in Nigerians with *O. volvulus* infection.

MATERIALS AND METHODS

Egoro-Eguare, a rural community located in Esan West Local Government Area of Edo State, Nigeria is our study area. It lies approximately lat 6^{o}N, 5^{o}E and longitude 6^{o}N, 8^{o}E. It is located about 7km away from Ekpoma, the headquarter of Esan West Local Government Area. Egoro-Eguare has a population of about 900 inhabitants who are predominantly farmers while some females are involved in pretty trading. Here there is absence of a school and market. There is a stream that is shaded with luxuriant green vegetation as the community lies within the rainforest belt of the state. This stream serves as the source of

recreational and domestic activities to the villagers. It constitutes breeding site of *Simulum* found within the community. The inhabitants had been subjected to ivermectin therapy by the State Ministry of Health Onchocerciasis Control Programme, Benin City, Nigeria. Ethical permission was obtained from the State Ministry of Health, Benin City, Nigeria. We carried out community mobilization campaign where the aims, scope and nature of our research were explained to the inhabitants in our study area for their consent. The consenting participants were assembled in the palace of the village head for further study. Here a pre-designed questionnaire on their names, age, weight and occupation were administered. They were subjected to physical examination individually in a room in search for the clinical presentation of the disease.

Two skin-snips were taken from the iliac crest bilaterally and transported to our Tropical Diseases Research Laboratory for further procession and examination microscopically as reported earlier (Nmorsi *et al*., 2002). The 98 volunteers with microfiladermia and different clinical features of Onchocerciasis and 35 control participants were recruited for further study. The presence of other obvious disease conditions namely HIV, malaria, intestinal parasitic infections were ruled out in these participants using standard kits and procedures.

The serum copper, selenium and zinc concentrations from the participants were determined using Atomic Absorption Spectrophotometer.

The data obtained from this study were subjected to statistical analysis using the chi – square test and correlation using the Micro Soft Excel Package.

RESULTS

Table 1 presents the clinical presentations of 98 volunteers with microfiladermia according to their age groups in years. In all, 4 clinical manifestations namely 48(48.9%) onchocercal dermatitis, 40(40.8%) leopard skin, 40(40.8%) and 9(9.2%) hanging groin were encountered. Leopard skin, onchocercal nodules and hanging groin were not reported among the *O. volvulus* infected inhabitants within the first decade of life. The highest prevalence of clinical manifestation of 11(100%) occurred among the individuals above 60 years old. The prevalence of the onchocercal dermatitis, onchocercal nodules, hanging groin and microfilarial load were positively correlated ($r = 0.81$, $r = 0.12$ and $r = 0.51$) respectively. The relationship between the onchocercal nodules and microfilarial load was negatively correlated ($r = -0.64$).

The serum trace elements, microfilarial load according to the age groups in years of the 98 *O. volvulus* infected volunteers are presented in Table 2. The highest microfilarial load of 20 mff/mg was reported among the infested volunteers within the 11-20 age groups in years, while the least occurred among the volunteers above 60 years old. The mean serum trace elements were copper 670.3±28.6 ng/ml, selenium 59.0±5.9 ng/ml and zinc 400.3±12.4 ng/ml. The mean concentration of copper was statistically different from their control subject (925±25.0ng/ml) at ($\chi^2 = 20.03$, $p>0.05$). The difference between the mean concentration of selenium and zinc of the infected and control volunteers were statistically not significant at ($\chi^2 = 1.61$, $p<0.05$), ($\chi^2 = 0.64$, $p<0.05$) respectively. The relationship between the microfilarial load and serum trace elements namely copper, selenium and zinc were negatively correlated at ($r = -0.93$, $r = -0.94$ and $r = -0.84$) respectively.

Table 1. The clinical presentations according to the age groups of 98 Volunteers with Microfiladermia

Age groups in years	No infected with microfilariae	Clinical Presentation			
		Onchocercal dermatitis no (%)	Leopard skin no (%)	Onchocercal nodules no (%)	Hanging groin no (%)
1 – 10	10	9(90)	0(0)	0(0)	0(0)
11 – 20	18	13(72.2)	2(11.1)	4(22.2)	1(5.6)
21 – 30	16	10(62.5)	3(18.8)	9(56.3)	3(18.8)
31 – 40	17	6(35.2)	5(29.4)	10(58.8)	2(11.8)
41 – 50	13	3(28.1)	9(69.2)	6(46.2)	2(15.4)
51 – 60	13	3(23.1)	10(76.9)	5(38.5)	1(7.7)
>60	11	4(36.4)	6(54.5)	6(54.5)	0(0)
Total	98	48(48.9)	40(40.8)	40(40.8)	9(9.2)

Table 2. The Serum trace elements and microfilarial load according to the age groups in years

Age group in years	**Microfilarial Load (mff/mg)**	**Copper ng/ml**	**Selenium ng/ml**	**Zinc ng/ml**
1 -10	10.5±4.1	664.5±50.5	62.5±3.5	419.0±13.2
11 – 20	20.0±3.1	631.8±45.3	46.8±7.0	384.4±44.3
21 - 30	16.5±4.2	641.0±46.7	57.2±2.5	386.4±38.4
31 – 40	12.0±1.1	669.2±25.3	58.3±2.8	393.6±41.2
41 – 50	12.5±3.5	671.3±52.1	60.3±2.8	399.0±10.2
51 - 60	8.3±4.1	689.0±24.0	63.0±3.5	404.5±10.5
>60	6.5±1.1	725.0±45.3	65.0±4.0	415.3±11.8
Mean	12.33±4.7	670.3±28.6	59.0±5.9	400.3±12.4
Control	-	925.0±25.0	78.5±15.2	433.0±8.0

DISCUSSION

Our data showed the prevalence of four clinical manifestations of ochocerciasis namely onchocercal dermatitis, leopard skin, onchocercal nodules and hamging groin. We observed a preponderance of infection towards the adult than the children. This denotes long standing and chronic presentation of this parasitic infection. These observations had been reported earlier (Nmorsi and kio 1994, Edungbola *et al*., 1987).

An important observation reported in our study is a plateau (fairly stable) type presentation of microfilarial load between 20 – 50 years while the children and the volunteers above 50 years of age had lower microfilarial load. This has economic repercussion considering the fact the inhabitants are predominantly farmers and the 20 – 50 years are the active productive age. This observation accords the reports of (Anderson and May 1991, Hudson and Dobson 1995, Nmorsi and Obiamwe 1992) where they reported a stabilizing (plateau) pattern of onchocerciasis with reduced infection in children and old age groups. This pattern of infection can be attributed to reduced exposure and enhanced immunity.

Our data which revealed lower concentration of trace elements than their control subjects reflects the impact of *O. volvulus* on these micronutrients. This assertion is further proved valid by the relationship between the serum concentration of the trace elements namely copper, selenium and zinc with the microfiladermia which were negatively correlated. Furthermore, this deduction is true considering the role of these micronutrients in human health. For instance, copper is involved in keeping our hairs and skin in good condition while repairing and maintaining connective tissues in our organs (Michels *et al*., 2005).

Another significant observation is the depressed zinc status among the Nigerians with onchocerciasis. This state of zinc deficiency reported in our investigation had been documented earlier in other disease conditions (Shankar and \Prasad 1988, Falutz *et al*., 1989). This observation is expected considering the central role of Zinc in human immune system as zinc deficient persons experience susceptibility to a variety of pathogens (Shankar and Prasad, 1989) thereby depresses immune function and leads to morbidity of diseases (Sandstead, 1991). Also Ibs and Rink (2003) documented that zinc deficiency depresses the ability of the body to respond to infection affecting both cell-mediated immune and humoral responses. Therefore this depressed zinc concentration profile will no doubt contribute greatly to the maintenance of the chronicity and long standing onchocerciasis in Egoro-Eguare despite the intervening ivermectin therapy.

The depressed selenium status in our *O. volvulus* infected participants reflects the depletion of this trace element which is known to possess antioxidant activities (Flohe, 1988) Selenium with its selenoenzymes, stutathione peroxidase and indeed zinc are cateforised as antioxidants. In the face of low serum selenium concentration, oxidative stress abound which can contribute to cell injury and oxidation of biomolecules (Fang *et al*., 2002). We believe that this will therefore contribute to the skin pathology and other clinical manifestations in onchocerciasis in Egoro-Eguare, Nigeria.

From our data, we found the interrelationship between serum trace elements and onchocerciasis which is chronic and long standing in Egoro-Eguare, Nigeria. Since administration of trace elements such as Zinc supplementation can improve the immune system in human diseases (Shankar and Prasad, 1998) and dietary antioxidants play an important role in preventing many human diseases (Fang *et al*., 2002), we

recommend the incorporation of dietary trace elements especially zinc, copper and selenium supplementations with current ivermectin in management of onchocerciasis.

Corresponding author:
Prof. O.P.G. Nmorsi
Tropical Research Unit,
Department of Zoology,
Ambrose Alli University,
Ekpoma. Nigeria.
nmorsiopg@yahoo.com

REFERENCES

1. Anderson R.M., May R.M. (1991). Infectious disease of humans oxford: Oxford University Press.
2. Anderson J., Fuglsang H., Marshal Y.E. (1976). Studies on Onchocerciasis. In United Cameroon Republic III. A four year follow up to 6 rainforest and 6 Sudan Savanna villages. *Transaction of Royal Society of Tropical Medicine; 70*: 762-73.
3. Edungbola L.O., Watts S. Kayode O.O. (1987). Endemicity and striking Manifestations of Onchocerciasis in Shaw, Kwara State, Nigeria. *African Journal of Medical Sciences, 16*: 147-56.
4. Falutz J, Tsoukas C and Deutsch G (1989) functional correoates of decreased serum zinc in human immunodeficiency virus (HIV) disease. *International Conference of AIDS. 5:* 468.
5. Fang YZ, Yang S and Wu G (2002). Free radicals, antioxidants and nutrition. *Nutrition. 18(10)*: 872-879.
6. Flohe L. (1988). Glutathione perixidase. *Basic life Sciences,* 49: 663-668.
7. Hambridge M (2000). Human Zinc Deficiency. *Journal of. Nutrition. 130*: 13445-13495.
8. Hudson P.J., Dobson A.P. (1995). Macroparasites: Observed patterns in naturally fluctuating populations. In: Grenfell B.Y., Bobson A. Peds. Ecology of infectious diseases in natural populations. Cambridge: Cambridge university Press. 144 -176.
9. Hussey DC and Clement CS (1996).Clinical problem in measles and management. *Annal of Tropical. Paediatric. 16*: 307-317.
10. Ibs K.and Rink L (2003) Zinc – Altered Immune Function. *J of Nutrition*. *133*: 1452S-1456S.
11. Koski KG and Scott MF (2003). Gastrointestinal nematodes, trace elements and immunity. Journal of Trace *Elements and. Experimental. Medicine. 16*:237-251.
12. Lockitch G (1989). Selenium: Clinical significance and analytical concepts. *Critical Reviews in Clinical Laboratory Sciences.. 27 (6)*: 483-541.
13. Michels HT, Wilks SA, Niyce JO and Keevil CW (2005). Copper alloys for Human Infections Disease Control. Material Science and Technology Conference paper. September 25-28, Pittsburgh, PA. Copper for the 21st Century Symposium.
14. Nmorsi OPG.and Kio F.E. (1994). Hypoendemicity of Onchocerciasis in Odiguetue, Ovia North East Local Government Area, Edo State, Nigeria. *Journal of Medical Laboratory Sciences 4*: 21-5.
15. Nmorsi OPG. and,Obiamiwe B.A. (1992). Onchocerciasis in Imeri, Ondo State, Nigeria. *Nigerian Journal of Parasitology 13*: 43-49.
16. Nmorsi OPG, Oladokun IAA, Egwunyenga OA and Oseha E (2002). Eye lesions and onchocerciasis in a rural farm settlement in Delta State, Nigeria. *SouthEast Asian Journal of Tropical Medicine and Public Health.33(1):* 29 – 32.
17. Nmorsi OPG, Ukwandu NCD, Alabi-Eric OJ, Popoola W and Osita-Emina M. (2007). CD4+, CD8+, Immunoglobulin Status and ocular Lesions among some onchocerciasis-infected rural Nigerians. *Parasitology Research*. *100(6)*: 1262-1266.
18. Sandstead H.H. (1991). Zinc deficiency a public health problem. *Archives of Journal Child Diseases 145*: 853-859.
19. Shankar AH, and Prasad AS (1998). Zinc and Immune function: The biological basis of altered resistance to infection. *American Journal of Clinical Nutrition. 68 (Suppl 2)*: 447S-463S.

Combining Ability and Heterosis of Oil Content in Six Accessions of Castor at Makurdi

Okoh, J.O, Ojo, A.A. and Vange, T
Department of Plant Breeding and Seed Science, University of Agriculture, P.M.B. 2373 Makurdi, 970001 Nigeria.
E-mail: okohjohn014real@yahoo.com, t_vange@yahoo.com

ABSTRACT: Six accessions of castor viz: - Mkd. Acc. 1, Mkd. Acc. 7, Mkd. Acc. 12, Mkd. Acc. 13, Mkd. Acc. 14 and Mkd. Acc. 27 were subjected to combining ability test. The study was conducted at the University of Agriculture, Makurdi in 2004 and 2005 planting seasons. The objective was to determine the effect of crossing on the oil content of these castor accessions. A Randomized Complete Block Design (RCBD) was used with three replications. The study revealed that oil content of castor seeds of the accessions used varies from 36.6% - 53.85%. Analysis of variance revealed significant differences for entries, parents and hybrids. The analysis for combining ability showed that GCA and SCA were significant in each of the year. This is an indication that both additive and non-additive gene actions are important in the inheritance of oil in castor. Percentage heterosis of the hybrids for the 2 years showed that in 2004, 9 hybrids had higher oil content than their mid-parent value. 7 hybrids had higher oil content than the better parent In 2005, 11 hybrids had higher oil content than the mid-parent value; and 8 hybrids had higher oil content than their better parent. This study revealed that heterosis existed among the parents used. The results indicates high chances that the hybrid vigour may be exploited in a breeding programme to improve castor oil content. [Nature and Science. 2007;5(4):18-23].

Keywords: Castor Accessions, heterosis, combining ability, Makurdi, Oil content.

INTRODUCTION

Castor plant which is essentially a tropical species (Weiss, 1983) can grow in all the states in Nigeria. Castor oil is derived from castor plant (*Ricinus communis* L.). It is a colourless to very pale yellow liquid with mild or no odour or taste. Castor oil has over 1000 industrial uses and because of this, its demand increases (Uguru and Abuka, 1998). A scientific investigation of the crop to improve its oil content will go a long way to meet up with the demand.

Utilization of hybrid vigour for higher yield and better quality products have been exploited in many crops including soyabean (Kaw and Menson, 1979), cowpea (Zaveri *et al.*, 1983) and Sorghum (Verma and singh, 1983). Gila *et al.* (2005) reported heterosis in some agronomic characters in Castor crosses. This study however, did not consider the oil content of castor. Estimates of Specific combining ability (SCA) and General combining ability (GCA) will also assist in determining the best combining parents that will be used in developing aspect for higher oil content.

This research effort is therefore to investigate the oil content of the castor accessions in Makurdi. The specify Objectives of this study are: (i) to determine the oil content in the accessions of castor; (ii) to estimate the GCA and SCA variances in these castor accessions.

Materials and Methods

Six accessions of castor viz:- Mkd. Acc. 1, Mkd. Acc. 7, Mkd. Acc. 12, Mkd. Acc. 13, Mkd. Acc. 14 and Mkd. Acc. 27 were selected from a germplasm evaluation based on their yield performance (Gila 2003, unpublished) and used as parents. These parents were crossed in a partial diallel to generate 15 hybrids. The parents and hybrids were planted for evaluation in a Randomized Complete Block Design (RCBD) with three replications, in 2004 and 2005.

The study was conducted at the University of Agriculture, Makurdi on Latitude $7^{0}41^{1}$ and Longitude $8^{0}37^{1}$. The agronomic practices were manually done. Single row plots were used, each 3m long and spaced 1m x 0.5m. Clean seeds from each plot were grounded into a paste using mortar and pestle.

Oil Extraction

The Flask was washed, dried and weighed. 200ml of petroleum spirit was poured into a quick fit round bottom flask. Ten grammes of the sample were placed in the thimble and were inserted in the centre of the extractor. Heat was supplied at 60^{0}C. When the solvent was boiling, the vapour rises through the

vertical tube into the extractor at the middle. The condensed vapour drips into the thimble in the centre, which contains the solid sample to be extracted wrapped in a filter paper.

The extract seeps through the pores of the thimble and fills the siphon tube, where it flows back into the quick fit round bottom flask. This was allowed for 8 hours.

The Petroleum spirit was recovered from the quick fit bottom flask. It was then dried in the oven and cooled in the desiccators, and weighed using mettler electronic balance.

Weight of oil = Weight of flask + oil - Weight of empty flask

$$\frac{\text{wt of oil}}{\text{wt of sample}} \times 100 = \% \text{ oil}$$

Percentage oil content was analyzed using ANOVA for each year separately because homogeneity of error variance did not exist. The sources of variation were further partitioned into GCA and SCA. The Model 1, Method 2 of Griffing (1956) was used for the analysis as presented by Singh and Chaudhary (1977).

Result and Discussion

Significant differences (P = 0.01) were found among the 21 entries. Parents and hybrids were significant for the two years as revealed by analysis of variance (Table 1).

Table 1: Sources, Degree of Freedom and Mean Squares from Analysis of Variance of Castor Accessions in 2004 and 2005 Cropping Season.

Sources	**d.f.**	**Mean squares**	
		2004	**2005**
Entries	20	18.83**	44.83**
Rep	2	0.008	0.0006
Parent	5	11.33**	24.48**
Hybrid	14	21.64**	46.44**
P vs H	1	17.11**	103.99**
Error	4	0.23	0.0023
Total	**62**		

** = Significant at 1%

The mean oil content of the entries in 2004 and 2005 is shown in Table 2. In 2004, the following parents (Mkd Acc. 12 and Mkd Acc. 7) have the highest oil content of 45.27% and 44.26%, respectively; while Mkd Acc. 14 have the lowest oil content. Among the crosses, Mkd Acc.1 x Mkd Acc. 13, Mkd Acc. 7 x Mkd Acc. 14 and Mkd Acc. 13 x Mkd Acc. 14 had the highest oil content of 48.28%, 47.50% and 45.17% respectively. In 2005, the following parents Mkd Acc. 12 and Mkd Acc. 13 had the highest significant per ent oil content of 45.93% and 42.88% respectively. Mkd Acc. 7 had the lowest oil content of 36.6%. Among the crosses, Mkd Acc. 7 x Mkd Acc. 13, Mkd Acc. 1 x Mkd Acc. 13 and Mkd Acc. 13 x Mkd Acc. 14 had the highest oil content of 53.85%, 48.35% and 48.10% respectively, while Mkd Acc. 1 x Mkd Acc. 7 had the lowest oil content of 39.55%. In Table 2, parents and hybrid means revealed slight variations in magnitude. The means for each entry were not exactly the same for the 2 years. Kulkarni (1959) reported that the rate of oil content varies from year to year, indicating that seasons have considerable effect on the rate of formation of oil. In this study, generally oil content varies from 36.6% - 53.85% (Table 2). This collaborates with the study of Akpan *et al*, 2006 that reported 30 – 55% oil content.

The following crosses have higher oil content than their parent: Mkd Acc 1 x Mkd Acc 13, Mkd Acc 1 x Mkd Acc 14, Mkd Acc 7 x Mkd Acc 13, Mkd Acc 7 x Mkd Acc 14, Mkd Acc 13 x Mkd Acc 14, Mkd Acc 13 x Mkd Acc 27, and Mkd Acc 14 x Mkd Acc 27. The crosses Mkd Acc 1 x Mkd Acc 12, Mkd Acc 1 x Mkd. Acc. 27, Mkd Acc 12 x Mkd Acc 13, Mkd Acc 12 x Mkd Acc 14, Mkd Acc 12 x Mkd Acc 27 have higher oil content than one of the parents in 2004 (Table 2). In 2005, crosses Mkd Acc 1 x Mkd Acc 13, Mkd Acc 1 x Mkd Acc 14, Mkd Acc 1 x Mkd Acc 27, Mkd Acc 7 x Mkd Acc 13, Mkd Acc 7 x Mkd Acc 14, Mkd Acc 7 x Mkd Acc 27, Mkd Acc 13 x Mkd Acc 14 and Mkd Acc 14 x Mkd Acc 27 have higher oil content than either of the parents; while crosses Mkd Acc 1 x Mkd. Acc. 7, Mkd Acc 1 x Mkd Acc 12, Mkd Acc 7 x Mkd Acc 12, Mkd Acc 12 x Mkd Acc 14 have higher oil content than the other parent but less than Mkd. Acc. 12 (Table 2).

Table 2: Mean Percent Oil Content for Castor Accessions in 2004 and 2005 Cropping Season.

Entries	**Percent Oil**	
	2004	**2005**
Parents		
Mkd. Acc. 1	40.84	40.27
Mkd. Acc. 7	44.26	36.6
Mkd. Acc. 12	45.27	45.93
Mkd. Acc. 13	42.04	42.88
Mkd. Acc. 14	40.27	41.73
Mkd. Acc. 27	42.5	42.10
LSD (0.05)	1.28	0.10
CROSSES		
Mkd. Acc. 1 x Mkd. Acc. 7	37.93	39.55
Mkd. Acc. 1 x Mkd. Acc. 12	41.25	41.25
Mkd. Acc. 1 x Mkd. Acc. 13	48.28	48.35
Mkd. Acc. 1 x Mkd. Acc. 14	44.92	45.9
Mkd. Acc. 1 x Mkd. Acc. 27	41.07	46.55
Mkd. Acc. 7 x Mkd. Acc. 12	41.55	41.82
Mkd. Acc. 7 x Mkd. Acc. 13	45.90	53.85
Mkd. Acc. 7 x Mkd. Acc. 14	47.50	47.42
Mkd. Acc. 7 x Mkd. Acc. 27	42.29	42.17
Mkd. Acc.12 x Mkd. Acc. 13	42.88	41.73
Mkd. Acc.12 x Mkd. Acc. 14	44.15	44.87
Mkd. Acc.12 x Mkd. Acc. 27	44.98	41.85
Mkd. Acc.13 x Mkd. Acc. 14	45.17	48.1
Mkd. Acc.13 x Mkd. Acc. 27	42.72	39.73
Mkd. Acc.14 x Mkd. Acc. 27	44.52	43.43
LSD (0.05)	0.57	0.074

Table 3 shows that analysis for combining ability revealed that GCA and SCA were significant (P = 0.01). Giriraj *et al* (1973) and Hooks *et al* (1971) reported that both additive and non-additive gene actions were important for oil content in castor. This suggests that additive and non-additive genes are responsible for controlling the inheritance of oil in castor.

Table 3: Sources, Degree of Freedom (D.F) and Mean Squares from Analysis of Combining Ability for Castor Accessions in 2004 and 2005 Cropping Seasons.

Source	**d.f.**	**Mean squares**	
		2004	2005
GCA	5	3.09**	9.18**
SCA	14	7.83**	17.84**
Error	40	0.08	0.00082

** = Significant at 1%

In this study, the GCA and SCA ratios of 1:19 and 1:14 in 2004 and 2005, respectively, showed that SCA contributes more to the inheritance of oil in castor.

Table 4: Estimates of The GCA and SCA Effects for Oil in 6 X 6 Crosses of Castor Accessions at Makurdi in 2004 and 2005 Cropping Season.

ENTRIES	**GCA EFFECTS**	
	2004	**2005**
PARENT		
Mkd. Acc. 1	-1.037	-1.40
Mkd. Acc. 7	0.33	-0.92
Mkd. Acc. 12	0.24	-0.25
Mkd. Acc. 13	0.7	1.52
Mkd. Acc. 14	0.42	0.97

Mkd. Acc. 27	-0.356	-0.93
S.E. (gi)	0.57	0.059
CROSSES	**SCA EFFECTS**	
Mkd. Acc. 1 x Mkd. Acc. 7	-4.42	-2.76
Mkd. Acc. 1 x Mkd. Acc. 12	-1.31	-1.73
Mkd. Acc. 1 x Mkd. Acc. 13	5.26	3.61
Mkd. Acc. 1 x Mkd. Acc. 14	2.18	1.71
Mkd. Acc. 1 x Mkd.Acc. 27	-0.87	4.27
Mkd. Acc. 7 x Mkd. Acc. 12	-2.11	-0.63
Mkd. Acc. 7 x Mkd. Acc. 13	1.81	14.93
Mkd. Acc. 7 x Mkd. Acc. 14	3.69	3.42
Mkd. Acc. 7 x Mkd. Acc. 27	-0.74	0.39
Mkd. Acc. 12 x Mkd. Acc. 13	-1.42	-2.87
Mkd. Acc. 12 x Mkd. Acc. 14	0.13	0.21
Mkd. Acc. 12 x Mkd. Acc. 27	1.71	-0.59
Mkd. Acc. 13 x Mkd. Acc. 14	0.69	1.98
Mkd. Acc. 13 x Mkd. Acc. 27	-0.98	-4.18
Mkd. Acc. 14 x Mkd. Acc. 27	1.10	-0.54
S.E. (Sii)	0.43	0.043

The larger SCA indicate preponderance of non-additive type of gene effects. The non-additive genetic variation can be successfully exploited for the development of hybrids. This can be utilized through multiple crossing.

The GCA effects ranged from –1.037 to 0.7, while SCA ranged from –4.42 to 5.26 in 2004. In 2005, the GCA effects ranged from –1.40 to 1.52, while the SCA ranged from –4.18 to 14.93 (Table 4). Mkd. Acc. 13 is the best combiner among these parents because it had the highest GCA effects of 0.7 and 1.52 in the 2 years. The best specific combiner for 2004 was Mkd. Acc. 1 x Mkd. Acc. 13; with SCA effect of 5.26. The best specific combiner for 2005 was Mkd. Acc. 7 x Mkd. Acc. 13 (Table 4).

Percentage heterosis of the hybrids for the 2 years showed that in 2004, 9 hybrids had higher oil content than their mid-parent value. 7 hybrids had higher oil content than the better parent (Table 5). In 2005, 11 hybrids had higher oil content than the mid-parent value; and 8 hybrids had higher oil content than their better parent. This study revealed that heterosis existed among the parents used.

Table 5: Percentage Heterosis of the Castor Hybrids in 2004 and 2005 Cropping Seasons.

Crosses		**2004**	**2005**
Mkd. Acc.1 x Mkd. Acc.7	x 1	-10.85	2.89
	x 2	-14.30	-1.79
Mkd. Acc.1 x Mkd. Acc.12	x 1	-4.23	-4.29
	x 2	-8.90	-10.19
Mkd. Acc.1 x Mkd. Acc.13	x 1	16.51	16.31
	x 2	14.84	12.76
Mkd. Acc.1 x Mkd. Acc.14	x 1	10.75	11.95
	x 2	9.99	9.99
Mkd. Acc.1 x Mkd. Acc.27	x 1	-1.44	13.01
	x 2	-3.36	10.57
Mkd. Acc.1 x Mkd. Acc.12	x 1	-7.19	1.33
	x 2	-8.22	-8.95
Mkd. Acc.1 x Mkd. Acc.13	x 1	6.35	34.19
	x 2	3.71	25.58
Mkd. Acc.1 x Mkd. Acc.14	x 1	11	21.06
	x 2	7.32	13.64
Mkd. Acc.1 x Mkd. Acc.27	x 1	-2.51	7.17
	x 2	-4.45	0.17
Mkd. Acc.1 x Mkd. Acc.13	x 1	-1.79	-6.03
	x 2	-5.28	-9.14

Mkd. Acc.1 x Mkd. Acc.14	x 1	3.23	2.37
	x 2	-2.47	-2.31
Mkd. Acc.1 x Mkd. Acc.27	x 1	2.48	4.57
	x 2	-0.64	-8.88
Mkd. Acc.1 x Mkd. Acc.14	x 1	9.42	13.68
	x 2	7.45	12.17
Mkd. Acc.1 x Mkd. Acc.27	x 1	1.06	-6.50
	x 2	0.5	-7.55
Mkd. Acc.1 x Mkd. Acc.27	x 1	7.56	3.60
	x 2	4.75	3.16

X1 = Mid-parent **X2 = Better parent**

Conclusion

The percentage oil content from accessions of castor used in this study was found to be 36.6 – 53.85%.

Additive and non-additive gene actions were also seen to be important in the inheritance of oil in castor. Since the GCA effect was significant, selection of diverse parents may be exploited. This could lead meaningful hybridization of parents with high GCA effect to get more segregants. Segregants that expressed hybrid vigour could be ultilized in improving on the oil content of castor. The breeding programme, for increasing oil content should take into account the additive and non-additive gene actions observed herein the study.

Corresponding to:
John O. Okoh
Department of Plant Breeding and Seed Science,
University of Agriculture,
P.M.B. 2373 Makurdi, 970001
Nigeria.
Cellular Phone: +234(0)8032370439
E-mail: okohjohn014real@yahoo.com

Received: 11/23/2007

R e f e r e n c e s

1. Akpan, U. G., Jimoh, A., and Mohammed, A. D. Extracting, Characterization & Modification of Castor Seed oil. Lenoardo Journal of Sciences. 2006. 45 – 52.
2. Bhardwaj, H. I.,. Mohammed, A. I., Weber, C. L., III & Lovell, G. R. Evaluation of Castor germplasm for agronomic and oil characteristics. P. 342 – 346. In: J. Jarnick (ed.) Progress in New Crops. ASHS Press. Alexandris, V. A. 1996. 342 – 346.
3. Chaudhary, B. D. and Singh, R. K. Biometrical Methods in qualitative genetic analysis. Rajinder Nagar, Ludhiana-141008. 1977. 140 – 145.
4. Gila, M. Preliminary Evaluation of castor germplasm in Makurdi (unpublished) 2003.
5. Gila, M. A. Ojo, A.A. and Adeyemo, M.O. Heterosis of some agronomic characters in Castor (*Ricinus communis* L.) Crosses. Proceedings of the 30th Annual Conference of Genetic Society of Nigeria held at University of Nigeria, Nsukka. 5- 8th sept. 2005. 29-31.
6. Giriraj, K., Mensinkai, S. W. and Sindagli Combining Ability of some qua ntitative character in 6 x 6 Diallel crosses of castor (*Ricinus cummunis* L.) Indian Journal J. Agric. Sci. 1973 (43) 3:319-322.
7. Griffing, B. A. Generalized treatment of diallel crosses in quantitative inheritance, Heredity 1956 (10)31 –50.
8. Hooks, J. A., Williams, J. H. and Gardner, C. O. Estimates of heterosis from a diallel cross of inbred lines of castor (*Ricinus communis* L.). Crop Science. 1971(11) 651 – 655.
9. Kaw, R.N. and P.M. Menson (1979). Heterosis in a temarent diallel cross in soybean. Indian J. Agric. 1979(49)5:322-324.

10. Kulkarni, L. G. Castor monograph published by the Indian Central Oil Seeds Committee, New Delhi. 1959 (26).
11. Marter, A. D. (1981). Market utilization and prospects. Tropical Product Institute, G152, (1981) 55 – 78.
12. Uguru, M. I. and Abuka, I. N. Hybrid Vigour and Genetic Actions for two qualitative traits in castor plant (*Ricinus communis* L.). Ghana Journal. Agric. Sci. 1998(31):81 – 82.
13. Verma, P.K. and R. Singh. Genetic analysis of Heterosis in sorghum. Indian J Agric. Sci. 1983 (53) (9):771-775.
14. Weiss, E. A.. Oil Seed Crops, Tropical Agricultural Series. Longman. 1983. 31 – 32.
15. Zaveri, P.P., P.. Patels, J.P. Yadvendra and R.M. Sha. Heterosis and combining ability in cowpea. Indian J. Agric Sci. 1983. (53)9: 793 – 796.

Quality Of Bread From Wheat/Cassava Flour Composite As Affected By Strength And Steeping Duration Of Cassava In Citric Acid

Owuamanam C. I.
Department of Food Science and Technology,
Federal University of Technology,
P. M.B 1526 Owerri Imo State Nigeria.
Email: icliffowums@yahoo.com

ABSTRACT: Cassava flour was prepared from tubers of TMS 30572 steeped in five varying concentrations of citric acid solution (1.0, 5.0, 10.0 15.0 and 20.0 % M/V db) and samples were generated for 24, 72 and 120 h. The resultant cassava flour was used in partial substitution 100% wheat flour at 90:10, 80:20 and 70:30 percent ratios in bread making. Sensory evaluation was conducted on the bread quality by 10 member panel on loaf volume, crumb texture, taste and overall acceptance using the 9-point hedonic scale. The bread from cassava flour steeped in 20% citric acid solution had the highest mean score of 6.32, for the loaf volume; taste, 5.16; crumb texture, 5.79 and overall acceptance, 6.22. The bread from 90:10 was rated the best in all the assessment made. On the other hand, steeping for 24 h gave the result in terms of bread taste, 4.69 and overall acceptance. The result indicates that it is possible to produce quality bread up to 30% substitution of wheat flour when cassava roots were pretreated with citric acid solution before milling into flour. Also, steeping in citric acid solution for 24 h gave the desired modification of cassava flour for a better bread quality. [Nature and Science. 2007;5(4):24-28].

Key words: cassava flour, citric acid, composite and bread quality.

INTRODUCTION

Asselbergs (1) defined bread as a food of any size and shape or form and consists of dough made from flour and water, with or without other ingredients, which have been fermented by yeast or otherwise leavened and subsequently baked or partly baked. High quality bread in terms of large volume, good crust and crumb texture is principally produced from wheat flour; from wheat- a temperate grown crop (11). The leavened wheat bread has become a favourite food of many households in developing countries which may be attributed to increasing populations, urbanization and changing food habits (12). Unfortunately, wheat cannot grow well in tropical climate and relying on imports would drain the scarce foreign exchange of these countries (8, 12).The concept of composite technology initiated by FAO in 1964 was targeted at reduction of fund out flow towards temperate countries by encouraging the use of indigenous crops such as cassava, yam, maize etc. in partial substitution of wheat flour (5, 14).

Several attempts have been made in the 1960s 1970s to produce wheatless bread or gluten –free bread in Nigeria (7, 14). In an effort to conserve currency, the government of Nigeria in 1987 ban wheat import but that was not sustained in subsequent years (2). The recent policy directive to mills in Nigeria to include 10% cassava flour in bread, biscuits and other confections manufacture was aimed at sustaining the production of cassava and to restrict fund out flow for import of wheat (13). According to Eggleston and Omoaka, (6) and Deflour, (4), getting quality cassava flour that will meet the need of the mills has remained a problem due to poor processing methods, varietal, age and environmental condition of growth of cassava.

The current production of unfermented cassava flour (12) for bread making however, may not address the issue of reduction of cyanide in cassava flour. Steeping in water, drying, milling etc. are known to improve flour functionality and also reduce levels of anti nutritional factors such as cyanide in cassava According to Iwuoha, (9), the improved functional characteristics of the flour are ultimately transferred to the recipient food systems. In the current study, peeled cassava chunks were steeped in varying concentrations of citric acid for a period of time, the resultant flours were used in different ratios with 100% wheat flour in bread making; and the baked loaves were subjected to sensory evaluation.

Materials and Methods

Cassava roots (TMS 30572) were harvested from the farm of Federal University of Technology, Owerri, Nigeria; peeled, washed and cut into chunks (5 cm thickness).

The chunks were steeped in previously prepared citric acid solution in five concentrations (SSC), (1.0, 5.0, 10.0, 15.0 and 20.0 % M/V) at loading rate of 1: 2 mass: volume. The steeping was carried out in plastic containers for a period (RSD) of 120h and samples collected for 24, 72 and 120h. The steeped out was further size reduced to 5mm thickness, oven dried at 65^{o}C, milled and sieved to pass 250µm and stored in cellophane bags.

Bread making

The straight dough method was used as modified by Onabolu *et al*. (12). Wheat flour was diluted with cassava flour at the ratios 90: 10, 80: 20, and 70: 30; the composite flour and other bread making ingredients (yeast, shortening, salt, sugar and water) were mixed in bowl mixer initially at low speed and later at high speed for the desired consistency. The dough was further kneaded, moulded, transferred into greased pans for proofing (for 45 min.) in a warm chamber at 43^{o}C. The proofed dough was transferred into the oven to bake at 180 - 200^{o}C and removed after baking; cooled at ambient temperature and wrapped.

Sensory evaluation

Ten member panelists drawn from usual bread consumers were used to assess the quality attributes of the baked loaves (for crumb texture, loaf volume, taste and overall acceptance). The samples were presented to with coded letters in identical white plates. The panelists were instructed to assess the samples based on 9-point hedonic scale ranging from (9)-like extremely to (1) disliked extremely as described by Ihekoronye and Ngoddy (7).

Statistical analyses of data

The scores of the quality attributes of the bread as a function concentration of citric acid (SSC) (5), root steeping duration (RSD) (3) and composite ratio (3) were fitted into a 5x 3x3 factorial experimental design and subjected to three-way ANOVA as described by Steel and Torrie (16). The means were separated using the least significant difference (LSD).

Results

The data in Table 1.0 shows the quality attributes of bread as affected by steeping concentration of citric acid solution. The loaf volume was significantly affected ($p<0,05$) by the percent increase in the citric acid solution. The bread from 20.0% SSC, had the highest loaf volume (6, 32) while the least mean score (4.12) was recorded for 1.0% SSC.

The taste of the bread was significantly affected ($p< 0.05$) by the increase of in citric acid solution. The highest mean score (5.16) was obtained for 20.0% SSC while 1.0%SSC gave the score (3.84).

Similarly the crumb texture of the bread increased significantly ($p<0. 05$) with increasing concentration of citric acid as the highest crumb texture of 5.79 was recorded for 20.0% SSC.. On the whole the panelists rated the bread from 20.0% as the best (6.22) followed by 15,0% (5.70) while the 1.0% SSC as least preferred with mean score of 4.19 in the overall acceptance.

The impact of composite ratio on bread quality

The data on the bread quality as affected by the composite ratio is shown in Table 2. The bread from 90:10, wheat/cassava composite flour had highest score for loaf volume, 6.25 followed by 80: 20, 4.99; while the 70: 30 had the least, 4.28.these values differed significantly under the condition of study $P< 0.005$.

The taste of the bread from 90:10 was preferred by the panelist (5.46) than the rest as shown in Table 2.0.

The 90:10 composite ratios resulted in high crumb texture, 6.03, followed by 80:20, 4.88, and 70:30, 3.93; these also differed significantly under the condition of study $P< 0.005$.

On the whole the panelist preferred the bread from the 90:10 ratios than the rest as shown in Table 2.0.

The impact of steeping duration in citric acid solution on the bread quality

The data in Table 3.0 show the effect of duration of steeping on sensory quality of bread. The loaf volume increased with increasing steeping duration. The highest score of 5.81was recorded for 120h while the least was obtained for 24h.

On the other hand, the panelists preferred the taste of bread from the 24h steeping duration, (4.69) followed by 72h, 4.49 while 120h had the least 4.26, these however differed significantly at $p< 0.05$.
The crumb texture of the 120h fermented had best rating 5.93, followed by 72h, 4.83 while the least value 4.08 was recorded for 24h as shown in Table 3.0.

Table 1: Mean scores of bread as affected by strength of citric acid solution

SSC % m/v	Loaf volume	Taste	Crumb texture	Overall acceptance
1.0	4.12 ± 1.03^{e}	3.84 ± 0.76^{e}	4.13 ± 1.34^{e}	4.19 ± 0.87^{e}
5.0	4.68 ± 0.93^{d}	4.02 ± 0.77^{d}	4.42 ± 1.21^{d}	4.69 ± 0.96^{d}
10.0	5.18 ± 1.03^{c}	4.48 ± 0.86^{c}	4.82 ± 1.19^{c}	5.30 ± 0.85^{c}
15.0	5.56 ± 1.08^{b}	4.89 ± 0.82^{b}	5.39 ± 1.10^{b}	5.70 ± 0.80^{b}
20.0	6.32 ± 0.92^{a}	5.16 ± 0.77^{a}	5.79 ± 1.00^{a}	6.22 ± 0.92^{a}
LSD	0.26	0.17	0.20	0.23

Means with uncommon superscripts letters of alphabets within the column differed significantly at $p < 0.05$

Table 2: Mean scores of bread as affected by percent composite ratios

Composite ratios(%)	Loaf volume	Taste	Crumb texture	Overall ac2ceptance
90:10	6.25 ± 0.99^{a}	5.46 ± 0.59^{a}	6.03 ± 1.07^{a}	6.20 ± 0.89^{a}
80:20	4.99 ± 0.91^{b}	4.38 ± 0.56^{b}	4.88 ± 091^{b}	5.18 ± 0.81^{b}
70:30	4.38 ± 0.96^{c}	3.60 ± 0.54^{c}	3.60 ± 0.97^{c}	4.28 ± 0.88^{c}
LSD	0.20	0.13	0.15	0.18

Means with uncommon letters of alphabets within the column differed significantly at $p < 0.05$

Table 3: Mean scores of bread as affected by duration of steeping in citric acid solution

Steeping duration (h)	Loaf volume	Taste	Crumb texture	Overall acceptance
24	4.51 ± 1.16^{a}	4.69 ± 0.08^{a}	4.08 ± 101^{c}	5.18 ± 0.81^{a}
72	5.21 ± 1.19^{b}	4.49 ± 1.05^{b}	4.83 ± 1.09^{b}	4.65 ± 1.04^{b}
120	5.81 ± 1.05^{c}	4.26 ± 0.84^{c}	5.93 ± 1.07^{a}	4.28 ± 0.88^{c}
LSD	0.26	0.17	0.20	0.23

Means with uncommon superscripts letters of alphabets within the column differed significantly at $p < 0.05$

Discussion

It was found that the loaf volume increased with corresponding increase in steeping solution concentration (SSC) which may suggest that the steeping solution (citric acid solution) modified the functional properties of cassava flour. It might as well be that the absorbed citric acid enhanced the activity of gluten in the wheat flour portion in the mix. Citric acid is a raising agent and its role as a flour improver has been reported by Smith (15).

The rating of bread from 20% SSC as the best in terms of taste in Table 1 might be that citric acid influenced the taste. The use of citric acid as a flavour enhancer in food systems has been reported by Macrae *et al.* (10). Citric acid is known for its ability to impact flavour, chelate heavy metals and deliver a "burst" of tartness in the recipient products.

The observed increase in crumb texture with corresponding increase in SSC% might be due to citric acid absorbed in cassava flour which enhanced the development of the texture of the bread. Citric acid has for long been used in the development of textural properties of food (10).

The ratio of flour composites was found to influence the sensory properties of bread. The highest loaf volume obtained in Table 2, for 90: 10, reflected the high content of gluten in the wheat flour portion which shows the superiority of wheat flour over other flour sources in bread making (3)
On the other hand, the high rating of the bread taste with the composite ratio may be associated with the complementary effect of citric acid in cassava flour.

Similar performance in crumb texture by 90: 10 ratios reinforces the decision of policy makers in Nigeria that millers should incorporate 10 percent cassava flour in bread making.

Steeping duration increased the loaf volume and crumb texture in Table 3. The highest loaf volume obtained for 120h (5.81) might suggest that more of the citric acid solution was absorbed with the resultant improvement in loaf volume and crumb texture.

The rating of taste by the panelist decreased as the steeping duration increased. The highest score obtained for 24h steeping duration (4.69) may suggest that when steeping in citric acid is a desirable step in cassava flour manufacture, it would be economically and technologically reasonable to limit the steeping duration to 24h. This is also supported by the highest rating of overall acceptance (5.18) for the steeping duration of 24h in Table 3.

Conclusion

The use of composite flour in bread making and other baked goods has become imperative for developing countries going by increasing cost of imported wheat. Steeping is a sure method of removing contaminants (residual cyanide) in food. Moreover, steeping in citric acid solution would play complementary roles as a modifier of texture, raising agent and as well as flavour enhancement which have been shown by the outcome of the investigations. It is deduce from the study that steeping for a period not exceeding 24h will give the best functional effect to baked goods. Finally steeping cassava in citric acid solution before milling is likely going to increase the percent ratio of cassava flour used in bread making and enhance the contribution of cassava to the nutritional wellbeing of developing countries. Other processing variables should be investigated and employed in improving the functionality of cassava flour.

Correspondence to:
Owuamanam C. I.
Department of Food Science and Technology,
Federal University of Technology,
P. M.B 1526 Owerri Imo State Nigeria.
E- mail icliffowums@yahoo.com

Received: 5/10/2007

References

1. Asselbergs, E.A. (1973). The FAO composite flour program documentation package 1:5-6 FAO Rome.
2. Bokanga, M. and Tewe O.O. (1998) Cassava aprremium raw material for food, feed industrial sectors in Africa. In: post harvest Technology and commodity marketing, proceeding of a post harvest conference (Ferris, R. S.B. ed.) 2 Nov-1 Dec. 1995, Accra Ghana. IITA, Ibadan.
3. Bushuk, W. (1996) Wheat chemistry and uses. Cereal Food World 31: 218-228.
4. Delfloor, I. (1995) Factors affecting the bread making potential of cassava flour in wheatless bread recipes. Ph.D dissertation Kathnolieke University, Lueven. In: Cassava Transformation, Africa's Best Kept Secret (Nweke, F.I., Spencer, D.S.C. and Lynam, J.K.(eds)). Michigan University Press. East Lansing. PP171.
5. Dendy, D.A.V. and Trotter (1988). Wheatless and composite technology awaiting adoption. Entwicklung und Landlicher Raum 86: 13-18.
6. Eggleston, G and Omoaka, P. (1994) Alternative breads from cassava flour In: Proc. Of the 9th Symposium of the International Society for Tropical Root Crops 20-26 Oct, 1991 Accra, Ghana (Ofori, F and Hahn, S. K. eds) IITA IBadan 243 - 248
7. Ihekoronye, A. I. and Ngoddy, P. O. (1985). Integrated Food Science and Technology for the Tropics Macmillan Pub Ltd London 270 – 281.

8. Iwe, M. O. (2003). The Science and Technology of Soybean Chemistry, Nutrition, Processing and Utilization. Region Communications Services, Enugu
9. Iwuoha, C. I. (2004). Comparative evaluation of physicochemical characteristics of flours from steeped tubers of white yam discorea rotundata poir, water yam (Discorea cayenensis lam). Tropicultura 22 (2): 56 – 63
10. Macrae, R., Robinson, R. K. and Sadler, M. J. (1993). Encyclopaedia of food science and technology and nutrition. Academic Press pp 734 – 743.
11. Okaka, J. C. (1997). Cereals and legume storage and processing technology. Breadmaking technology. Data and micro systems pub. Enugu Nigeria pp 79.
12. Onabolu, A. Abass, A. and Bokanga, M (2003). New food products from cassava. IITA Ibadan pp 1 – 26
13. Raw Material Research and Development Council RMRDC (2004) Report on survey of Agro Raw Material in Nigeria, Fed. Min. of Sci. and Tech. Abuja (median ed.) pp 99.
14. Satin, M. (1988). Bread without wheat. New Scientist, April 28, pp 56 – 59
15. Smith J. (1991). Food additives users' handbook. Blackie and Sons Ltd. pp 59 – 61.
16. Steel and Torrie, J. H. (1980) Analysis of variance111: factorial experiment In: principals and procedures of statistics A biometrical approach. 2nd edn. McGraw-Hill Intl. coy, London pp 336-376.

Ion implantation damage in GaN layers investigated by an ellipsometric method

B. Bouafia[1], Dj. Boubetra[2]

Optics Laboratory, Setif University 19000 Algeria, Centre Universitaire Bordj Bou Arreridj 34000 Algeria
E-mail: boubetra@gmail.com

Abstract: Ion beam damage in semiconductors is connected with marked changes in dielectric function. In the low energy range, the damage is localized to a thin surface layer and the optical properties are sensitive to the ion species and energy and to the dose implanted. This can be detected by ellipsometric measurements. To show this, a section of an Ar ion beam was recorded by scanning ellipsometry of GaN/GaAs and GaN/Si that had been exposed to 500 eV-3000 eV ion beam. For more detailed analysis, it is necessary to develop a suitable layer Model that can be fitted to the ellipsometric data. Such a procedure allows to restore the depth resolution, which is normally not an intrinsic feature of ellipsometry**.** [Nature and Science. 2007;5(4):29-33].

Keywords: Ion beam damage, Ellipsometry, Implantation, Amorphization

1. INTRODUCTION

Radiation damage theories are based on the assumption that a lattice atom struck by an energetic atom must receive an amount of energy to be displaced from its lattice site. Therefore, the deposited ion energy can be used as well as the number of the produced defects [1]. It is well know that the most used theory of ions transport in the matter is the LSS Theory [2]. According to this theory, the ion range has Gaussian distribution with projected range Rp, and projected range straggling R.

The investigation of implantation parameters (ranges, straggling, and damage distributions) requires methods with a depth resolution in the order of monolayers. Ellipsometry is such a method, even suited to enlighten details of the collision processes, because ion implantation often causes changes in the optical state of the target (especially in the case of semiconductors).

The amorphization of semiconductors crystal by ion implantation [3, 4, 5] or by deposition [6, 7] with marked changes of the dielectric function wich can be detected with a high sensitivity by ellipsometry. In the low-energy range, the damage is localized to a thin surface layer. For a more detailed analysis of ion target-interactions, it is necessary to develop suitable multi-layer model that can be fitted to the experimental data [5, 8-10]. Such a procedure allows to restore a depth resolution, which is normally not an intrinsic feature of ellipsometry.

It will be shown in the presented paper, that using special developed model [11] and ellipsometric measurements these changes can provide informations about relevant parameters of the amorphization process as the amorphization state and the critical concentration.

The method will be demonstrated here for the case of low-energy argon implantation in gallium nitride on gallium arsenide and on silicon. Gallium nitride on arsenide alloys and silicon is promising for optoelectronic devices working in the visible wavelength zone [12].

2. EXPERIMENTAL

Gallium nitride samples with GaN thicknesses of about 600 nm to 900 nm were implanted with argon ions from a Kaufman-type source with energies from 500eV to 3000eV. GaN layer thickness and ion energy have been adjusted that the maximum of the range distribution was located in the interface. The value of the ion dose determines the kind of the buried damaged layer (below or above the amorphous threshold, voids) and its extent in the depth.

The GaN films were fabricated by reactive magnetron sputtering in Ar 99,99% - N_2 99,99% gas mixture. A 99,99% purity Ga was used as target. The start pressure was 10^{-3} Pa. The substrate was located at 50 mm downstream from the target. The films were deposited at 0,6Pa. The partial pressure N2/Ar was 1,75. The substrates used in these experimental work were quartz for transmission measurements and GaAs with (100) orientation, ($n=2.10^{17}cm^{-3}$) and Si with (111), orientation ($n=1.10^{18}cm^{-3}$) for ellipsometric investigations.

The structure of the sample was investigated by X-ray diffraction. The analysis shows an amorphous structure of the GaN layer at ambient temperature. The GaN Layer does not show a luminescence.

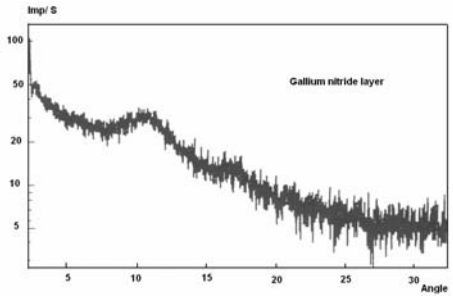

Figure 1. X-ray diffraction diagram of reactive sputtered GaN layer is the figure caption.

Experimental results of optical transmission as function of wavelength of GaN/quartz film with quartz substrate as reference is shown in Figure 2. The interferences maxima in spectra. Curves are located very closely. This indicates that GaN has very high transmission and possess low absorption in the visible a part of the spectrum (λ>400 nm). As indicated in Fig.2 the average transmittance of GaN film is about 85%.

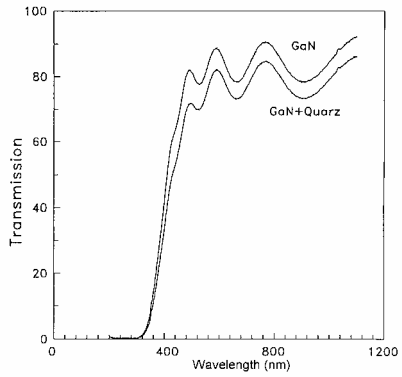

Figure 2. Optical transmission of gallium arsenide in dependence of the wavelength..

The ellipsometic measurements were accomplished using rotating analyzer ellipsometer (Sentech Instruments, Germany) with the fixed laser wavelength 632,8 nm (1,96eV). The angle of incidence has been chosen to 70° at this angle the laser spot is elliptical with an area of about 6 mm^2. Some measurements at other angles were only performed to verify the model. The measuring results of ellipsometry are available in the form of the ellipsometric angles ψ and Δ that are correlated with the amplitude and the phase of the complex reflectance ratio:

$$\rho = \frac{r_p}{r_s} = \tan\psi e^{i\Delta} \qquad (1)$$

where r_p and r_s are the reflection coefficients of the p- and s-polarized components.

3. Results and analysis

The amorphization behaviour has been analyzed by developed optical model. The model used here concerns the lower and medium dose range, I.e, doses below the threshold of Ar void formation. In the model, it will be assumed that the maximum of the damage depth distribution is located not far from the interface (for example GaN/GaAs) and that the distribution can be approximated by a Gaussian (Fig. 3). The first condition is well satisfied in the chosen energy range for GaN layer thicknesses. The approximation of the damage distribution by a Gaussian is quite good, because only the part in the GaAs

respectively Si must be considered attributed to the missing optical influence of ion bombardment in the GaN.

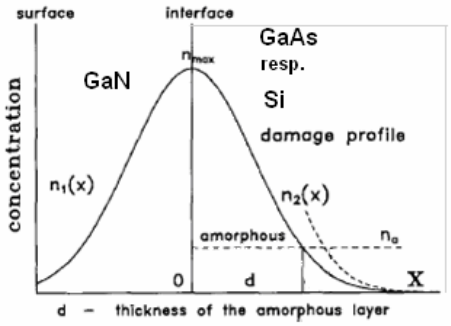

Figure 3. Schematic diagram of the damage distribution ray diffraction diagram of reactive sputtered GaN layer

Two regions can be distinguished (see fig.4). First, the region of highly damaged GaAs respectively Si above the amorphization threshold, which results in an optical homogeneous layer with the refractive index $\tilde{n} = n - ik$ for amorphous semiconductor, even though the argon ions and the displacement events are not homogeneously distributed. Second, the region that is influenced by the tail of the argon depth distribution. Since no complete amorphization is reached in this region, $\tilde{n} = n - ik$ will change depending on the depth [13].

The thickness d of the amorphous layer d is given by the parameters of the damage distribution. If the maximum of the assumed Gaussian damage distribution is exactly located in the interface, d^2 is simply given by:

$$d^2 = 2\delta^2 \ln \frac{n_{\max}}{n_a} = 2\delta^2 \ln \frac{D}{D_a} \qquad (2)$$

while δ is the standard deviation of the damage depth distribution, n_{max} the maximum concentration of the defects, n_a the threshold defect concentration of (optical) amorphization, D the ion dose, and D_a the amorphization dose leading to $n_{max} = n_a$.

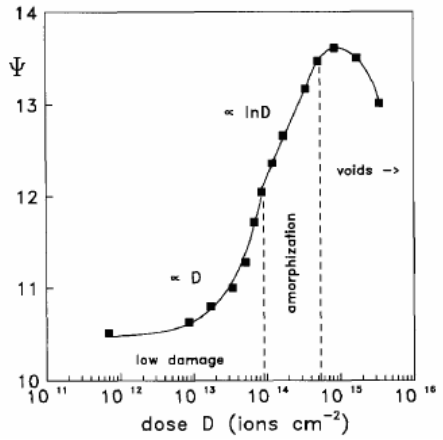

Figure 4. Measured Ψ values for the 1500 eV implantations in dependence on the Ar ion dose

From ψ and Δ values both the thickness and the complex refractive index $\tilde{n} = n - ik$ of the respective amorphous zone can be derived by fitting model calculations to the measure values. Concerning the amorphization behaviour, the thickness of amorphous GaAs has been found 8 nm. For amorphous GaAs the refractive index value $\tilde{n} = 4.30 - i0.70$ was an acceptable fit for all values investigated here.

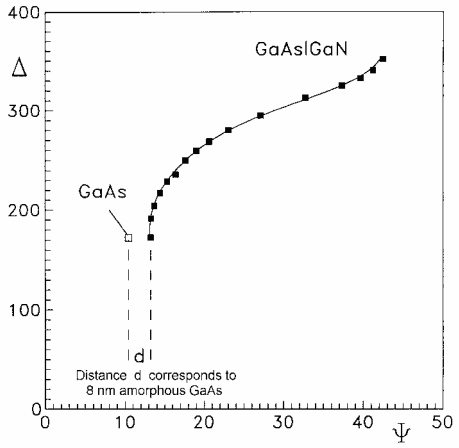

Figure 5. Experimental ellipsometric ψ and Δ curve

This complex refractive index is characterized by comparatively high n and k values compared with crystalline GaAs ($\tilde{n} = 3.85 - i0.19$), which are typical of amorphous GaAs created by ion damaged [14] or deposition [6]. The here found refractive index agrees within some percent with the reported values.

4. Conclusion

It has been shown that one wavelength ellipsometry has proved to be sufficient to characterize the amorphization by low energy, in contrast to methods that use spectroscopic ellipsometry. Statements to ion damage distributions and amorphization thresholds are possible in principle.

It was the intention of this paper to present a method consisting of ellipsometric measurements combined with a model that is easy to handle and that allows to determine ion implantation damage depth at low ion energies.

ACKNOWLEDGEMENTS

This work was supported in part by Deutsche Akademischer Austausch Dienst – Germany.

CORRESPONDENCE AUTHORS:
B. Bouafia, Dj. Boubetra
Optics Laboratory
Setif University 19000 Algeria
Centre Universitaire Bordj Bou Arreridj 34000 Algeria
E-mail: boubetra@gmail.com

Reveived: 11/10/2007

REFERENCES

1. H. Ryssel and I. Ruge, *Ionenenimplantation*,(GeestPortig K.- G, Leipzig, 1978).
2. J.Lindhard, M.Scharff and H.E. Schiott, Range Concepts and Heavy Ion Ranges (Notes On Atomic Collisions, II)*Mat. Fys. Medd. Dan. Vid. Selsk, 33 (1963).*
3. M. Fried., T. Lohner, W.A.M Aarnink, L.J. Hanekamp, and A. van Silfhout,.J. Appt. Phys. 71, 2835 (1992).
4. T. M. Burns, S. Chongsawangvirod, J. W. Andrews, E.A. Irene, G. Mc.Guire, and S. A. Chevacharoeukul, J. Vac. Sci. Technol. 89, 41 (1991).
5. Y.Z. Hu, J-W. Andrews, Li M. and E-A. Irene, In situ spectroscopic ellipsometric investigation of argon ion bombardment of single- crystal silicon and silicon dioxide films *Nucl. Instr.. Methods Phys. Res. B59/60, 76. (1991).*

6. X. M.Teng , H. T. Fan, , S. S. Pan, C.Ye, and G. H. Li,, Optical properties of amorphous $GaAs_{1-x}N_x$ film sputtering with different N_2 partial pressures, *Journal of Vacuum Science & Technology A:Vacuum, Surfaces, and Films -- September 2006 -- Volume 24, Issue 5, pp. 1714-1717 (2006).*

7. I. V. Rogozin, and A. N.Georgobiani,, Bulletin of the Lebedev Physics Institute 34, 114 (2007).

8. T. Miyazaki and S. Adachi, Spectroscopic Ellipsometry Study of Si Surfaces Modified by Low-Energy Ar^+-Ion Irradiation, *Jpn. J. Appl. Phys. Part1 A32,4941 (1993).*

9. G.F. Feng, R. Zallen, J.M. Epp and J.G. Dillard, Raman-scattering and optical studies of argon-etched GaAs surfaces , *Phys. Rev. B 43, 9678 (1991).*

10. M.Gal, P. Kraisingdecha and C,Shewe, *SPIE Proc, 2141, 88 (1994).*

11. M. Bouafia, N. Moussaoui, Dj. Boubetra, L.Bouamama, and D.Bouzid, Mathematical modelling of amorphous layers growth by low energy ion implantation, *Proc.OASIS,Algeria.(2006)*.

12. S.Nakamura, , M.Senoh, , S.Nagahama, ,S. Iwasa, T.Yamada, , T.Matsushita, H.Kiyoku, and Y.Sugimoto, *InGaN-Based Multi-Quantum-Well-Structure Laser Diodes Jpn. J. Appl. Phys. 35, L74 (1996).*

13. T.Motooka, K. Watanabe, Damage Profile Determination of Ion-Implanted Si Layers by Ellipsometry, J. Appl. Phys-- Volume 51, Issue 8, pp. 4125-4129 (1980).

14. G.E. Jellison,. Optical functions of GaAs, GaP, and Ge determined by two-channel polarization modulation ellipsometry *.Jr.OPT. MATER 1, 151 (1992)*.

Correlation Research of the Directors Capability and the Corporate Governance Performance of Chinese Listed Companies

Zhang Jianying, Duan Yun

School of Management, Harbin Institute of Technology, Harbin, Heilongjiang 150001, China
Email: zzjjyy0757@sina.com
Telephone: 01186-451-8641-4011

Abstract: At present，the transformation of corporate governance is a basic problem that china is facing. Board is the heart of the corporate in a modern enterprise's organization，so a probe into the capability of directors has practical significance to the governance of listed corporation. In this article we give a relevance analyze between the performance of corporate governance and the capability of directors by the means of data statistic，with the aim that it can show the demonstrability that the domination assignment in our country should be based on the ability of the directors，so that we'll have a rational board structure which can give us a better corporate Performance. [Nature and Science. 2007;5(4):34-42].

Keywords: Listed corporate, The capability of directors, Corporate governance, Performance

1. Introduction

Nowadays with the economic globalization, the development of China Capital Market is depended on the quality of the listed companies to a great extent. We are facing the topic for discussion about how to enhance the governance quality and international competency. Although a lot of attention is focused on the maturity of governance structure and principle in academic area, the most significant factor of corporate governance, the executive, is neglected. Therefore, it is not the right way to the problem. After building the system of basic modern enterprise, the board will become the key factor of corporate governance. Under the background of economic system switcher, there are still some problems in the board of listed company in China, which concentrates in the following aspects: 'Along One' state-owned stock, unreasonable structure board of directors, the bureaucratic mechanism of the board and the disqualified capability of board directors. Among these, the capability of board directors, the inner factor, plays as the decision function to the performance without any doubt. Therefore, the key points of corporate administrations are the follows: taking the board of directors as the reform objective point, obtaining from director's capability and adjusting board of directors' capability to match the governing structure to improve the governance and enhances the company benefit.

2. The capability of directors in the listed company and the performance of corporate governance

The capability of directors means the whole capability and knowledge of directors to effectively implement leadership and achieve the targets of enterprise. We can say that the capability of directors is directly and specifically related to the future of company. Hence, the directors must be equipped with all kinds of capabilities which are applicable in extensive kinds of jobs. In other words, they should be combined with noble moral and excellent talent. The directors compose the board, and therefore, the board is the key of corporate governance in the listed companies. Different academies will divide the board into different structure according to their researches. The one that is more authoritative is the definition under entrusting and agency theory. It concludes that the portion and quality of exterior directors and independent directors, the non-duality of chairman and chief executive officer, audit office subordinated to board of directors and so on. According to the characters of China and China state-owned companies, the author holds that the components of board including the state-owned stock agent (state-owned director), the enterprise agent (enterprise director), the operator and the independent director constitutes. Directors' capability of Board and reasonable match of each constituent part have significant and decisive influence on company performance without doubt.

Performance means the approved working behavior, procession and result of employees. Speaking of the organization, the performances are the competition situations of mission in aspects quantity, quality and efficiency. The analysis of performance of corporate governance is according to some indexes to valuate and assess the structure and benefit of corporate governance, which is based on the Idea, principle and system of corporate governance, the system of justice and the notion about culture and value in each

country[1]. In this article, the author assesses the two main factors which can valuate the performance, stock value and directors capabilities, based on the need of research. And the author tries to demonstrate the promotion utility of reasonable match of capabilities to the corporate performances, which is based on the correlation between stock and directors' capabilities①.

Table 1. The standard of appraisal of directors' capabilities

Index	Standard and number
Magnificent	Very Important—1, Normal Important—2
Rank	Excellent—10，Good—8，Medium—6，Bad—4，Worsen—2

3. The correlation between directors' capabilities of listed companies and corporate performances

The author picks out 39 companied from the Shanghai Stock Exchange as the sample② and analyze the relationship between directors' capabilities[2]. The specific procedures are as follows:

3.1 The qualification and quantification of the evaluation of directors' capabilities

(1) The qualification of evaluation of directors' capabilities

The author qualitative appraisal the capability of directors in the following ways: the first one is the moral capability; the second one is the decision capability. The specific contents include the follows

Directors' capabilities

- Moral capability: Legal consciousness, wealth view, team cooperation, political quality, self-idea, risk consciousness, benefit view, value and
- Decision capabilities: Financial decision-making, strategic decision, market decision-making, physical distribution decision-making, human affairs decision-making, purchase decision-making, industrial decision-making, information decision-making, investment decision-making, production decision-making and so on

(2) The quantitative appraisals of directors' capability

The author utilizes the method of expertise's valuation to appraise the capabilities after deciding the index. Through proof reading, questionnaire and personal conversation, the expertise group appraises the personal capabilities of each directors based on the appraisal standard, and then utilizes the following formula to get the moral capabilities f_1, decision capability f_2, personal capabilities of each director f. The formula to compute director's capability is as follows

$$f_1 = \frac{\sum_{i1=1}^{n_1} d_{i_1} b_{i_1}}{n_1} \tag{1}$$

$$f_2 = \frac{\sum_{i2=1}^{n_2} d_{i_2} b_{i_2}}{n_2} \tag{2}$$

$$f = f_1 + f_2 \tag{3}$$

The b means the significance of each qualification index of capability; d is the rank to it and n is the number of index.

3.2 The correlative analysis between the components of board and corporate performances

During the corporate governance, it is the board rather than the respective directors who is the key of corporate governance. Therefore, the author further analyzes the impact of components of the board on the corporate performances. Based on the above analysis, we can see the value F of each component of the board.

$$F = \frac{\text{The sum value of various directors } (f)}{\text{Number of Directors}} \times 10 \quad (4)$$

After computing, the specific data are the following in table 2[③]:

Table 2. The value of each component of the board

Name of Company	Stock value	State trustee(F_1)	enterprise trustee (F_2)	operation (F_3)	Independent trustee(F_4)
YYRJ	84.1	10.5	16.8	20	14.7
LXQX	83.2	10.4	16.6	20	12.4
TTYY	82.3	12.4	14.5	20	14.7
XZTL	82.1	9.8	14.3	18.9	16.2
TTGF	81.7	8.9	12.5	20	14.6
SGJX	81.4	8.7	16.1	20	14.4
ZXTX	80.9	8.6	14.1	20	13.3
JDAL	80.9	8.4	13.8	19.6	14.2
GYGS	80.9	7.9	13.7	20	15.4
QJZY	80.6	7.9	13.8	20	15.8
GZKG	80.5	8.9	14.1	18.8	12.9
SZGX	80.1	9.0	13.1	19.2	14.1
HCGF	80.1	8.4	13.6	20	13.8
MSYH	80.1	11.5	12.7	20	11.4
NHGS	80	12	12	19	10.9
NHFZ	79.9	7.9	11.3	18.9	13.4
SHYY	79.9	8.0	10.6	17.8	13.8
QJSL	79.9	8.4	11.8	18.4	12.6
GLLY	79.9	11.2	12.4	17.1	10.9
MTKJ	79.9	11.3	12.5	16.8	10.7
YHKJ	79.8	11.3	12.5	16.9	10.7
HRZY	79.8	11.2	12.3	17.2	10.3
SCGF	79.7	11.1	12.1	17.8	10.6
KMZY	79.7	11.2	12.4	16.9	10.4
DSGF	79.6	9.8	11.6	18.1	10.1
GHYX	79.6	9.8	10.1	18.1	11.6
LRGF	79.6	9.4	10.9	18	11.1
HJGF	79.6	9.3	10.5	18.3	11.5
SDLH	63.4	8	11.2	15	11
DAAJ	63	7.4	11	15	11.2
STLJ	62.9	7.3	10.7	15.1	11.1
BMGF	58.8	7.1	10.2	14.8	10.8
DLCS	58.8	7.0	10.0	14	12.1
DRGF	58.8	7.0	10.0	14	12.1
JFTZ	56	6.8	8.7	16	15.2
ZJGS	55.8	6.7	8.8	15.9	15.1
MNRY	55	6.5	8.3	16	15.0
KLDQ	53	6.2	8.1	15.4	14.9
YNDL	52.3	6.0	8.8	14.7	14.3

The author utilizes these data to compute the Pears' Correlation r_s [3] and gets the results in Table 3. Then he inspects these data by the Z exam in statistics. The r_s is:

$$r_s = 1 - \frac{6\sum d^2}{n\left(n^2 - 1\right)} \tag{5}$$

Z is the following:

$$z = \frac{r_s - 0}{\frac{1}{\sqrt{n-1}}} \tag{6}$$

Table 3. Pears correlation result

	Stock value	State director	Enterprise director	Operators	Independent director
correlation	1.000	. 566**	. 941**	. 894**	. 243
Significance	.	. 000	. 000	. 000	. 136
N	39	39	39	39	39

PS: The significance is 0.05

Based on the table above, we can see that all of state directors, enterprise directors, operators and independent directors have absolutely positive correlation with stock value ($0 < r_s = 0.556, 0.941, 0.894, 0.243 < 1$). Moreover, the state directors, enterprise directors and operators have a higher correlation with the stock values ($0.5 < r_s = 0.556, 0.941, 0.894 < 1$), especially the enterprise trustees. Therefore, we can say that the directors are excellent and qualified in the listed companies with good achievements, vice verse.

3.3 The correlative analysis between capability of board and corporate performance

The performances of listed companies have the positive relationship with the components of board. Then, we can analyze the relationship between capability of the whole board and the corporate performances.

Y stands for the stock value, Dependent variable, and *X* stands for the capability of the board, variable. And *X=F1+ F2+ F3+ F4*, so we get table 4:

Table 4. The relationship between capability of whole board and corporate performances

Name of Company	Stock value （Y）	（X）	X*X	X*Y	Y*Y
YYRJ	84.1	62	3844	5214.2	7072.81
LXQX	83.2	59.4	3528.36	4942.08	6922.24
TTYY	82.3	61.6	3794.56	5069.68	6773.29
XZTL	82.1	59.2	3504.64	4860.32	6740.41
TTGF	81.7	56	3136	4575.2	6674.89
SGJX	81.4	59.2	3504.64	4818.88	6625.96
ZXTX	80.9	56	3136	4530.4	6544.81
JDAL	80.9	56	3136	4530.4	6544.81
GYGS	80.9	57	3249	4611.3	6544.81
QJZY	80.6	57.5	3306.25	4634.5	6496.36
GZKG	80.5	54.7	2992.09	4403.35	6480.25
SZGX	80.1	55.4	3069.16	4437.54	6416.01
HCGF	80.1	55.8	3113.64	4469.58	6416.01
MSYH	80.1	55.6	3091.36	4453.56	6416.01

NHGS	80	53.9	2905.21	4312	6400
NHFZ	79.9	51.5	2652.25	4114.85	6384.01
SHYY	79.9	50.2	2520.04	4010.98	6384.01
QJSL	79.9	51.2	2621.44	4090.88	6384.01
GLLY	79.9	51.6	2662.56	4122.84	6384.01
MTKJ	79.9	51.3	2631.69	4098.87	6384.01
YHKJ	79.8	51.4	2641.96	4101.72	6368.04
HRZY	79.8	51	2601	4069.8	6368.04
SCGF	79.7	51.6	2662.56	4112.52	6352.09
KMZY	79.7	50.9	2590.81	4056.73	6352.09
DSGF	79.6	49.6	2460.16	3948.16	6336.16
GHYX	79.6	49.6	2460.16	3948.16	6336.16
LRGF	79.6	49.4	2440.36	3932.24	6336.16
HJGF	79.6	49.6	2460.16	3948.16	6336.16
SDLH	63.4	45.2	2043.04	2865.68	4019.56
DAAJ	63	44.6	1989.16	2809.8	3969
STLJ	62.9	44.2	1953.64	2780.18	3956.41
BMGF	58.8	42.9	1840.41	2522.52	3457.44
DLCS	58.8	43.1	1857.61	2534.28	3457.44
DRGF	58.8	43.1	1857.61	2534.28	3457.44
JFTZ	56	46.7	2180.89	2615.2	3136
ZJGS	55.8	46.5	2162.25	2594.7	3113.64
MNRY	55	45.8	2097.64	2519	3025
KLDQ	53	44.6	1989.16	2363.8	2809
YNDL	52.3	43.8	1918.44	2290.74	2735.29
TOTAL	2893.6	2008.7	104605.9	150849.1	218909.8

Based on the data above, we can get the following

$$S(XY)=\sum_{i=1}^{39}X_iY_i-39\overline{XY}=1813.841$$

$$S(XX)=\sum_{i=1}^{39}(X_i-\overline{X})^2=1147.559$$

and

$$\hat{b}=S(XY)/S(XX)=1.580608$$

$$\hat{a}=\overline{Y}-\hat{b}\overline{X}=-7.21455$$

Get the linear formula

$$Y=\hat{a}+\hat{b}X=-7.21455+1.580608X \quad (7)$$

Table 5 is the statistic result of SPSS.

Based on the above analysis, we can get to know that the higher the capability of board, the higher the stock value. There is the positive correlation between capability of whole board and corporate achievements.

Table 5. Coefficient Table

Model	Non-standard coefficient		Standard coefficient	T	Standard error
	coefficient	Standard error	Coefficient		
constant	-7.215	9.244		-0.78	0.44
X	1.581	0.178	0.824	8.856	0

4. The adjustment and match of directors' capabilities in corporate governance

The corporate governance is one kind of ownership right which is based on the contractual relationship as the implementation foundation, the resources disposition as the implementation content and the board of directors as the governance structure center. Its basic function lies in the surveillance control and the strategic instruction, and essential target lies in between the coordinated correlation main body the benefit to solute the proxy question. Under this situation, the board of directors is in the strategic core of corporate governance of listed companies.

$$F_1 = \frac{\text{The sum of various trustees' value}(f_1)}{\text{Number of Trustees}} \times 10 \quad (8)$$

$$F_2 = \frac{\text{The sum of value of the same kind trustees}(f_2)}{\text{Number of trustees}} \times 10 \quad (9)$$

Based on the former analysis, we can get the conclusion that the difference of capabilities exists in the corporate governance among the listed companies in China: the weak decision capability and moral capability of state directors, the strong decision capability and moral capability of operators, the relative weak decision capability and relative strong moral capability of enterprise directors and the relative strong decision capability and relative weak moral capability of independent directors.

In order to enhance the performances and avoid the above problems, the listed companies should set up the following model

$$P = f[G(r_g, l_g), Q(r_q, l_q), S(r_s, l_s), K(r_k, l_k)] \quad (10)$$

P is the performance of directors, G is the state directors, Q is the enterprise directors, S is the operators, K is the independent directors, r is the moral capability, l is the decision capability.

When P is the max,

$$G(r_g, l_g) = Q(r_q, l_q) = S(r_s, l_s) = K(r_k, l_k) \quad (11)$$

During the governance, it can be done as: keep the balanced relationship among state directors, enterprise directors, operators and independent directors. This means focusing on the interior of board directors. To be specific, it operates as the following: enhancing the moral capability of independent directors, moral capability and decision capability of state directors and decision capability of enterprise directors. Although the capability can be extended infinitely, we should realize that it is a long time to promote the individual capability, which makes the companies draw up a long-term training program. However, there is still a limitation of this model that the moral capability and decision capability, such as the proportion of stocks, are considered in it.

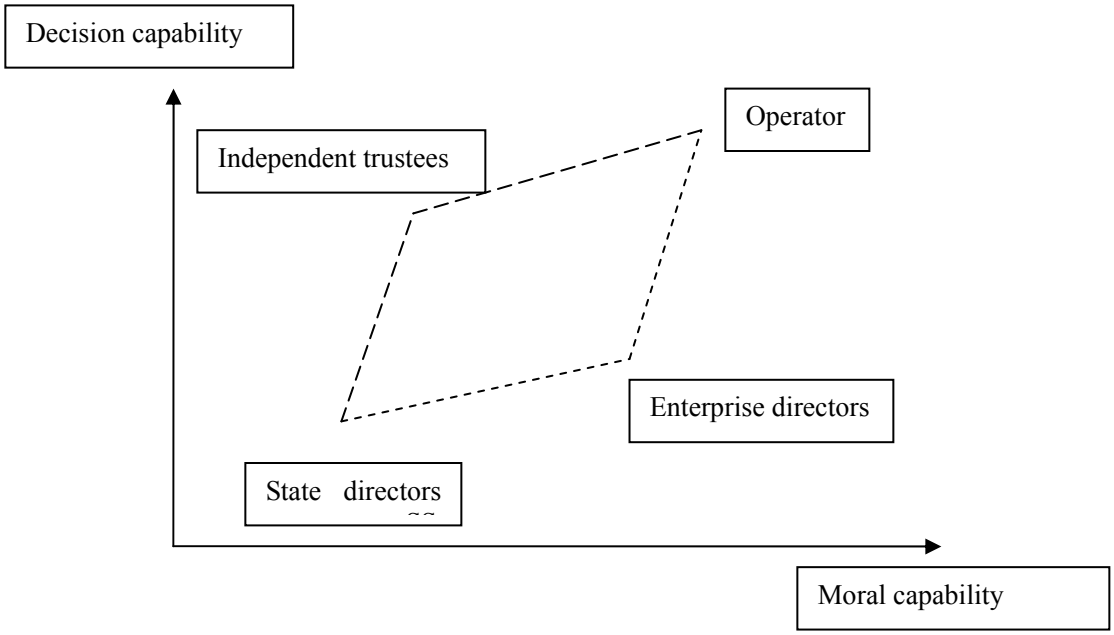

Figure 1. The difference of capability among components of the board

Hence, we need to extend the application of this model. *c* is the proportion of the stocks and *e* is the proportion of seats in the board. Assumed that all of the weak are minus *r* and *l* is constant. Then we can get the following conclusions:

$$P \begin{cases} P_g = (c_g + e_g)(-r_g - l_g) & (12) \\ P_q = (c_q + e_q)(r_q - l_q) & (13) \\ P_s = (c_s + e_s)(r_s + l_s) & (14) \\ P_k = (c_k + e_k)(-r_k + l_k) & (15) \end{cases}$$

From formula (12), we can see because $-r_g - l_g$ <0, so $c_g + e_g$ and P_g .If we want to increase the value of P_g , we need to reduce the value of $c_g + e_g$. In China, the stocks are highly centralized and state department and state-owned enterprises take up majority of the board. Hence, we can increase the number of other components of the board to reduce the proportion of state directors in the board l_g to solve the problem about the 'Along one' phenomenon and inside controlling, when c_g is unchangeable. When it is inside controlling, the independence of decision is weak. It only stands for the benefit of major stockholder and lacks of diversification[4]. Therefore, the decision capability of the board can be enhanced by the increased number of directors.

From formula (14) and (15), the value of l will increase with the increasing value of $c + e$. We can not doubt about the impact of high moral capability and decision capability of operators on the performances. Hence, we should improve the aspect of operators. That is enhancing the system of limitation and incentives to operators and making the income of operators depend on not only the value of

options but also the price of stocks. This both is advantageous in the reassignment manages superintendent's enthusiasm, and may avoid the short-term plundering behavior which the operator possibly appears, causes them to focus on enterprise's long-term development and the long-term benefit[5]. From the formula (15), we know that $c_k + e_k$ increase with the increasing of $l_k(c_k + e_k)$. Therefore, the number of independent directors should be increased in order to enhance independence of the board and refine the governance performances. This can be supported by the case of Guangzhou Baiyunshan Medicine Production Company which hired two independent directors to appraise the adjustment of production structure and increase its 80% of its profit in 1999. In US, the proportion of independent directors in the listed companies accounts for 62%. Considering about China's situation, the proportion of that should be 30%[6]. However, the formula also provides the information that with the increasing value of $c_k + e_k$ the value of $-r_k(c_k + e_k)$ will decrease. It means that we will face the moral risk with the increasing of independent directors. But there is still no statement about the punishment to the dereliction of duty of independent directors. Hence, the independent director definitely may be bought by other directors or the holding shareholder and violate benefit of the company and other shareholders.

From the formula (13), we know that $\uparrow r_q$, $\uparrow P_q$ and $\uparrow e_q$, $\uparrow r_q$ therefore, we should increase r_q to increase P_q; and if we want to increase r_q, we can increase e_q. In other words, we should employ the advantage of good moral capability when we match the capability of the board. And this provides the ways to avoid the moral risk of increasing the number of independent directors and makes more enterprise directors to go to Board of supervisors. It is said in China's Enterprise Law that the board of supervisors is composed by the shareholder and staff representative with suitable proportion company. The concrete proportion is stipulated by the articles of incorporation. The staff represent in board of supervisors is elected by the company staff democratic election.

5. Conclusion

In fact, the governance of the listed company is a system project which is related to the interior and exterior factors. About the interior factors, the expanding capability, leader capability and creative capability of each directors should be trained by the methods of study and practice, and the director member's theoretical level, the capability of processing complex business and controls the overall situation should be strengthened unceasingly. And then the overall capability of board should be enhanced and the components of board should be matured. Talking about the interior of the board, the following should be done based on the enhanced capability of the directors' capabilities: ① In order to progress the efficiency of the board, all the responsibilities and rights should be stated on the contract; ② Appointment mechanism of directors should be optimized and the professionals who are proficient in law, operation and governance should be collected to be the directors. ③ The local trustee system should be consummated to make listed directors normal and independent regardless of all achieves from the management decision-making to the moral personality in order to maximize gambling function among members of board. Speaking of exterior, we should govern the pattern international hastens with the reality based on the company, further consummates the produce market, the capital market, the manager market and so on exterior market system, creates the condition for the company exterior government mechanism display function.

In a word, the corporate governance urges the board of directors to make, the science, the high grade decision-making comprehensively, thus solves company's government problem in the essence, and take the time to be listed as our country national economy growth the further impetus function.

Correspondence to:
Zhang Jianying, Duan Yun
School of Management
Harbin Institute of Technology
Harbin, Heilongjiang 150001, China
Telephone: 01186-451-8641-4011
01186-139-0465-9188 (mobile)
Email: zzjjyy0757@sina.com

Notes:

① In fact, stock value can usually be the symbol of a company's benefit. So the author thinks that we can analysis the correlation between directors' capabilities and stock value instead of director's capabilities and corporate performance.

② Data resources: Yongyou is listed first in the Chinese Public company board governance. Newspaper of Economic View. 2002.12.23.

③ Data in the case is based on the Newspaper of Economic View and statistic formula (1) and (2).

References:

1. Wu Yun. Human Resource Management [M].Harbin: Harbin Engineering University Press. 2002.
2. Li Wei'an, Wu Lidong. Teaching Book of Corporate Governance [M].Shanghai: Shanghai Renmin Press. 2002.
3. Nankai University Corporate Governance Evaluation Project Group of Corporate Governance Research Center. A Emperical Study Between Corporate Governance index and Governance Performance of Chinese Public Companies [J]. Management World. 2004 (2).63-74.
4. He Zejun. Problem and Resolvation of Board Decision Function in Chinese Public Companies [J].Journal Henan of Textile College. 2005(3).20-22.
5. Heinz Weihrcih, Hanold Koontz. Management: A Global Perspective [M].Beijing: Economic Science Press. 2004.125-150.
6. Zhou Li. Comparation and Inspiration of Corporate Governance Structure in Nation and Abroad [J]. Hunan: Society Science.2005(4):92-94.

The Consideration of Cohesive Forces Perpendicular to the Tensile Layer in Bubbles, Droplets, Capillary Rise and Depression

Kent W. Mayhew

68 Pine Glen cres., Ottawa, Ontario, Canada, K2G 0G8, kent.mayhew@gmail.com

Abstract: The application of the Young-Laplace equation to bubbles, droplets, capillary rise and depression have been generally accepted for centuries, because it approximates experimental evidence. Consequentially, any cohesive forces perpendicular to the tensile has been omitted from due consideration. In this treatise, we shall investigate the mechanical implications of also considering the cohesive forces perpendicular to the tensile layer, arriving at a new perspective. [Nature and Science. 2007;5(4):43-52].

Keywords: Capillary Rise, Capillary Fall, Capillary Depression, Bubbles, Droplets, Cohesive forces

Introduction

Whether a resultant force is dynamic or static, that force when applied perpendicular to an area results in a pressure felt by that area. This concepts holds in every realm of physics except for one! Most accept the intermolecular cohesive forces along a curved tensile layer result in a pressure change across the tensile layer, without any consideration being given to the intermolecular cohesive forces perpendicular to the said tensile layer. This has rendered the science of tensile layers into that rare case where resultant forces perpendicular to an area do not contribute to pressure felt by that area. Accordingly, this paper will consider the ramifications of considering a liquid's cohesive forces perpendicular to its tensile layer, determining that such consideration may be warranted.

The science of tensile layers is too often portrayed as if there is no ambiguity. Interestingly, the question as to should tensile layers be contemplated purely in terms of some mechanical description[1,2,3], or based upon some thermodynamic consideration, i.e. Helmholtz free energy[2,4,5,6], is an ongoing debate. A verbal description for its existence Helmholtz free energy being[2]: "The interaction of a given molecule with its (nearest) neighbors leads to a reduction of its potential energy, i.e., intermolecular forces act to stabilize the system. However, the molecules at the surface region of this condensed matter have a smaller number of nearest neighbors, and therefore their potential energy is not decreased by as much as in the interior of condensed phase."

The mathematical description for the Helmholtz Free energy (F) is[7]: $F \equiv E - TS$. If F is actually obtained from[7]: $TS = E + PV$. Then comparing these two equations one would be inclined to say that: $F = -PV$, therefore: $\Delta F = -\Delta(PV)$.

Although well accepted, this is problematic! Changes to Helmholtz free energy are contemplated in terms of temperature change (ΔT) at constant entropy (S) and volume change (ΔV) at constant pressure (P), plus any changes in energy associated with chemical potential, surface area etc. For the isothermal case, with no change to chemical potential, the change in Helmholtz free energy in differential form is [2]:

$$dF = -P_1 dV_1 - P_2 dV_2 + \sigma dA \qquad 1)$$

Where: σ is the surface tension, dA is the change in surface area and subscripts "1" and "2" represent the two phases, which are separated by the tensile surface. 1) assumes that the energy changes associated with tensile layers, only signifies a volume change of both phases plus the energetics associated with the increased tensile layer. Seemingly forgotten is that fact that a curved tensile layer signifies a pressure change, hence any conjecture that tensile layer formation is an isobaric process is troublesome at best. Part of the justification resides in the fact that we can mathematically obtain certain results by doing so, as Pellicier[2] does for the Young-Laplace equation. Beyond the mathematical justification, the logic is seemingly weak. Accordingly, we must seek an improved logic based mathematical model.

Perhaps the reason for the acceptance of the Helmholtz free energy interpretation of tensile layers is that the mechanical description of tensile layers is similarly troubled. Consider the verbal description for its existence is[3]: "For a molecule in the bulk liquid the resultant repulsive form its nearest neighbors and the

resultant attractive force from its farthest neighbors are both zero on the average." "In the surface there is an unbalanced force on a molecule; it is directed inwards because the decreasing density in the surface layer implies that there are fewer neighbors to give an outward repulsive force". As plausible as such an explanation sounds, the implication is that the unbalanced forces are perpendicular to the tensile layer. So why are these unbalanced forces not considered?

The mechanical description is approximated by the Young-Laplace equation. For a spherical shaped tensile layer residing between a liquid and gas, the Young-Laplace equation is[8]:

$$P_l - P_g = 2\sigma / r \qquad 2)$$

Wherein the subscripts "*l*" and "*g*" respectively signifies the liquid and gas phase, with *r* being the tensile layer's radius of curvature. As valid as 2) may be for obtaining a result based upon the cohesive forces along a tensile layer, one must ponder: What would happen if we added to this, a consideration of the unbalanced forces resulting from cohesive forces perpendicular to the tensile layer? Hence, this paper was written.

Simple Derivation of the Young-Laplace Equation

Let us review the Young-Laplace equation derivation. There a numerous methodologies for deriving 2), such as the one given by Adamson[9]. Herein, we shall take simpler approach in deriving 2), which was previously published by this author[10] thus is given herein purely for review purposes, with the intention of adding clarity.

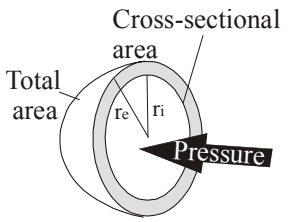

Fig. 1: Shows the pressure in a sphere and its cross-sectional area

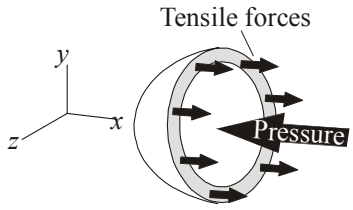

Fig 2: Shows the pressure in a sphere being countered by the tensile forces, along the *x*-axis

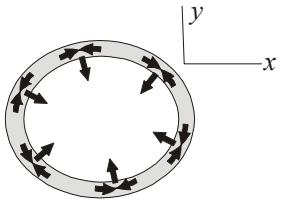

Fig.3: Shows that the pressure along the *x*-axis is equated to an inward squeezing by the tensile layer along the *x*-*y* plane.

When deriving the Young-Laplace equation, one may start with the following fundamental principle of hydrostatics. The force in a particular direction from a uniform pressure on a curved surface equals the pressure times the cross-sectional area of this surface in the direction of the desired force[11]. Consider the cross-section of a spherical tensile layer, as is shown in Fig. 1. If r_i is the radius to the inside of the tensile layer, then the cross-sectional area is: πr_i^2. If the pressure under consideration is along the *x*-axis, as shown in Fig. 2, then the cross-sectional area is measured in the *y*-*z* plane. Applying the principle of hydrostatics we can say, the total force perpendicular to the cross-sectional area is the force of elongation (F_e)[10]:

$$F_e = \Delta P \pi r_i^2 \qquad 3)$$

Where: $\Delta P = P_g - P_l$, which is the pressure difference, across the tensile layer. Equilibrium means that the surface tension must be equal and opposite to this force of elongation. Consider the pressure to be along the *x*-axis, is countered by the tensile force along the *x*-*y* plane, as is shown in Fig 2. If the bubble's surface tension is squeezing inward as a function of its length then the total surface tension (τ_1) along the ring of tensile layer, as illustrated in Fig. 3, is[10]:

$$\tau_1 = 2\pi R\sigma \qquad 4)$$

Where: $R = (r_i + r_e)/2$. Consider the tensile layer to be thin therefore: $R = r_i = r_e = r$ =r. Equating the tensile forces to the force of elongation, i.e. 3) to 4) and dividing by: πr_i^2, we obtain:

$$\Delta P = 2\sigma / r \qquad 5)$$

Obviously, 5) is another way of writing the Young-Laplace equation, that being 2).

Bubbles, Droplets and the Young-Laplace Equation

Traditionally, the Young-Laplace equation is used to define the pressure inside of a bubble surrounded by a liquid, the pressure inside of a liquid droplet surrounded by a gas, as well as in the analysis of both capillary rise and depression. The Young-Laplace equation only considers the cohesive forces along the tensile layer conveniently omitting the liquid molecule's cohesive forces perpendicular to the tensile layer, as is shown by the white arrows in Fig. 4 and 5. If we now consider the cohesive forces perpendicular to the tensile layer, the resultant tension perpendicular ($\tau_{\perp}$) to the tensile layer is taken over a ½ sphere, whose magnitude is[10]:

$$\tau_{\perp} = \sigma \pi r_d \qquad 6)$$

As illustrated in Fig 4, the cohesive forces perpendicular to a bubble's tensile layer would be directed into the surrounding liquid, from the bubble's tensile layer. Subtracting the cohesive forces perpendicular to the tensile layer, as defined by 6), from the cohesive forces along the tensile layer, as defined by 4), the pressure within a bubble (P_b) immersed in a liquid becomes[10]:

$$P_b = \sigma / r_b + P_l \qquad 7)$$

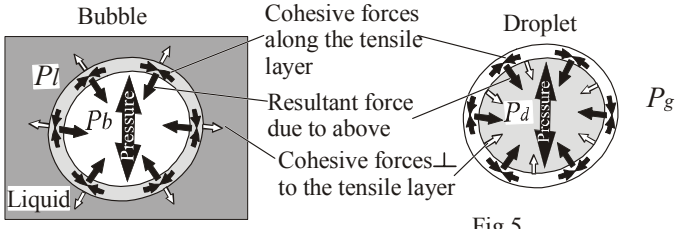

Fig 4

Fig 5

In both the above Fig 4 and Fig 5 we see two sets of forces. Black arrows are due to the intermolecular cohesive forces along the tensile layer while the white arrows are due those perpendicular to the tensile layer.

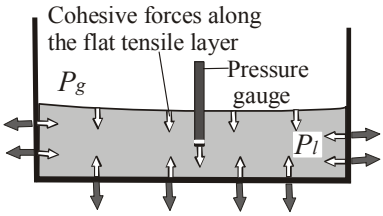

Fig. 6 Shows the cohesive forces in a container of liquid. Although the pressure in the liquid is higher due to the intermolecular cohesive forces, the affinity of those same forces to the pressure gauge would prevent the gauge from reading any pressure increase.

Conversely for a droplet, as illustrated in Fig 5, the cohesive forces perpendicular to the tensile layer would be directed into the droplet. Adding the cohesive forces perpendicular to the tensile layer, as defined by 6), to the cohesive forces along the tensile layer, as given by 4), results in the pressure within the droplet (P_d) becomes[10]:

$$P_d = 3\sigma / r_d + P_g \qquad 8)$$

Until now, most researchers believe that the pressure within both a bubble and droplet are well understood, that being defined by 4). Certainly, this was this author's belief until researching the phenomena and noticing huge discrepancies in the theory. The extent of this problem can be seen by comparing Debenedetti[12] who has the pressure inside of a bubble, lower than the pressure of the

surrounding liquid, to Adamson[9] has the pressure inside of a bubble greater than the pressure of the surrounding liquid. They both cannot be right.

Logic seemingly dictates that one should be able to readily probe either a bubble or a droplet with a pressure gauge. However, trying to actually measure the pressure within a spherical bubble is next to impossible. It only becomes feasible if the bubble is rigidly adhered to a surface, however the consequences of that rigid attachment should influence the pressure reading.

As for a droplet, inserting a pressure probe into it is easily accomplished. Even so, when either a bubble or droplet is rigid attached to some surface to which its tensile layer has an affinity, the shape is rarely perfectly spherical which will influence the pressure reading. Moreover, if we are considering all resultant intermolecular cohesive forces, then we must consider that the resultant cohesive forces of the liquid perpendicular to the probe's surface, which will be directed into the liquid. Hence will lower the actual pressure reading. In order to visualize this, imagine the container of liquid illustrated in Fig. 6. Considering all resultant intermolecular cohesive forces, we realize that along the container's base and walls the liquid's intermolecular forces are directed into the liquid but these are countered by the strong affinity the liquid has for the container. The only intermolecular cohesive resulting in pressure increase within the liquid would be those perpendicular to the relatively flat surface tensile layer. Obviously these are directed down into the liquid. However, the pressure gauge, due to the affinity between the pressure gauge's probe's end and the surrounding liquid, would result in a resultant cohesive force directed into the liquid therefore the gauge would not measure the pressure increase.

Interestingly, for a soap bubble, it was realized that the cohesive forces perpendicular to the tensile layer would cancel, leaving the accepted traditional result[10]:

$$\Delta P = 4\sigma / r_b \qquad 9)$$

Capillary Rise and Depression: The Traditional Approach

Capillary rise is the elevation of a liquid by some height (h) within a capillary tube when the liquid has an affinity towards the capillary tube and the tubes radius is sufficiently small. In capillary rise, traditional theory incorporates the idea of contact angle (ϕ), and considers the tensile surface to be spherical with a radius defined by the capillary tube's radius (r_c). The traditional equation is for capillary rise being[9]:

$$h = 2\sigma \cos\phi / \rho g r_c \qquad 10)$$

It seems strange that the curved tensile layer would have a radius simply defined by the tube's radius, even though it has a contact angle. Logic should dictate that the greater ϕ is, then the larger the tensile layer's radius should be. When, r_c is sufficiently small, then: $\phi \to 0$, then: $\cos\phi \to 1$, which results in:

$$h = 2\sigma / \rho g r_c \qquad 11)$$

Interestingly, 11) is also traditionally used to define capillary depression, that being the fall of a liquid by some height (h) within a capillary tube when the liquid has no affinity to the capillary tube. For capillary depression, the traditional approach is treat the radius of curvature of the liquid as being equal to the capillary tube's radius, which is to say: $\phi \to 0$, hence the use of 11).

The correlation between 11) and the Young-Laplace equation [2) or 5)] can be best illustrated by contemplating capillary rise. That column of liquid has a volume (V) and a density (ρ), giving the force due to gravity exerted by the weight of the column of liquid in the capillary tube is:

$$mg = V\rho g = \pi r_c{}^2 h \rho g \qquad 12)$$

Equating 12), to the tension as defined by 4), we obtain:

$$\pi r_c^2 h\rho g = 2\sigma\pi r_c \qquad 13)$$

Dividing through by: $\pi r_c^2 \rho g$, one then obtains 11).

Capillary Rise and Cohesive Forces Perpendicular to the Tensile Layer

In order to arrive at a more general formulation that being approximately the tensile layer as elliptical, we will consider what forces are acting in the *y*-direction in Fig 7. The cross-sectional area of an approximate ellipse parallel to the *x*-*z* plane is:

$$A_{xz} = \pi r_x r_z \qquad 14)$$

Multiplying the pressure change (ΔP_y) along the *y*-axis by the cross-sectional area in the *x*-*z* plane (A_{xz}) gives the force of elongation (F_{ey}) along the *y*-axis:

$$F_{ey} = \Delta P_y \pi r_x r_z \qquad 15)$$

F_{ey} is countered by the tension squeezing along the *x*-*y* plane. Since the tensile surface approximates a ½ ellipse, whose length along the *x*-*y* plane is: $\pi(r_x + r_y)/2$. Therefore, the tension along the positive *y*-axis due to intermolecular cohesive forces along the tensile layer [$\tau_{(y\,:\,along)}$] is:

$$\tau_{(y\,:\,along)} = \sigma\pi(r_x + r_y)/2 \qquad 16)$$

Since the tensile layer has an inner (r_i) and exterior/outer radius (r_e), as was discussed when deriving 4), we double 10). Therefore, for capillary rise, the tension along the positive *y*-axis due to the intermolecular cohesive forces along the tensile layer is:

$$\tau_{(y\,:\,along)} = \sigma\pi(r_x + r_y) \qquad 17)$$

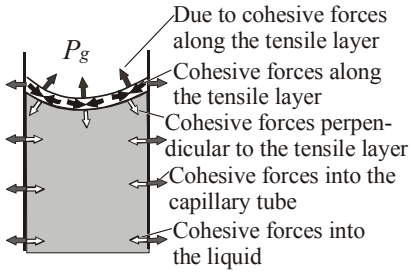

Fig. 7 Shows all the intermolecular cohesive forces within the liquid in capillary rise.

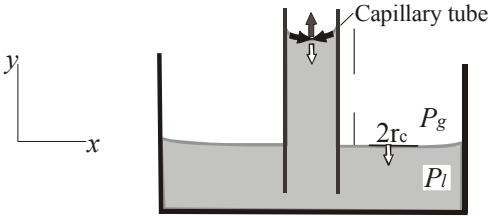

Fig. 8 Shows capillary rise of height *h*. Shown are the intermolecular cohesive forces that must be considered that being both those along and perpendicular to the curved tensile layer in the capillary plus those perpendicular to the flat tensile layer.

Obviously, when the capillary layer is spherical then: $r_x = r_y$, and 17) simply equates to 4), i.e. $\tau_{xy} = \tau_1$, giving the traditional result. Specifically, for the case of: $r_c = r_x = r_y$, then 17) becomes the Young-Laplace equation for capillary rise, which in this case would be:

$$\tau_{(y\,:\,along)} = 2\sigma\pi r_c \qquad 18)$$

Next consider the liquid's cohesive forces perpendicular to the tensile layer [$\tau_{(y\,:\perp)}$] in the capillary tube. Since they are of the same magnitude as those along the tensile layer, we can approximate them by writing:

$$\tau_{(y:\perp)} = -\sigma\pi(r_x + r_y)/2 \qquad 19)$$

The negative sign meaning $\tau_{(y:\perp)}$ is directed along the negative *y*-axis hence downward into the liquid. Therefore, the net tension felt by the liquid inside of the capillary due to all cohesive forces within the capillary tube (τ_{cyl}) must be:

$$\tau_{cyl} = \tau_{(y\,:\,along)} + \tau_{(y:\perp)} \qquad 20)$$

Realizing that $\tau_{(y\,:\,along)}$ and directed upward, while $\tau_{y\perp}$ is directed downward, we obtain:

$$\tau_{cyl} = \sigma\pi(r_x + r_y) - \sigma\pi(r_x + r_y)/2 \qquad 21)$$

Collecting the terms, for capillary rise we obtain:

$$\tau_{cyl} = \sigma\pi(r_x + r_y)/2 \qquad 22)$$

We do not concern ourselves with the intermolecular cohesive forces between the capillary tube and liquid as shown in Fig. 7 because they are perpendicular to the capillary rise with the resultant force directed into the capillary tube. This does not imply that they are not important because it is the liquid's affinity to the tube that allows for the rise in the first place. Is 22) the summation of all cohesive forces felt by the liquid inside the capillary? The answer is no!

As was discussed previously for Fig. 6, there are cohesive forces perpendicular to the relatively flat tensile layer, which will need consideration. Considering, the pressure exerted along an arbitrary line, whose length is $2r_c$ the equivalent tension felt along the arbitrary line (τ_a), would be:

$$\tau_a = 2r_c\sigma \qquad 23)$$

As far as the contents of the capillary tube, is concerned, the direction of τ_a is directed upward along the *y*-axis. The tension as defined by 23) must be added to 22) to calculate the total tension that results in capillary rise:

$$\tau_{tot} = \tau_{cyl} + \tau_a = \sigma\pi(r_x + r_y)/2 + 2r_c\sigma \qquad 24)$$

Equating τ_{tot} to the weight, as defined by 12), we obtain:

$$\pi r_c^{\,2} h\rho g = \sigma\pi(r_x + r_y)2 + 2\sigma r_c \qquad 25)$$

Dividing by: $\pi r_c^{\,2}\rho g$, we obtain:

$$h = [\sigma\pi(r_x + r_y)/2 + 2\sigma r_c]/\pi r_c^{\,2}\rho g \qquad 26)$$

If $r_c = r_x$, then we can rewrite 26) as:

$$h = [\sigma\pi(r_c + r_y)/2 + 2\sigma r_c]/\pi r_c^{\,2}\rho g \qquad 27)$$

27) becomes the general equation for capillary rise. For the special case of the tensile layer being spherical then: $r_c = r_y$. Collecting terms we obtain:

$$h = \sigma(1 + 2/\pi)/\rho g r_c \qquad 28)$$

Which can be rewritten as[10]:

$$h = \sigma(1.64)/\rho g r_c \qquad 29)$$

Although 29) is not identical to the traditionally accepted value [10) or 11)] for capillary rise, we can see that it is close, implying that our consideration of cohesive forces perpendicular to the tensile layer warrants consideration. What is most important is 27), which tells us that the greater the value of r_y in comparison to r_c the higher the capillary rise would be. Moreover, in capillary experiments the tube is generally wetted prior to the experiment, which should increase r_y thus increasing height (h), which helps explain why basing capillary rise on the Young-Laplace equation has remained unchallenged.

We can view the above analysis another way. Consider that capillary rise is the difference of two phenomena. 1) the upward force due to the cohesive forces along the tensile layer, as defined by the Young-Laplace equation when the tensile layer is spherical. 2) the difference between the cohesive forces perpendicular to the curved tensile of the top of the capillary and the cohesive forces perpendicular to a flat tensile layer whose length is: $2r_c$.

Capillary Depression and Cohesive Forces Perpendicular to the Tensile Layer

Capillary depression/fall seemingly correlates better with the Young-Laplace equation than does capillary rise. However, the current theory for capillary depression a is poor at best and as was the case in capillary rise, current theory fails to address the fact that cohesive forces are acting in 3 directions along the tensile surface, hence the parabolic shape.

For capillary depression, once again the area of the ellipse in the x-z plane is given by 14), while the force along the y-axis is given by 15). Therefore, for capillary depression, the tension along the positive y-axis due to the intermolecular cohesive forces along the tensile layer is has a magnitude defined by 17) but is now along the negative y-axis, as illustrated in Fig 9. Therefore:

$$\tau_{(y\,:\,along)} = -\sigma\pi(r_x + r_y) \qquad 30)$$

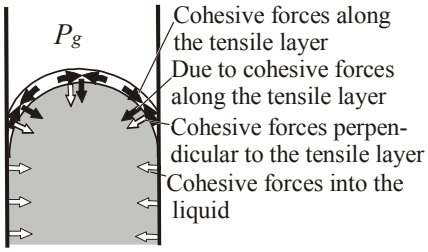

Fig. 9 Shows all the intermolecular cohesive forces within the liquid in capillary depression/fall.

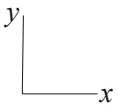

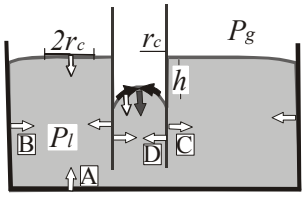

Fig. 10 Shows capillary depression of height h. Shown are the intermolecular cohesive forces that must be considered. Those being both along and perpendicular to the curved tensile layer in the capillary plus those perpendicular to the flat tensile layer plus those directed into the liquid along the container walls and capillary tube.

For the liquid's cohesive forces perpendicular to the tensile layer ($\tau_{y\perp}$) in the capillary tube, which are directed into the liquid, once again that would be defined by 19) and be directed along the negative y-axis hence downward into the liquid, as illustrated in Fig 9. Therefore, the net force felt by the liquid inside of the capillary due to all cohesive forces within the capillary tube (τ_{cyl}) must be would still be defined by 20) but the result now becomes:

$$\tau_{cyl} = -\sigma\pi(r_x + r_y) - \sigma\pi(r_x + r_y)/2 \qquad 31)$$

Collecting the terms, for all the cohesive forces along the curved tensile layer within the capillary tube in capillary depression, we obtain:

$$\tau_{cyl} = -3\sigma\pi(r_x + r_y)/2 \qquad 32)$$

32) is written as if it represents all the cohesive forces within the capillary. However, looking at Fig 9 we can see that the cohesive forces of the liquid directed into the liquid along the capillary tube, were not considered. Although, due to strong affinity between the capillary tube and liquid in capillary rise, these forces were omitted from the analysis, this may not be the case for capillary depression, which we will discuss later on in this section. Considering the cohesive forces perpendicular to a tensile layer, the difference between that exerted along a curved tensile layer and an equivalent section of flat tensile layer, is still defined by 23). The net result becomes:

$$\tau_{tot} = \tau_{cyl} + \tau_a = 2r_c\sigma - 3\sigma\pi(r_x + r_y)/2 \qquad 33)$$

The value of τ_{tot} will be negative, indicating that the resultant tension is along the negative *y*-axis. Equating τ_{tot} to the gravitational force as defined by 12), we obtain:

$$\pi r_c{}^2 h\rho g = 2\sigma r_c - 3\sigma\pi(r_x + r_y)2 \qquad 34)$$

Dividing both sides of 34) by: $\pi r_c{}^2\rho g$, we obtain:

$$h = [2\sigma r_c - 3\sigma\pi(r_x + r_y)/2]/\pi r_c{}^2\rho g \qquad 35)$$

If: $r_c = r_x$, then 35) becomes:

$$h = [2\sigma r_c - 3\sigma\pi(r_c + r_y)/2]/\pi r_c{}^2\rho g \qquad 36)$$

For an approximation to the currently accepted equation for capillary depression we assume that the tensile surface is close to being spherical, therefore: $r_c = r_y$ and we now obtain:

$$h = (2r_c\sigma - 3\sigma\pi r_c)/\pi r_c{}^2\rho g \qquad 37)$$

Dividing 37) through by r_c we obtain:

$$h = \sigma(2 - 3\pi)/\pi r_c\rho g \qquad 38)$$

Which becomes:

$$h = -2.36\sigma/r_c\rho g \qquad 39)$$

The traditionally accepted theory for capillary depression is also based upon the Young-Laplace equation, but is directed along the negative y-axis, hence is the negative of 11). We can see that the traditional value is 85% of our calculated value. It must be emphasized that our approximation, as given by 39) is based upon the tensile surface being spherical and its radius being exactly that of the capillary. For the case of the capillary depression of mercury is a glass capillary tube, that is seemingly often the case. Since in capillary depression experiments, the tube is not wetted prior to experiment, the difference between our result, 39), and the traditional result, 40), must be explained. Firstly, in our analysis we did not consider all the tensile forces directed into the liquid. Looking at Fig 10 we can see that we omitted the following:

A) The cohesive forces directed upwards into the liquid from along the base of the container.
B) The cohesive forces directed into the liquid from the along the walls of the container.
C) The cohesive forces directed into the container of the liquid from along the capillary tube.
D) The cohesive forces directed into the capillary tube from along the capillary tube.

As for A), these cohesive forces and those from along the top of the liquid should be uniform throughout the liquid. The only real difference is the difference between the curved tensile in the capillary tube and that of an equivalent line of a flat tensile. Accordingly our analysis could have included these but we would have arrived at the same result!

However, the same cannot be said if due consideration was given to B), C) and D). Since all these cohesive forces are perpendicular to the capillary depression, then they probably do not affect the result. Having said that, this may warrant more consideration.

Secondly, another explanation for why 40) is so strongly believed may lie in the process of measurement.

Measurement in Capillary Action

Whether one is talking about capillary rise or capillary fall, this author believes that the measurement of *h* should be made along a line passing through the centroid of the section containing the curved tensile layer in the capillary tube, as illustrated in Fig 11. And not to either the top or bottom of the curved tensile layer in either capillary rise or fall, as is done traditionally.

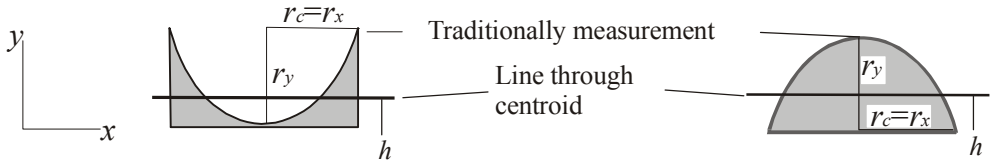

Fig. 11 Shows the top of a tensile layer in capillary rise on the left and the top of a tensile layer in capillary fall on the right. In both cases the height (*h*) should be measured to the plane which defines the center of mass of the capillary section.

.

For the case of capillary rise this would mean that the traditionally measured location gives a slightly higher value for the *h* than it should be. Conversely, for capillary depression the traditionally measured value would be lower than it should be, hence providing an explanation as to why 40) is so strongly believed by those using traditional theory.

Clarification

For clarification, the derivation of 7) ,8) and 9) can be found in this author's paper[10], entitled: "Energetics of Nucleation". Since the paper primarily dealt with nucleation, 29) and 39) were simply stated, in order to demonstrate to the reader, that the treatment of all cohesive forces may warrant due consideration. Hence the more formal derivation and discussion of 29) and 39) were left for this paper.

Conclusions

In this treatise we did not prove that the intermolecular cohesive forces perpendicular to tensile layers must be considered when contemplating a pressure change across a tensile layer, whether it be curved or flat. By considering all the intermolecular cohesive forces, meaning both along and perpendicular to the tensile layer in capillary action, we arrive at results that are close (82.5-85%) to the traditionally accepted value when the tensile layer is approximated to being spherical! Considering, the tensile layer as being elliptical resulted in an improved approximation, although a precise calculation can only be attained, by considering the tensile layer's exact shape. Interestingly, for capillary rise the act of wetting the capillary tube should result in a higher height of rise, by increasing r_y in comparison to r_x .

In both capillary rise and depression, the measurement of height is often taken to be the highest point in the curved tensile surface, rather than a line passing through its centroid. For capillary rise this means that the measured height is too large, while in capillary depression it would be too small, thus reinforcing the traditional theory.

We also realized the some of the difficulties exist in measuring the pressure with a bubble and/or droplet. Furthermore, when measuring the pressure within most liquids, whether it is a droplet or a container of liquid, the measurement of pressure will be lowered due to any affinity between the liquid to

the end of the probe, hence nullifying from the reading any pressure increase within the liquid due to the intermolecular cohesive forces directed perpendicular to the tensile layer and into the liquid.

We are no longer befuddled by the enigma as to why we simply omit the intermolecular cohesive forces perpendicular to the tensile layer. Certainly, logic dictates that there is a resultant force associated with such cohesive forces, therefore a pressure/tension associated with them. Interestingly, the concept of contact angle was not required in our analysis leaving the astute reader to ponder whether contact angle may be a result, rather than some reason as conveyed in traditional theory[9].

The paper is a treatise demonstrating that when one considers all the intermolecular cohesive forces, both along and perpendicular to a tensile layer that one does arrive at some interesting results. In many ways it is an elaboration of some concepts originally discussed in an earlier paper by this author, which dealt with the theory of nucleation (paper entitled: Energetics of Nucleation). Since that paper dealt with nucleation, certain equations concerning the pressure change across curved tensile layers were simply stated. It must be emphasized that the derivation of those stated equations were given to the reviewers but no comments were made.

The paper Energetics of Nucleation was deemed controversial and was not going to be published, until this author found some data from an experiment performed in 2001, in which a laser was shot into degasified water and the energy required for nucleation was calculated. The data in question could not be explained by the research group but was an exact fit to what this author was saying, hence publication. The Lauterborne group in Germany, who performed the experiment in question, has confirmed the exactness of fit.

I am an independent researcher whose interest lay in nucleation theory and thermodynamics. I have also another paper concerning work that has been accepted for publication by Physics Essays and another currently in the review process. Neither of those papers deals with cohesive forces and tensile forces that being the paper presented herein.

Correspondence to:
Kent Mayhew
68 Pine Glen cres.
Ottawa, Ontario, Canada, K2G 0G8
Email: kent.mayhew@gmail.com

References

1. Zhmud, B.V., Tiberg, F., Hallstensson, K., J. Colloid and Inter Sci. 228 pp 263-269 (200)
2. Pellicier, J., Manzanares, J.A., Mafe, S., Am. J. Phys 63 (6) pp 542-547 (1995)
3. 3 Berry, M.V. Phys. Educ., 6 pp 79-83 (1972)
4. Navascues, G., Rep. Prog. Phys. 42 Pp1131-1186 (1979)
5. Boucher, E.A., Rep. Prog. Phys. 43 Pp497-546 (1980)
6. Reif F. "Fundamentals of Statistical and Thermal Physics", McGraw-Hill, New York 1965
7. Walton, Alan, J., Phys. Educ. 7 Pp491-498 (1972)
8. Adamson, A.W.,"Physical Chemistry of Surfaces, 3rd edition" John Willey and sons 1976
9. Mayhew, K.W. Phy. Essays, 17 Pp 476-495 (2004)
10. Fogiel, M. Problem Solver in Strength of Materials, Research and Education Association, New York, 1983 (page 197)
11. Debenedetti, P. "Metastable Liquids: Concepts and Principles", Princeton University Press, Princeton 1996

Evaluation Of Bioremediation Of Agricultural Soils Polluted With Crude Oil By Planting Beans Seeds, Phaseolus Vulgaris

Aboaba, O.A., Aboaba, O.O., Nwachukwu, N.C., Chukwu, E.E. And Nwachukwu, S.C.U.

Department Of Microbiology, University Of Lagos, Yaba, Lagos, Nigeria.
Department Of Pblic Administraton, National Open University, Victoria Island, Lagos, Nigeria
simboaboaba@yahoo.com

ABSTRACT: The impact of crude oil on agricultural land, germination, growth and morphology of beans seeds (Phaseolus vulgaris) after bioremediation of agricultural soils polluted with crude oil using selected strains of Pseudomonas putida (PP) was investigated (E). A similar polluted agricultural soil not inoculated with PP served as a control (C). In e, the residual oil concentration decreased from 0.260 at week zero to 0.002g/g soil at week 10 representing about 92% oil reduction. The corresponding values for c were 0.240 and 0.170g/g soil respectively and this is equivalent to about 17% oil reduction. The levels of oil reduction in both E and C were confirmed by the results of gas liquid chromatography which revealed smaller peaks for E. At day 16 during germination experiments, there was 40% germination in E and 20% in C. For C, the mean seedlings height was 5.20 cm and all displayed abnormal morphology such as stunted growth and chlorosis. Thus treatment of oil-polluted agricultural land with PP culture as bioremediating agent can produce soils which can grow healthier plants than where bioremediation has not taken place. In conclusion, beans seeds germination and the general morphology of the seedlings seem to be reliable biological indices for the evaluation of the recovery of crude oil-impacted land after bioremediation protocols using selected microorganisms. [Nature and Science. 2007;5(4):53-60].

Keywords: Crude Oil, Pollution, Bioremediation, Pseudomonas Putida, Agricultural Soil And Seed Planting

INTRODUCTION

Land, a major factor of production and an employer of human resources for agricultural purposes for food production, has become a necessity especially in countries where fertile arable land is scarce (Atlas, 1991; Harley and Englande, 1992). To avoid poor yields of agricultural produce caused by planting in oil-impacted land, the regaining of the soil fertility upon pollution is very important and may involve some waste management such as bioremediation protocols (Atlas, 1991: Achana et al, 2005: Nwachukwu, 2001). This can be achieved using a selected strain of Pseudomonas putida (PP) which was examined as a part of the objective of this study. Even after bioremediation of oil-impacted land, there is the critical need to evaluate and ascertain the recovery of the land in terms of soil structure and fertility before planting. The best method to achieve this is by a biological method. Thus, the effectiveness of the bioremediation programmes put in place in the oil-impacted soils were evaluated by planting bean seeds (Phaseolus vulgaris) as the major aim of this study. Also, the percentage germination and growth profiles of beans seeds as biological evidence of the recovery of the oil-impacted soils were examined.

MATERIALS AND METHODS

Duplicate oil-impacted agricultural soils (4kg each) to the level of 2.04%w/w pollution collected from Niger Delta area of Nigeria was bioremediated by application of 350ml of the developed culture of Pseudomonas putida (PP) containing 3.80 x 106 cfu/ml in nutrient broth (E). The duplicate setups (C) contained all the materials present in E but without PP culture. At two weeks intervals, inoculation of E with PP culture and C equivalent amount sterile distilled water was repeated for a period of ten weeks. During this period, changes in the residual crude oil concentration by both gravimetric and gas liquid chromatographic methods (Yveline et al, 1997), population density of total bacteria on nutrient agar and PP on selective Pseudomonas medium (Oxoid) and fungi on potato dextrose agar (Oxoid) were monitored. At the end of the bioremediation period (10 weeks), the soil samples were tested to check whether or not the oil pollutant was eliminated by planting selected ten healthy beans seeds (Phaseolus vulgaris) (PV) per replicate of soil E and comparing the morphological characteristics such as percentage seed germination, leaf structure, height, etc of the seedlings obtained with those of C (Nwachukwu et al., 2001). Using Pseudomonas spp as test organisms with a mean generation time (T) in tropical soil ecosystem polluted

with crude petroleum as 14.84 days as previously determined (Chukwu et al., 2005), the time required for the environment to recover completely on terms of microbial load was estimated using the model (Dawes, 1969):

$$\frac{\text{Log } N_t - \text{log } N_0}{\text{Log } 2} = \frac{t}{T}$$

Where N_t = highest exponential growth phase population density of PP at time t; N_0 = initial exponential growth phase population density at time zero, t_0; t = exponential growth phase time; T = mean generation time of PP in oil-impacted tropical soil ecosystem. Thus, in this case, N_t = 1.511 x 10 8 cfu/g, N_0 = 1.82 x 10 5 cfu/g and T= 14.84 days.

The socio-economic aspects of this study involved interviewing some people from Niger Delta area of Nigeria as regards their demand for land as an important factor of productions, the other possible ways of augmenting their income and the government policy and implementation strategies about their environments grossly polluted with crude oil. To achieve this, 200 male and 200 female adults in the Niger Delta area were interviewed through the use of questionnaires.

RESULT AND DISCUSSION

Figure 1 shows the growth profiles of Pseudomonas putida (PP) during inoculum development. The broth inoculated with PP showed increases in optical density over the period. Thus, the culture was at its exponential stage when it was applied as a bioremediating agent to the agricultural soil samples polluted with crude oil. In contrast, the control broth showed little or no increase in optical density over the period suggesting the absence of microbial contaminants in the broth systems during inoculum development. Thus, any observed differences between C and E could be attributed to the culture inoculated into E. generally, the microbial populations increased persistently for the first few weeks and this was much more remarkable in E than observed for C (Fig.2). The predominant microorganisms identified for both E and C replicates included Bacillus spp, Lactobacillus spp (bacteria); Candida spp and Penicillium spp (fungi). In addition, Pseudomonas spp occurred abundantly in E and this could be attributed to the inoculated culture into E as a bioremediating agent. In E, the residual oil concentration (ROC) decreased from 0.026 to 0.002 g/g soil at week 10. The corresponding values for C were 0.024 and 0.017 g/g soil respectively (Fig.3). Moreover, GC profiles of ROC showed remarkable reductions in peaks and the values for biomarkers namely nC17/ pristane and nC18/ phytane ratios were much more pronounced in E (Fig.4) supporting the gravimetric values observed for ROC. Furthermore, the percentage seed germination in E was 40% at day 12 with the seedlings reaching a mean height of 7.75cm at day 16. The equivalent values for C were 10% AND 5.50cm respectively giving the difference of about 48% in seedling heights (Fig.5). Generally the growth profiles in PV were poor in C with pronounced abnormal morphology when compared with results obtained for E (Fig.6). This is in line with our previous reports although cress seeds (Lepidium spp) were used (Nwachukwu et al., 2001). When the values obtained for N_t, N_0 and T were fitted into the above model, the time probable (t) required for the oil-impacted agricultural soils (E) to recover completely in terms of microbial load from the day of putting in place the bioremediation protocols was estimated at 26.14 weeks. Consequently, it would take the polluted soil ecosystem (E) approximately 26 weeks from the day of sampling to return to the normal conditions obtainable in the equivalent unpolluted agricultural land in the Niger Delta region. This estimation is valid only on the condition that no crude petroleum or petroleum products would be further introduced into the environment. This is because chronic addition of oil pollutant as a result of imminent oil spills due to the activities of oil industries located in the area or to natural blow-outs from oil deposits could increase the recovery time (Atlas, 1991). From the responses of the people in the Niger Delta area interviewed, 344 (86%) were farmers involved in practices such as intensification of agricultural production with shortening of traditional rotation methods and permanent monocropping without sufficient time for replenishment of nutrients. This is further worsened by the chronic crude petroleum pollution in the area with attendant high degree weathering of the environment and poor yield. Incidentally, the government policies about the high attendant socio-economic problems confronting the farmers as a result of the pollution of their agricultural land are not clearly defined. For the control (C), the recovery time could be longer than observed for E but was not estimated using the model. This is because the population density of bacteria in C had not reached its exponential peak to allow the application of the model in order to estimate the recovery time for C (Dawes, 1969).

Significance and impact of study:

This study confirms that treatment of oil-impacted agricultural land with a selected culture of Pseudomonas putida can produce soils which are capable of growing healthier plants than where bioremediation and bioaugmentation has not taken place. Moreover, from the results of this study, planting of PV seeds seems to be a good biological index that can be used in evaluating the level of recovery of agricultural land upon pollution with crude oil. This is because of the low oil concentration of 0.002 and 0.017g/g soil in E and C respectively at week 10 was probably responsible for the low percentage germinations and the gross biological damages usually observed in crude oil-impacted ecosystems. Thus, a selected culture of P. putida isolated from tropical ecosystems (Nwachukwu, 2001) seems to be a suitable bioremediating agent of oil-impacted agricultural land while P. vulgaris seeds are highly sensitive to crude oil toxicity; its germination efficiency is therefore, a good biological index of evaluation of the rehabilitation of land upon pollution with crude petroleum or petroleum products.

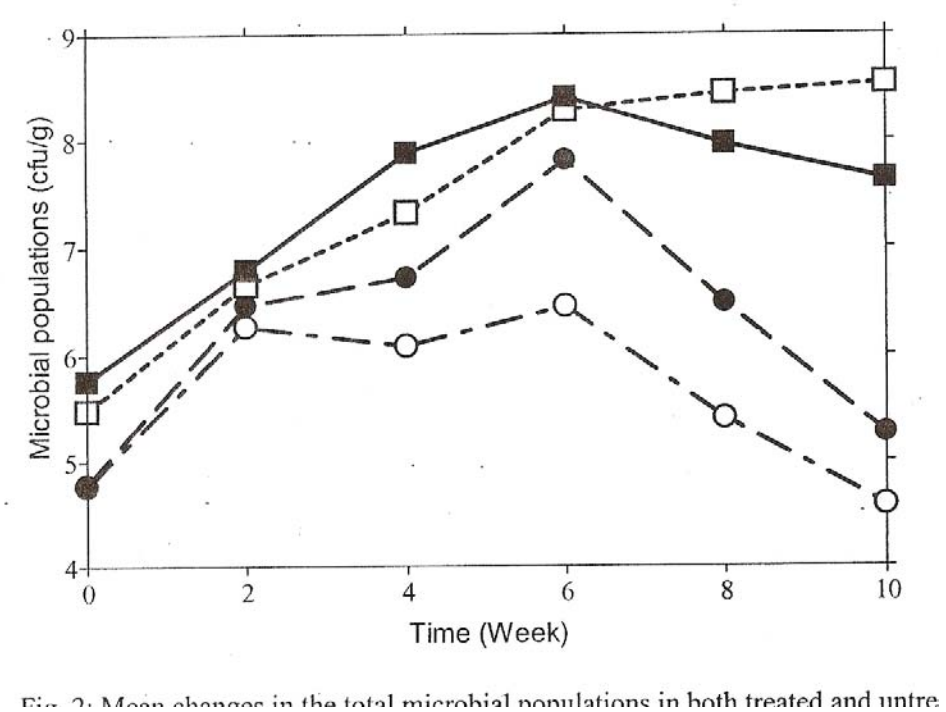

Fig. 2: Mean changes in the total microbial populations in both treated and untre

Figure 1. Micobial populations

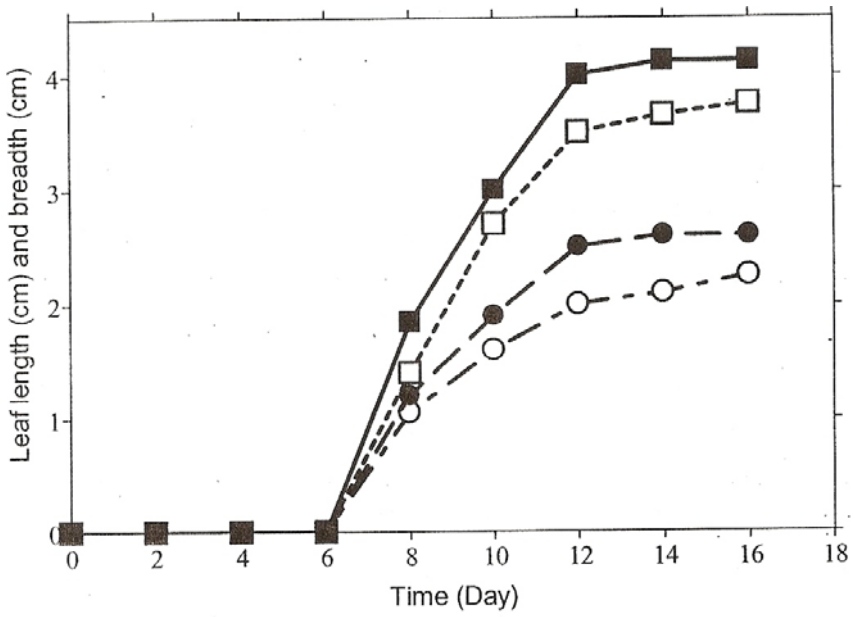

Mean leaf length and leaf breadth of bean seedlings planted in oil polluted ural soils after bioremediation. , leaf length in treated and; , untreated soil; adth in treated and; , untreated soil samples.

Figure 2. Mean leaf and leaf breadth of bean seedling

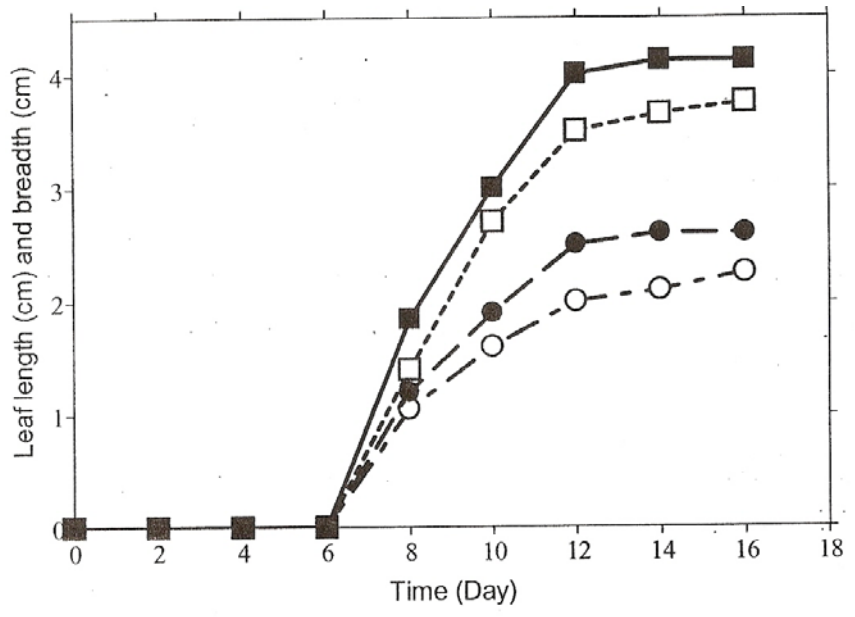

Figure 3. Leaf length and leaf breadth

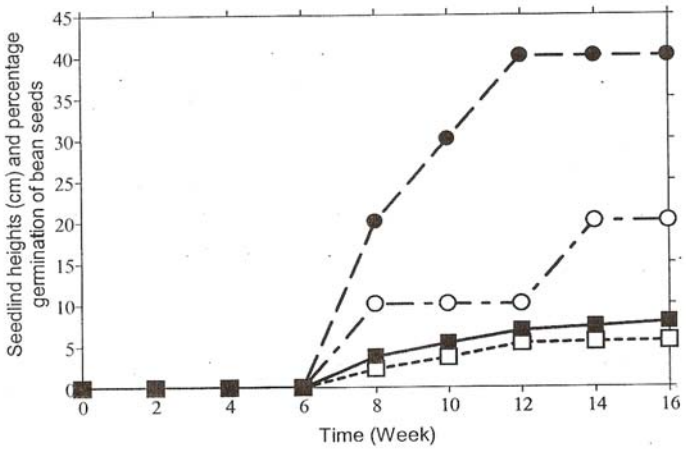

Figure 4. Seedling heights

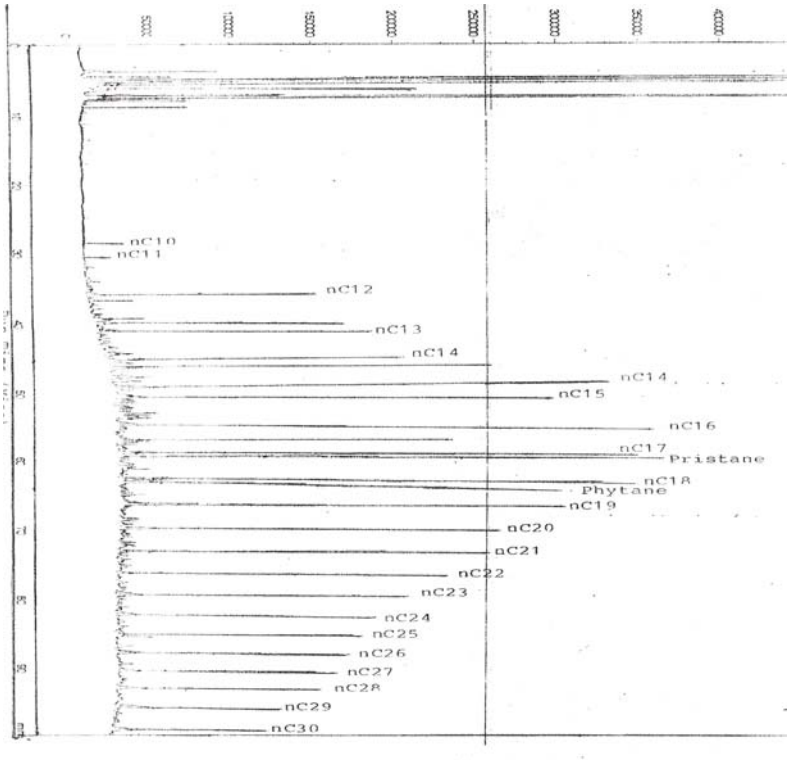

Figure 5. Chromatography

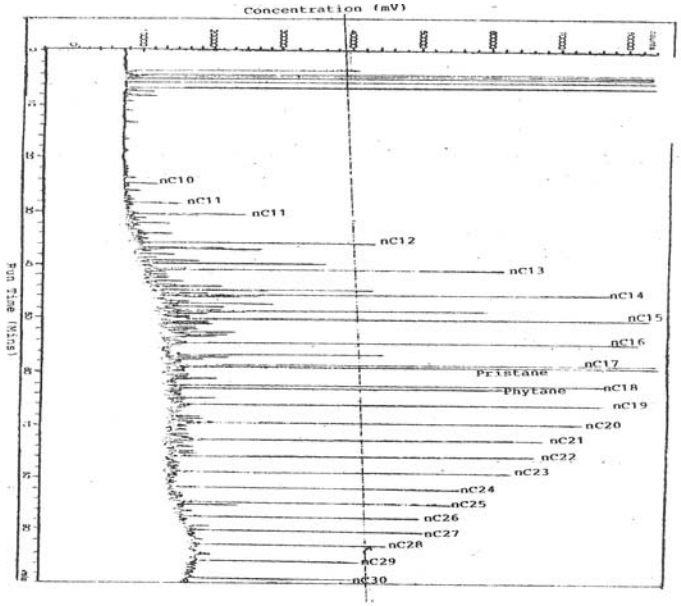

Figure 6. Chromatography

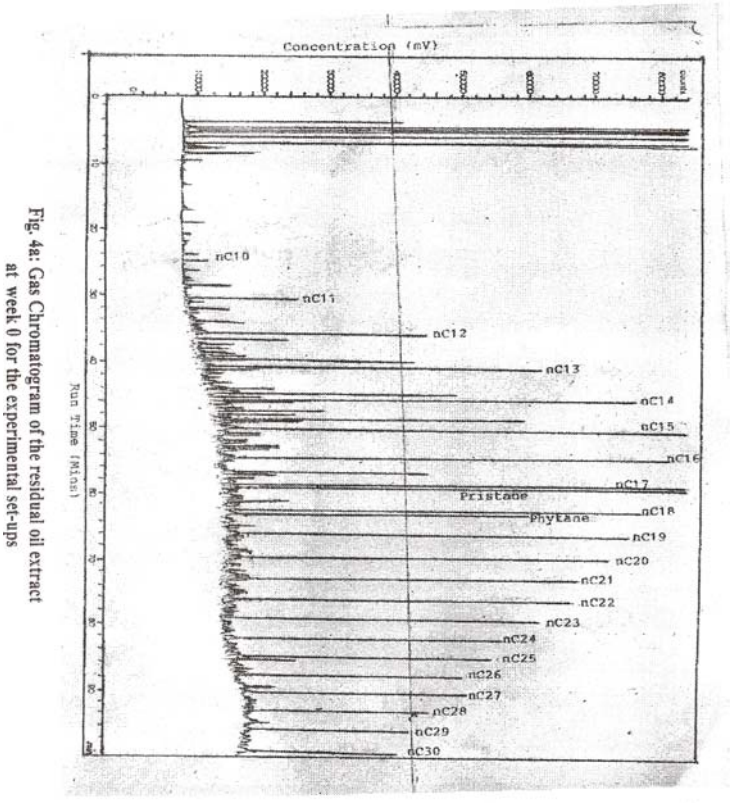

Fig. 4a: Gas Chromatogram of the residual oil extract at week 0 for the experimental set-ups

Figure 6. Gas Chromatography

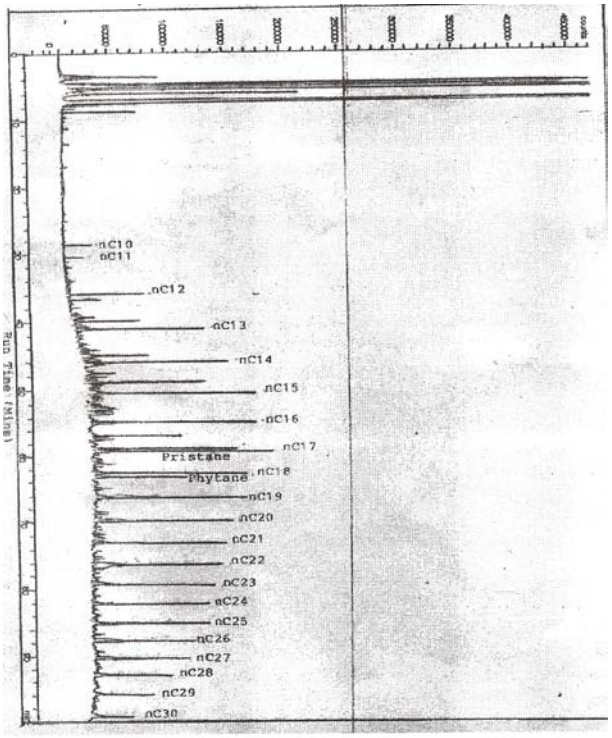

Figure 6. Gas Chromatography

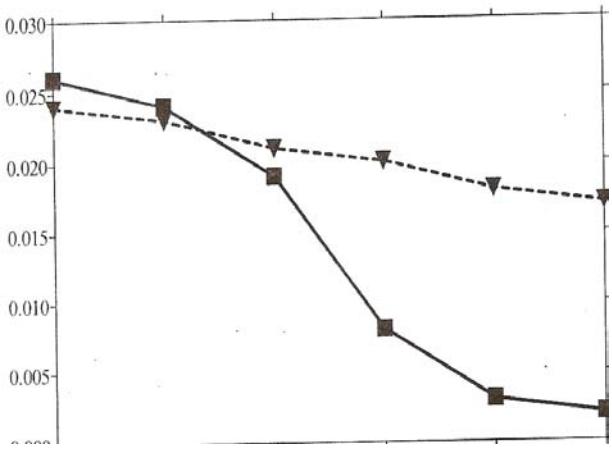

Figure 7.

CONCLUSION

From the results of this study, rehabilitation agricultural land polluted with crude petroleum at the Niger Delta area or elsewhere could be facilitated by inoculation with a selected culture of Pseudomonas putida. The poor percentage seed germination in both the experimental (40%) and control (10%) replicates is, therefore, an indication of crude oil phytotoxicity and the broad range of ecological damage associated with oil spillage in natural ecosystems.

Correspondence to:
Aboaba, O.A., Nwachukwu, S.C.U.
Department Of Microbiology,
University Of Lagos,
Yaba, Lagos, Nigeria
simboaboaba@yahoo.com

REFERENCES

1. Atlas, R.M (1991) Microbial hydrocarbon degradation: Bioremediation of oil spills J. Chem Tech. Biotech. 52:149-156
2. Archana D. D, Sopan T, I, Sanjay B.A and Nilesh D.W,(2005).Ecofriendly approach of urban solidwaste management: A case study of Jalgaon city, Maharashta. J.Environ. Biol.26 (40:747-752.
3. Chukwu, L.O. and Nwachukwu, S.C.U (2005). Impact of refined petroleum spills on water quality, macro-invertebrate and microbial communities of a tropical aquatic environment. J. Environ. Biol. 26(3): 449-458.
4. Dawes, E.A (1969). Quantitative problems in Biochemistry, 4th edition. (Edinburgh and London: E & S. Livingstone Ltd).
5. Hartley, W.R and Englande, J.A.J (1992). Health risk assessment of the migration of unleaded gasoline, a model for petroleum products. Water Sci. Technol. 25: 65-72.
6. Nwachukwu, S.C.U (2001). Bioremediation of sterile agricultural soils polluted with crude petroleum by application of Pseudomonas putida with inorganic nutrient supplementations. Current Microbiol. 42: 231-236.
7. Nwachukwu, S.C.U., James, P and Gurney, T.R (2001). Impacts of crude oil on the germination and growth of cress seeds (Lepidium spp) after bioremediation of agricultural soil polluted with crude petroleum using “adapted” Pseudomonas putida. J. Environ. Biol. 22(1): 29-36.

Relationship of Inflammation/Thrombosis and C-reactive protein (CRP), Plasminogen Activator Inhibitor 1 (PAI-1), Inteleukin-6 (IL-6), Inteleukin-1 (IL-1), Tissue Factor (TF), Tumor Necrosis Factor-alpha (TNF-α), tTssue Plasminogen Activator (tPA), CD40

Ma Hongbao *, Cherng Shen **

* Michigan State University, East Lansing, MI 48824, USA
mahongbao2000@yahoo.com

** Department of Electrical Engineering, Chengshiu University, Niaosong, Taiwan 833, Republic of China, cherngs@csu.edu.tw, 011886-7731-0606 ext 3423

Abstract: This project is to elucidate the relationship between systemic inflammation and plaque disruption and thrombosis. The implications of this could greatly define the mechanism leading to acute cardiovascular events including myocardial infarction and strokes. Also, this could lead to novel therapeutic and preventive approaches. The proposal seeks to investigate the kinetics of inflammation markers prior to and during an acute cardiovascular event. The feasibility depends on a valuable model developed by Dr. Abela's laboratory. This is an atherosclerotic rabbit model that can be pharmacologically triggered to develop plaque disruption and thrombosis. Thus, the inflammatory process can be monitored through an event. This rabbit atherosclerotic model is ideally suited to test potential therapeutics. **Specific Aim 1** will investigate the mechanism of C-reactive protein (CRP) in the development of acute thrombosis. CRP has been shown to increase plasminogen activator inhibitor 1 (PAI-1) and tissue factor (TF) in cell culture. This will be evaluated in an *in vivo* model and the kinetics and sequence of expression of markers will be demonstrated in the applied project. CRP effects on TF and CD-40L/CD-40 pathway activation will be evaluated. Platelet aggregation and adhesion will be measured in atherosclerotic rabbits with higher soluble CD40L following vascular injury in a dual organ perfusion chamber with and without antiplatelet agents. CRP, TF, IL-6 and CD40 will be evaluated following thrombus triggering in 20 rabbits compared to 20 control rabbits. **Specific Aim 2** will use immunohistochemical methods to demonstrate the localization of inflammatory markers in the arterial wall with local temperature rise. **Specific Aim 3** will use thermal model to analyze the generation of local temperature following vascular injury. This will be done both in a special *in vitro* thermally isolated and *in vivo*. **Specific Aim 4** will study the relationship between the inflammation factors and the effect of UV excimer laser on the thrombosis in the atherosclerotic rabbit. [Nature and Science. 2007;5(4):61-74].

1. Specific Aims

In order to study relationship of inflammation and thrombosis, an atherosclerotic rabbit model will be used (1) and C-reactive protein (CRP), plasminogen activator inhibitor 1 (PAI-1), inteleukin-6 (IL-6), inteleukin-1 (IL-1), tissue factor (TF), tumor necrosis factor-alpha (TNF-α), tissue plasminogen activator (tPA), CD40, and temperature will be measured.

Specific Aim 1. To Determine the Mechanism of CRP-mediated Vascular Thrombosis.

Aim 1a will test the hypothesis that increased serum CRP induces thrombosis by increasing PAI-1 and TF levels. We propose to determine *in vivo* physiological mechanisms underlying CRP induced PAI-1 and TF by investigating the kinetics of CRP, PAI-1 and TF level changes.

Aim 1b will test the hypothesis that CRP induced TF is mediated via CD40/CD40L (CD40 ligation) activated pathway, and CRP mediated upregulation of PAI-1 is mediated by inhibition of tPA leading to acute thrombus formation *in vivo*. Time-course immunohistochemical studies will be conducted to determine the localization of CD40, CD40L, TF, tPA and PAI-1.

Aim 1c. To test the specificity of CRP, PAI-1, and TF mediated thrombosis, we will administer neutralizing antibodies to CRP, PAI-1, and TF to reduce the thrombotic events.

Aim 1d will test the hypothesis that platelets from rabbits with atherosclerosis will have significantly higher levels of soluble CD40/CD40L production.

Specific Aim 2. Mechanism of Injury-induced Arterial Wall Temperature Increase and Mediatory Role of CRP.

Aim 2a. Using temperature measurement as a diagnostic marker of intensity of the inflammatory response, the arterial wall temperature will be measured at sites of arterial injury and correlated to the changes in serum CRP concentrations.

Aim 2b will evaluate the relationship among tissue cholesterol levels, expression levels of CRP, PAI-1, tPA, TF, CD40/CD40L, and local temperature rise in the aortic atherosclerotic plaques. To determine the causative factors of temperature rise in the atherosclerotic lesions, we propose to determine levels of CRP, PAI-1, tPA, TF and CD40/CD40L in the atherosclerotic plaques and correlate these data to arterial wall temperature and cholesterol levels.

Aim 2c will evaluate the effect of administration of antibodies directed against TF, CD40, CD40L, PAI-1 and tPA and CRP antibodies on the changes in arterial wall temperatures.

Specific Aim 3. Thermal Modeling of Injury Site to Obtaining Quantitative Relationships Between the Rate of Heat Generation and Associated Temperature Rise.

Aim 3a will determine the heat released during clotting of blood using a calorimeter experiment. The information can in turn be utilized to calculate the expected temperature rise associated with clotting in an artery in the body.

Aim 3b. Using numerical methods for the heat transfer processes involved in the arteries, estimates can be prepared relating the amount of heat generated to the temperature rise expected in response to the heat addition.

Aim 3c. Using methods of inverse heat transfer analysis, measurements taken in Specific Aim 2 can be analyzed to compute the amount of heat generated at the site of an injury.

Specific Aim 4: Relationship Between Inflammation Factors and Effect of Excimer Laser Ablation of Thrombus.

Aim 4a will test the effect of UV excimer laser on thrombosis in atherosclerotic rabbit. Our previous *in vitro* studies showed that UV excimer laser alters platelet aggregation based on total energy and greater laser power resulted in higher rate of thrombus ablation (2).

Aim 4b will study if the inflammation factors in the serum of rabbit are correlated to the UV excimer laser effect on thrombus formation/ablation and platelet activities *in vitro* and *in vivo*.

2. Background and Significance

2.1 Atherosclerosis, Systemic Inflammation and Thrombosis.

Increasing number of studies has demonstrated that atherosclerosis is associated with inflammation and acute coronary events. Buffon et al demonstrated that in an acute cardiovascular event related to a lesion in one coronary artery was associated with inflammation in the adjacent and non-involved artery by angiography (3). A compelling amount of data using different technologies have demonstrated that often more than one plaque is ruptured both in the culprit artery with thrombosis and in adjacent non-occluded arteries at the time of an acute myocardial event (4). Rioufol et al demonstrated multiple atherosclerotic plaque ruptures in patients during acute coronary syndrome by conducting intravascular ultrasound scan of all three coronary arteries in 24 patients with acute coronary syndrome (5). Furthermore, patients with acute cardiovascular events seem to have plaques that have ruptured in other arterial beds such as the carotid arteries at the time of the event (6). Thus, it is almost inevitable to assume that the outcome at a specific arterial site is being influenced by a systemic process. Additional supportive data regarding the systemic nature and effects of atherosclerosis comes from the strong association between peripheral vascular disease and coronary artery disease (7). In fact, carotid arterial wall thickness has been used as a strong index of coronary artery disease and predictor of future events (8). Also, as with coronary artery disease, the elevation in CRP is an indicator of future development of claudication and symptomatic peripheral vascular disease (9). All these observations seem to support that coronary artery disease is part of a systemic condition reflected by the presence generalized inflammation. Further, as with coronary artery disease, the elevation in CRP is an indicator of future development of claudication and symptomatic peripheral vascular disease. Systemic inflammatory marker CRP also has recently been shown to play an important role in promotion of atherothrombosis by increasing recruitment of monocytes (10) and by increasing recruited monocyte synthesis of TF (11). It has also been shown that CRP exerts its proatherothrombotic effect directly on endothelial cells (ECs) by increasing PAI-1 in the EC resulting in platelet aggregation and thrombosis. PAI-1, a marker of impaired fibrinolysis exert its atherothrombogenic effects by inhibiting

conversion of inactive plasminogen to active plasmin, a fibrin-degrading protease, by binding and inactivating tPA and urokinase plasminogen activator (12, 13). Further, PAI-1 has been shown to have the highest affinity for tPA in plasma and thus has been suggested to be the major regulator of tPA activity in the blood (14). Indeed, decreased fibrinolysis due to increased PAI-1 activity, PAI-1 and tPA complexes, and decreased tPA levels have been demonstrated in patients with coronary artery disease. PAI-1 is also increased in atherosclerotic plaques, and blood of patients with atherosclerosis, especially increased in diabetic patients (15). Interestingly, diabetic patients are known to be at greater risk for acute cardiovascular events. Also, CRP is markedly higher in patients with metabolic syndrome as well as diabetes (16). Importantly, increased PAI-1 levels have been shown to enhance thrombosis, and administration of antibodies directed against PAI-1 has been shown to be effective in prevention of the thrombosis development (17-21). Furthermore, a recent study has shown that transgenic mice expressing human PAI-1 develop coronary arterial thrombosis (22). CD40 a membrane-bound glycoprotein is expressed in B lymphocytes, dendritic cells, monocytes, and ECs (23). Its ligand, CD40L is expressed in activated T cells, smooth muscle cells, macrophages (23, 24) and activated platelets (25). Further, procoagulant activity of platelets has been shown to be via the CD40/CD40L pathway (25, 26). Importantly, recent study has shown that activated platelets increase TF in human monocytes (27). Since TF expression in monocytes and macrophage has been shown to be induced by cross-linking processes, it is plausible that CD40L expressing platelet interaction with CD40 expressing monocytes and macrophages cross link to induce TF production from the monocytes and macrophages. Interestingly, an increasing number of studies support a key role for the CD40/CD40L pathway in atheroma progression. Patients with unstable angina have significantly higher levels of soluble and membrane-bound forms of CD40L (28). Recent studies have also suggested that activated platelets can express CD40L and trigger inflammatory response and TF expression in ECs through interaction with CD40 (29). The linkage between systemic inflammation and coagulation, and possibly thrombosis may involve TF. Circulating TF is detected in patients with unstable angina (30), and high levels are expressed on macrophages in unstable plaques (31). It has also been shown in monocytes that CRP induces the production of inflammatory cytokines and promotes monocyte chemotaxis and TF expression (10, 11). Increased monocyte TF expression during infection or tissue necrosis may be at least partially mediated by an increased CRP level (11). This study and others strengthen the hypothesis that CRP is associated with clinical events by altering clotting status through induction of monocyte TF (11, 32).

2.2 Arterial Wall Temperature as a Reflection of Inflammation.

A strong physical marker for inflammation is temperature elevation. In fact, inflammation has been traditionally defined by ‘calor’ - heat , ‘rubor’ - redness, ‘dolor’ - pain and ‘turgor’ - swelling. Recently, studies have demonstrated that increased arterial temperature as an index of inflammation may be a marker of increased risk for plaque rupture and thrombosis. Cassells et al demonstrated temperature elevation at specific sites of plaques extracted during carotid endarterectomy procedures. At histologic examination, the sites with higher temperature had a greater concentration of inflammatory cell density (33). Stephanadies et al conducted several studies measuring temperature in human coronary arteries using a thermal sensing catheter. They demonstrated a wide local temperature dispersion in coronary arteries of patients who presented with acute cardiovascular events but not in patients with normal arteries or stable angina symptoms (34). Both the physical and the biochemical data seem to track together suggesting that both temperature and elevation in inflammatory molecules are involved in the process leading to and possibly causing the acute cardiovascular event. However, it is probably thrombus formation that is the common end pathway that is the result of this process. Thus, thrombus formation may be a common denominator that can be used to access the extent of local inflammation.

Despite some inconsistencies in the temperature measurements in detecting “vulnerable plaque”, detection of local inflammation and thrombus may be equally valuable data in the assessment of immediate outcome and potential future cardiovascular events. Thermistors have been used with sinusoidal heating to determine thermal parameters in small arteries. This work by Anderson and Valvano (35) was performed in canine kidneys, but has wide applicability for arterial thermal measurements. Studies of heat transfer in blood flow in artery and vein pairs have been studied by Roemer (36). Analytical solutions were compared to numerical calculations for heat transfer in blood vessels by Zhu and Weinbaum (37). Green's functions were used in the exact solutions in this work and axial variation was observed with this formulation for the first time. Radiative heating of biological tissues was examined by Klemick et al (38). A numerical grid

was used in this work, which would be similar to the analysis proposed presently. A solution of the Pennes equation was given by Chan (39) using the boundary element method. As a predecessor to the work by Zhu and Weinbaum (37), this solution did not allow temperature variation in the axial direction. The body of research for arterial heat transfer is mature enough to allow a solid foundation on which to compute temperature rises due to the biochemical reactions, proposed for investigation as part of the present proposal.

3. Preliminary Studies

3.1 Cholesterol Content Was Directly Correlated With Amount of Thrombosis. Using the atherosclerotic rabbit model of plaque disruption and thrombosis, we demonstrated that the amount of cholesterol content in arterial wall is directly correlated with amount of thrombus formation (r=0.98; p=0.003) (40).

3.2 CRP Increased Significantly with Thrombus Formation. With the atherosclerotic rabbit model our results showed that levels of CRP increased significantly with thrombus formation (41). Also, pravastatin preserves vasomotor response after balloon angioplasty (42) and beta-carotene preserves endothelium dependent relaxation in atherosclerotic rabbits (43).

3.2 Possible Mechanism of Systemic Inflammation Mediated Local Thrombosis. **With the same model as 3.1, results showed that rabbit serum IL-6 concentration increase and reached peak level by 24 hours after thrombus triggering. This rise in IL-6 levels was preceded by the subsequent rise of serum CRP from 24 hours after Russell viper venom (RVV) and histamine administration reaching the peak levels by 48 hours. Sustained CRP as well IL-6 levels were observed from 48 to 72 hours. Interestingly, we observed concurrent rise of IL-6 and PAI-1 up to 24 hours. Importantly, the delayed second increases of serum PAI-1 levels were observed from 60 hours after RVV and histamine triggers. Immunohistochemical staining of section from thoracic aorta of atherosclerotic rabbits demonstrated that TF presented in the sites where thrombus formed.**

3.3 *In vitro* Testing of the Thermal Response of Arteries to Injury. With a dual perfusion chamber to measure the temperature of arteries injured by balloon catheter, our results showed that temperature rose of approximately $1^{o}C$ at the injured location.

3.4 *In vivo* Vascular Injury Elicits a Local Temperature Response. At 48 hours after rabbit thrombus triggering, a 4F special thermal catheter was advanced via a femoral cut down using fluoroscopic guidance. Temperature increased in the thrombus present site but not in the thrombus absent site.

3.5 Continuous Platelet Aggregation Measurement Using Laser Light Scattering. Using laser light scattering method to continuously measure platelet aggregation and ^{111}In-labeled platelets to measure platelet adhesion, we showed that platelet activity was increased when the platelet passed through an injured artery (44, 45).

3.6 Effect of Laser on Platelet Function and Stress Protein. Platelet rich plasma (PRP) circulating in a chamber was lased by 308 nm UV excimer laser with various energies and the platelet aggregation was measured by laser light scattering. The results showed that at the lower laser energy there was no significant platelet aggregation while at higher energies there was a significant increase in platelet aggregation (2). Heat shock protein 70 is reduced in rat myocardium following transmyocardial laser revascularization (46).

3.7 Effects of Aspirin on Platelets During Laser Procedure. Using the dual organ chamber, the results demonstrate a significant reduction in platelet aggregation by aspirin when measured by laser light scattering method.

3.8 Type and Amount of Debris Formed by Laser Ablation. Rabbit thrombi were formed by fibrinogen (5 mg/ml), thrombin (0.3 unit/ml) and $CaCl_2$ (1.5 mg/ml) then lased by UV excimer laser. The results demonstrated that at higher energies and catheter size resulted in greater amount of thrombus ablation and debris generation.

3.9 Gross and SEM of Thrombus Debris Formed by Laser Ablation. Gross and SEM images demonstrated that size, shape and structure of thrombus debris formed by excimer laser were correlated to the accumulated laser energy.

3.10 Hemoglobin Release into Medium. After lasing 1 ml rabbit whole blood with 2.0 mm fiber at 35 mJ/pulse and 10 Hz for 1 min, about 25% hemoglobin was released into the buffer.

4. Research Design and Methods

Rabbit Atherosclerosis Inducing and Thrombus Triggering (1): Each year, fifty NZW rabbits will be used. Control-control group (n=10) rabbits are fed a regular diet for 6 months. Control group (n=20) and thrombus group (n=20) rabbits are undergone balloon deendothelialization and were then maintained on a 1% cholesterol enriched diet (Harlan-Sprague Dawley, Inc., Indianapolis, IN) alternating with regular diet every month for a total of 6 months. Under general anesthesia (ketamine 50 mg/kg and xylazine 20 mg/kg, i.m.) balloon-induced deendothelialization of the aorta is performed using a 4F Fogarty arterial embolectomy catheter (Baxter Healthcare Corporation, Irvine, CA) introduced through the right femoral artery cutdown. The catheter was advanced in a retrograde fashion to the ascending aorta and pulled back three times. Thrombus group rabbits will be triggered thrombus by RVV (0.15 mg/kg, i.p., Sigma Chemical Co., St. Louis, MO) and histamine (0.02 mg/kg, i.v., Sigma Chemical Co., St. Louis, MO).

Aim 1a. Our preliminary data showed that serum CRP levels are significantly higher in the atherosclerotic rabbits, which have thrombi, compared to the atherosclerotic rabbits without thrombi formation *in vivo* (41). To determine whether two of the major regulators of thrombosis (PAI-1 and TF) are involved in CRP-associated thrombosis, venous blood will be collected from the ear vein at an interval of 6 to 72 hours from the cholesterol fed atherosclerotic rabbits post administration of RVV and histamine. The serum will be immediately stored at -80°C until further use. To measure kinetics of CRP-mediated thrombosis, time-dependent changes of serum CRP, PAI-1, IL-6, IL-1, TNF-α, and estrogens will also be investigated using ELISA. Briefly for rabbit CRP ELISA, 50 µl of anti-rabbit IgG capture antibody will be added to each well of 96-well plates (Dynatech Laboratories, Chantilly, VA) and incubated overnight at 4°C. The wells will be then washed with phosphate buffered saline (PBS) containing 0.1% tween 20, and 50 µl of rabbit serum diluted in 1:1000 ratio in 10% fetal bovine serum (FBS) and 1× PBS were added to each well. The wells will be washed and 10 µg of horseradish peroxydase conjugated anti-rabbit IgG detection antibodies will be added. The wells will be then washed with PBS containing 0.1% tween 20 prior to addition of 65 µl of 5,5 -tetramethyl- benzidine (TMB) liquid substrate. Within 30 minutes following addition of TMB substrate, the reaction will be stopped with 100 µl of 1 M H_2SO_4. The absorbance at 450 nm will be measured using microplate reader (Molecular Device, Sunnyvale, CA). IL-6, IL-1 and TNF-a levels will be measured using ELISA kits (BD Bioscience, San Jose, CA). Serum PAI-1 levels will be measured using rabbit PAI-1 kit according to the manufactures instructions (Molecular Innovations, Southfield, MI). To measure changes in TF pathway of blood coagulation, factor VII coagulant activity will be measured using plasma prepared at room temperature to avoid cold activation before being frozen at -80°C. FVII coagulant activity (FVIIc) will be then determined in a two-stage chromogenic assay containing thromboplastin (CoA-Set FVII, Chromogenics AB, Mølndal, Sweden).

Aim 1b will test the hypothesis that CRP induced TF is mediated via CD40/CD40L activated pathway, and CRP mediated upregulation of PAI-1 is mediated by inhibition of tPA leading to acute thrombus formation *in vivo*. To address this specific aim, time-course studies will be conducted to identify the portion of CD40, CD40L, TF, tPA and PAI-1 secreting cells using fixed peripheral blood from atherosclerotic rabbits. Briefly, peripheral blood will be fixed with addition of 1% formaldehyde followed by dilution at 1:200 with PBS. Erythrocytes will be removed by addition of FACS lysis solution for 10 minutes at room temperature. Samples will then be incubated for 30 minutes at room temperature with various antibodies including fluorescein isothiocyanate (FITC)–conjugated anti-CRP, anti-CD40, anti-CD40L, anti-TF and anti-PAI-1. Approximately 10^4 cells will be analyzed by FACS Vantage equipped with a G3 Mac computer and CellQuest software (Becton-Dickinson, San Jose, CA). Monocytes will be identified by gating for $CD14^+$ cells. T cells will be identified by gating for $CD4^+$ cells and $CD61^+$ will be used for identifying platelets. Furthermore, the levels of arterial wall cholesterol will be correlated to the serum levels of CRP and to the tissue levels of CD40, CD40L, TF, tPA, PAI-1.

For immunohistological analysis, rabbit aortas will be rapidly removed and frozen in liquid nitrogen followed by snap-freeze in OCT compound (Tissue-Tek) after the rabbit are killed. Cryostat sections (7 µm) of the aorta will be prepared, and air-dried 30 minutes at room temperature prior to washing with 0.1 M PBS followed staining with the respective antibody: anti-CD40, anti-CD40L, anti-TF and PAI-1, and anti-CRP. As negative controls, isotype control IgG will be used. After incubation with the appropriate biotinylated, affinity-purified secondary antibodies, the sections will be incubated with alkaline phosphatase-labeled streptavidin solution and visualized using a fast red substrate kit. Quantitative analysis of atherosclerotic lesions was performed by a single observer blinded to the experiment protocol. All images will be captured by microscope equipped with camera and analyzed using Adobe Photoshop 6.0 and

National Institute of Health Image 1.62 Software. For all samples, the average value for 5 locations for each animal will be used for analysis.

Aim 1c. To test the specificity of CRP, PAI-1 and TF mediated thrombosis, we will administer neutralizing antibodies to CRP, PAI-1 and TF to reduce the thrombotic events. Administration of CD40 and CD40L antibodies will also be conducted to demonstrate the specificity of CD40/CD40L mediated TF upregulation. Selected or acceptable antibodies will be injected intraperitoneally at doses 50, 100, 250, 500, and 1000 μg prior to administration of RVV and histamine for additional 72 hours. All animals will be killed at the end of 12, 24, 48 and 72 hours post RVV and histamine injection. Aortic thrombi formation will be examined as previously described. The number and size of thrombi will be measured using planimetry of digitized images of the aorta after exposure of the intimal surface. Also, total serum creatine kinase (CK) levels will be obtained. Serum will be obtained prior to triggering and at 12, 24, 48 and 72 hours post triggering. CK activity will be analyzed using U-V vis spectrophtometer (Hewlett-Packard 8542A U-V, Palo Alto, CA). This will provide an index of myocardial infarct size. Furthermore, triphenyltetrazolium chloride staining will be used to determine the amount of remaining viable myocardium and unstained infracted areas. Surface areas of infarction proportional to viable myocardium will be determined at four levels starting at the apex to the base of the heart.

Aim 1d will test the hypothesis that platelets from rabbits with atherosclerosis will have significantly higher levels of soluble CD40/CD40L production. Using a dual organ perfusion chamber, we will evaluate platelet aggregation and activation of platelets that have a greater production of soluble CD40L in the presence and absence of anti-inflammatory agents (such as aspirin, ibrufen, statin). Measurement of soluble CD40L will be analyzed by using commercially available ELISAs (Bender MedSystems, San Bruno, CA). Platelet aggregation and adhesion will be measured as previously reported by the PI using a unique method of laser light scattering (44). The advantages of this system are that it allows for continuous real time measurement of platelet aggregation over time. Furthermore, it allows simultaneous comparison of platelet aggregation after circulation through balloon injured arteries in the presence or absence of various antiplatelet agents. Also, it provides a means to evaluate platelet adhesion to the injured arteries by using ^{111}In-labeled platelets added to the circuit. The technique relies on the scattering of a He-Ne laser beam passed through cuvettes connected to tubing that drain the balloon-injured arteries. From the angle of incidence of the scattered light, the average volume of aggregates and the number of particles can be calculated from the ratio of the scattering light at 1 to 5 degrees spread on a diode array of a multichannel analyzer.

Aim 2a. We have previously demonstrated that temperature will rise at the site of acute vascular injury using balloon catheters. This is associated with the development of thrombus. In fact, temperature rise seems to be correlated with the development of thrombosis. Under general anesthesia, rabbits will be catheterized using fluoroscopic guidance. A right femoral cut down will be used to access a 4.5F introducer and 4F balloon catheter to induce arterial wall injury. Vertebrae will be used as landmarks to identify these sites for post-mortem analysis. Blood samples will be collected prior to and following injury via the right femoral access site. Measurement of CRP will be conducted in a similar manner as described in Specific Aim 1a. Temperature measurements will be obtained using an expanding basket catheter that allows contact of thermistors with the arterial walls (Figure 1). This was demonstrated in the section on preliminary data.

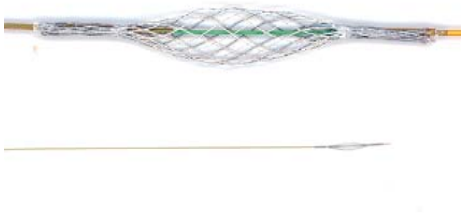

Figure 1. (Top) Basket catheter tip with expanding mesh that brings the thermistors in contact with the arterial wall. (Bottom) full catheter body (4F) that can be advanced from the femoral vein to map the temperature of the entire aorta.

Aim 2b. Immunohistochemistry methods will be performed using the aortas from rabbits subjected to temperature measurements in Specific Aim 2a and 3a. Markers used for immunohistochemistry include TF, PAI-1, CRP and CD40/CD40L. Temperature and thrombus will be correlated based on the post-mortem analysis and localization. Arterial wall cholesterol will be measured and correlated to the immunohistochemical markers and temperature.

Aim 2c. Antibodies to inflammatory molecules will be used in this setting to determine if temperature response can be normalized.

Aim 3a will determine heat released during thrombosis. Experiments have been performed in the past, attempting to measure this energy release using a water bath. However, the large mass and specific heat of the water bath imparts a damping effect on the temperature rise of the blood sample. This temperature rise should otherwise be observable in a sample isolated from its surroundings. Because of difficulty in detecting temperature change *in vivo* or in areas with large thermal sinks, it is necessary to determine the temperature changes in a thermally isolated setting. In order to accomplish this, blood samples will be placed in a series of test tubes held in an insulating polystyrene holder. The insulated holder will in turn be placed in an insulated enclosure, heated to the ambient temperature of the test tubes to minimize the temperature difference between the air and the small portion of the tubes exposed to the air. Additionally, this heated space will be used to bring all of the test tubes to a uniform temperature just prior to the start of the experiment (Figure 2).

Blood is drawn from rabbits and placed in several test tubes. These are then placed in a polystyrene block, which is drilled to facilitate a tight fit for the tubes, so as to avoid the circulation of air around the outside surface of the tubes. The tubes extend very little above the top surface of the polystyrene block, only as necessary to permit removal. The top surface of the tubes is also covered with an insulating blanket. This minimizes the potential for convective heat transfer from the air to the blood or vise versa. The primary objective is to trap any heat released by the reaction associated with clotting to the volume of the blood and the test tubes. Each tube is provided with two thermocouples for redundancy, with one located in the upper part of the tube and one in the lower part. The thermocouples in turn are read by a data acquisition system. Additionally, two thermocouples are placed in the experimental chamber to record the average chamber air temperature throughout the experiment.

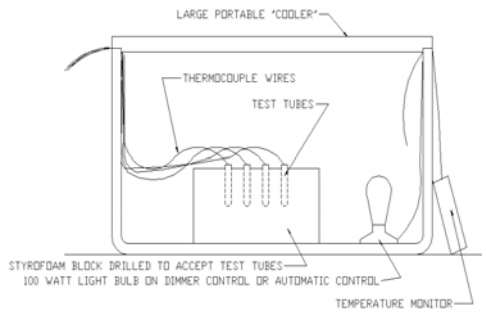

Figure 2. Clotting Calorimeter Experiment. Blood samples will be taken and placed in a series of test tubes held in an insulating polystyrene holder. Clotting will be induced by the addition of Thrombin. Temperature measurements as a function of time can be recorded by a data acquisition system throughout the experiment.

Once the blood has been added to the test tubes, temperature measurements from the thermocouples through data acquisition system can be observed and recorded. Certain time is required during this transient period to allow the samples to come to thermal equilibrium. Once changes in temperature with respect to time have subsided, the clotting can be induced by addition of thrombin and formal recording of temperature with respect to time can begin. The readings on all thermocouples in all tubes are recorded at intervals not greater than 30 seconds. Additionally, temperature of the air in the chamber is recorded at the same interval. As the chemical reactions associated with the clotting take place, the heat given off raises the temperature of the test tube and the blood with a negligible amount of heat lost to the surroundings, due to the insulating properties of the polystyrene block and the blanket cover.

Temperature measurements are taken until the temperature rise resulting from the heat released from the clotting reaction appears to stop. This is evidenced by a stabilization of the temperature, wherein the temperature appears to no longer rise as a function of time. At this apparent stabilization point, the experiment is continued and measurements are recorded until the overall time past the stabilization point is equal to the time of stabilization, as measured from the point of the introduction of the thrombin at the start of the experiment. The purpose of recording the extended post-stabilization data is for analysis of heat loss rates from the tubes in the experimental enclosure. Each year, blood from normal (n=10); atherosclerotic (n=20) and thrombus triggered rabbits (n=20) will be used and compared to determine any differences that may be altered by varying systemic conditions.

Aim 3b will involve direct numerical temperature profiles for arteries in which injuries or clotting have taken place. For computing the temperature in the artery wall, thermal conduction will be assumed, in cylindrical coordinates, with a convective surface on the interior and either a convective surface or a semi-

infinite solid boundary condition on the exterior. Due to the potential irregularities in the region on the injury, a numerical solution will be developed. The full three-dimensional transient heat conduction equation in cyclindrical coordinates, with constant properties is

$$\frac{1}{r}\frac{\partial}{\partial r}\left(r\frac{\partial T}{\partial r}\right)+\frac{1}{r^2}\frac{\partial}{\partial \theta}\left(r\frac{\partial T}{\partial \theta}\right)+\frac{\partial^2 T}{\partial z^2}+g=\frac{1}{\alpha}\frac{\partial T}{\partial t}$$

where r is the distance from the centerline of the artery, θ is the circumferential coordinate, z is the axial coordinate, t is time, and T is the temperature as a function of r, θ, z and, t. Additionally, α is the thermal diffusivity and g is the volume energy generation rate as a function of r, θ, z and, t.

Given the relatively small size of arteries, on the order of centimeters, and the accompanying long time associated with the duration of the anticipated heat generation, on the order of tens of minutes, it should be reasonable to consider the heat conduction in the artery to be steady-state. This can be verified by considering the dimensionless time for a transient of this duration, assuming a thermal diffusivity of approximately 10^{-7} m^2/s. Using these assumptions gives

$$t^* = \frac{\alpha t}{L^2} = \frac{(10^{-7})(1200)}{(.01)^2} = 1.2$$

With a dimensionless time greater than 1, the conduction transient following the injury is nearly complete. Therefore, a steady state analysis is not unreasonable. A geometric simplification can be employed as well. A two dimensional analysis could be used when variations are expected to be minimal in one of the three dimensions in the cylindrical coordinate system, depending upon the location and size of the injured area of the artery. If a long injury or clot along one side of an artery is to be examined, variation of temperature in the axial direction could be ignored and variations in the radial and circumferential directions could be calculated. An illustration for a sample grid for this type of situation is shown in Figure 3.

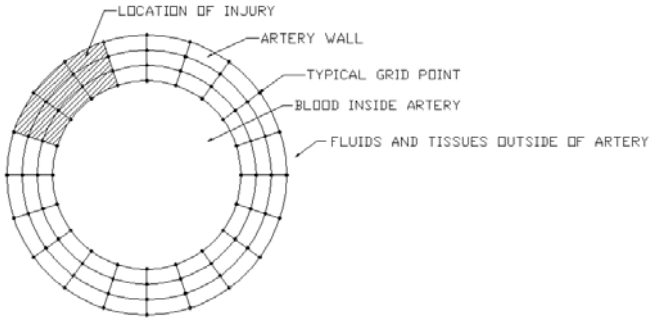

Figure 3. Two dimensional numerical grid for calculation of temperatures in the artery for a circumferentially dependent orientation of an injury site. This is a two dimensional problem which can be computed much more rapidly than a three-dimensional case, and is best suited for small local injuries.

In this case, the differential equation would reduce to

$$\frac{1}{r}\frac{\partial}{\partial r}\left(r\frac{\partial T}{\partial r}\right)+\frac{1}{r^2}\frac{\partial}{\partial \theta}\left(r\frac{\partial T}{\partial \theta}\right)+g=0$$

with boundary conditions on the inside and outside surfaces, respectively, of

$$k\left.\frac{\partial T}{\partial r}\right|_{r=r_i} = h_i\left(T(r=r_i) - T_{blood}\right)$$

$$k\left.\frac{\partial T}{\partial r}\right|_{r=r_o} = h_o\left(T_{fluids} - T(r=r_o)\right)$$

The internal energy generation term would only apply in the affected area modeling the injury. Elsewhere it would be zero. Similarly, if an injury is assumed to completely surround the artery in one location, variation in the circumferential direction could be ignored and the radial and axial dimensions alone could be considered. This situation is depicted in Figure 4, where a two dimensional finite difference grid is shown in the axial and radial directions. In this case, the applicable differential equation is

$$\frac{1}{r}\frac{\partial}{\partial r}\left(r\frac{\partial T}{\partial r}\right) + \frac{\partial^2 T}{\partial z^2} + g = 0$$

with boundary conditions on the inside and outside surfaces, respectively, of

$$k\left.\frac{\partial T}{\partial r}\right|_{r=r_i} = h_i\left(T(r=r_i) - T_{blood}\right)$$

$$k\left.\frac{\partial T}{\partial r}\right|_{r=r_o} = h_o\left(T_{fluids} - T(r=r_o)\right)$$

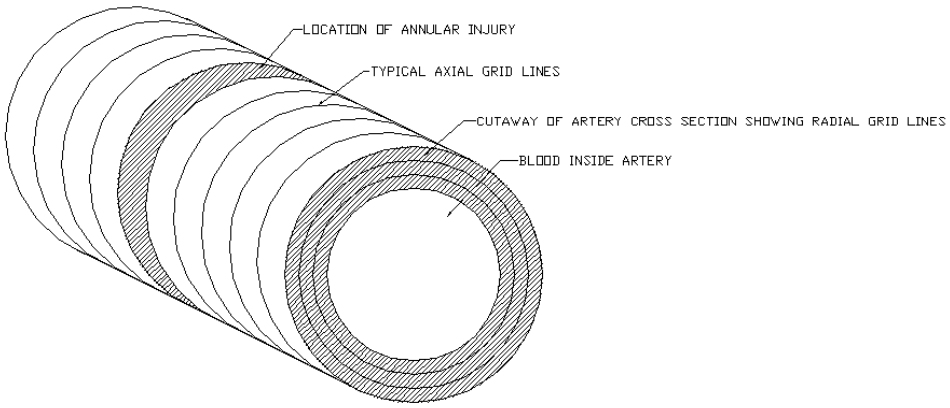

Figure 4. Two dimensional numerical grid for calcula- calculation of temperatures in the artery for an axially dependent orientation of an injury site. This is a two dimensional problem which can be computed much more rapidly than a three-dimensional case and is best suited for cases where the injury exists over the entire circumference of the artery.

The internal energy generation term would only apply in the affected area modeling the injury. Elsewhere it would be zero. Both of these differential equations could be solved for various sizes and configurations of injuries, so as to be correlated with the experimental measurements and applied using the inverse methods in Specific Aim 3c. These equations are anticipated to be solved using a custom made finite difference method, as opposed to using a commercial software package because of the repetitions to be used by the inverse methods.

Aim 3c will involve the analysis of experimentally measured data from Specific Aim 2. Temperature measurements can be taken using a thermal catheter *in vivo*, measuring the temperature response to injury or clotting. Temperature measurements taken by the thermal catheter can be fitted using inverse heat transfer analysis (47). The essence of the procedure is to compute values of temperature rise, as functions of position and time, in the artery in response to a unit volumetric energy generation rate within a certain number of finite control volumes within the grid. Assuming that one of the two dimensional steady state

grid systems mentioned in Aim 3b is to be used, the computation will depend only on position in two dimensions with no dependence on time. This can be expressed as a function which is typically designated as $\varphi_{i,j}(r,\theta)$ or $\varphi_{i,j}(r,z)$ depending on whether the problem is being considered in the z or the θ direction. In either case, the i and j subscripts designate the location of the internal energy generation, in terms of which finite control volume contains the internal energy generation. Using a numerical grid solution, the r, θ and z dimensions can be thought of as indices as well. Therefore, for each point on the grid, a temperature rise given by $\varphi_{i,j}(r,\theta)$ or $\varphi_{i,j}(r,z)$ will be calculated. There will be as many values of the unit temperature function as there are finite control volumes in the grid for each point on the grid. Of course, many of these are redundant and will not need to be calculated, but there are potentially thousands of these function values.

Using the principle of superposition, the actual temperature rise at a given point in the grid will be the sum of the contributions from each of the finite control volumes. With the unit temperature rise functions $\varphi_{i,j}(r,\theta)$ or $\varphi_{i,j}(r,z)$ calculated and tabulated, this temperature rise will be the sum of each of the individual functions multiplied by the magnitude of the internal energy generation in the corresponding finite control volume. This is

$$T(r,\theta)=\sum_{\substack{i=1\\j=1}}^{\substack{i=m\\j=n}} g_{i,j}\phi_{i,j}(r,\phi) \qquad or \qquad T(r,z)=\sum_{\substack{i=1\\j=1}}^{\substack{i=m\\j=n}} g_{i,j}\phi_{i,j}(r,z)$$

where $g_{i,j}$ is the magnitude of the internal energy generation in the finite control volume with indices i and j and m and n are the number of nodes in the r and θ or the r and z directions, respectively. Given a collection of temperature measurements with respect to position, the location and magnitude of the heating in the artery due to injury or clotting can be computed. This method then gives a quantitative measure of the location and extent of injury or disease in the artery.

Aim 4a. Rabbit thrombi *in vitro* and *in vivo* will be ablated by UV excimer laser (308 nm excimer laser, Spectranetics CVS-300^{TM}, Spectranetics, Colorado Springs, CO) with 0.7, 0.9, 1.7 and 2.0 mm diameter optical fibers. Saline is flowed through the central hole by a syringe pump. Within the laser ablation the fiber is pushed through the thrombus by a hand-control micrometer and the speed depends on the laser power. As a control, some tests are done with only fiber without laser to test the mechanical effect on thrombus. The buffer with the ablated debris is collected in a beaker. After treatment the buffer is centrifuged to separate the debris. The debris is dried and weighted. The remaining thrombus in the tube is dried at 70^{o}C over night (48, 49). Meanwhile, some tubes with thrombus are dried without treatment and weighed to calculate the ratio of wet/dry weight of thrombus. The lost thrombus weight is calculated from this ratio and the remaining thrombus dry weight. Particle size measurement is done by a modified Coulter counter and laser scattering method. The Coulter counter's output pulse signal is converted to digital signal by the A-D converter in the controller of a multi-channel analyzer and recorded as a computer data file. The pulse high (proportion to particle volume) distribution is calculated with a home-written software.

Aim 4b. CRP, PAI-1 and TF in the serum of rabbits (lased and non-lased) will be measured with ELISA and the protein contents will be correlated to the thrombus formation/ablation and platelet activity.

In the whole project, rabbits will be used as the multi-purpose. Endothelium and smooth muscle cells from hearts and arteries of the 3 rabbit groups will be primary cultured for the reference observation and histology will be made by the standard method.

Data Analysis: The temperature rise as a function of time is plotted at the conclusion of the experiment, including measurements taken beyond the stabilization time. Using the values available for the mass and specific heat of the glass test tube and the blood, the amount of heat released can be determined by the product of these two quantities and the temperature change. Using the measurements from the post-stabilization period, the rate of heat lost from the test tubes as a function of the temperature difference between the tubes and the experimental chamber can be computed, namely an effective convection coefficient. From this effective convection coefficient, the quantity of heat loss during the experiment is computed and is added to the heat release computed from the temperature rise in the test tubes in order to compute the total amount of heat released in the clotting reaction. The heat released during the clotting process on a per-gram basis will then be known, which can be used in other analyses where temperature is measured in connection with clotting and injury. This in turn, using inverse heat transfer techniques, allows

an analysis of the magnitude of clotting and injury having taken place when only temperature measurements are available.

Data comparing the three groups will be compared using a Student's t-test. Also, multivariate analysis will be made comparing the serum level of CRP, IL-6 and other inflammation markers relative to the temperature elevation achieved. Each group of rabbits will consist of 10 to 20 animals. These are powered to be able to distinguish significant differences based on the probability of less than 0.05.

Expected Findings/Potential Problems: It is expected that we will see a significant temperature rise, on the order of several degrees Celsius, as heat is released from the reactions associated with clotting. The stabilization point is expected to occur in the neighborhood of 20 to 30 minutes after the addition of the thrombin. The rate of heat loss from the samples to the surroundings of the experimental enclosure is expected to be negligible or nearly so. But, it is also possible that the temperature rise may not be measurable by the means of detection employed. Because thrombus continues to contract for many hours, temperature monitoring many need to be followed for up to 24 hours. Thus, the point of stabilization may also be somewhat different from that anticipated, which would require the experiment to be repeated with a different sampling frequency.

It is expected that a temperature rise can be calculated throughout the tissue of the artery in response to heating due to an injury in a particular location. It is also expected that it will be possible to correlate these numerical results with empirical measurements taken *in vivo* as part of Specific Aim 2. A potential problem is in attempting to estimate the size and shape of the injury used in the empirical measurements in order to make the correlation with the numerical model. Physical examination of the injury site for the artery used may be necessary in order to better estimate the size and location of the injury. Additionally, the injury may resemble neither the size nor shape. In this case, a three dimensional model may be required, which would be considerably more computationally expensive, requiring a considerably more complicated program as well. This would reduce the potential output in terms of results that could be generated for the thermal aspects of the injuries in the artery wall.

For the *in vivo* measurements, the small temperature rises anticipated, which are only expected to be one order of magnitude above the limit of detection of the thermal catheter at best, dictates that measurement errors will be large in comparison to the temperature rise. This brings about a significant challenge in the application of inverse methods. Similarly, the difficulty associated with determining the location of the catheter, both axially and circumferentially, during the *in vivo* measurement of temperature adds to the challenge imposed on the inverse thermal analysis.

Advantages of the Method: (1) Nearly all thermal energy released from the reaction is accounted for by observing temperature rise. (2) Heat lost to the surroundings can be accounted for by watching temperature decay with no accompanying heat generation. (3) Thermal energy released can be examined in isolation without the interfering influenced of an *in vivo* experiment.

Correspondence to:
Ma Hongbao
Michigan State University
East Lansing, MI 48824, USA
mahongbao2000@yahoo.com

References

1. Abela GS, Picon PD, Friedl SE, Gebara OC, Federman M, Tofler GH, Muller JE. Triggering of plaque disruption and arterial thrombosis in an atherosclerotic rabbit model. Circulation 1995;91:776-784.
2. Ma H, Huang R, Abela GS. Excimer laser irradiation alters platelet aggregation based on total energy. Lasers in Medicine and Surgery 2004;16 (Supplement):6.
3. Buffon A, Liuzzo G, Biasucci LM, Pasqualetti P, Ramazzotti V, Rebuzzi AG, Crea F, Maseri A. Preprocedural serum levels of C-reactive protein predict early complications and late restenosis after coronary angioplasty. J Am Coll Cardiol 1999;34:1512-1521.
4. Fujimori Y, Morio H, Terasawa K, Shiga T, Hatano M, Osegawa M, Uchida Y, Morita T. Multiple plaque ruptures in patients with acute myocardial Infarction: an angioscopic evidence of systemic cause of plaque instability. J Am Coll Card 2002;37:307A.

5. Rioufol G, Finet G, Ginon I, Andre-Fouet X, Rossi R, Vialle E, Desjoyaux E, Convert G, Huret JF, Tabib A. Multiple atherosclerotic plaque rupture in acute coronary syndrome: a three-vessel intravascular ultrasound study. Circulation 2002;106:804-808.
6. Chang MK, Binder CJ, Torzewski M, Witztum JL. C-reactive protein binds to both oxidized LDL and apoptotic cells through recognition of a common ligand: Phosphorylcholine of oxidized phospholipids. Proc Natl Acad Sci USA 2002;99(20):13043-13048.
7. Aronow WS, Ahn C. Prevalence of coexistence of coronary artery disease, peripheral arterial disease, and atherothrombotic brain infarction in men and women > or = 62 years of age. Am J Cardiol 1994;74(1):64-65.
8. Salonen JT, Salonen R. Ultrasonographically assessed carotid morphology and the risk of coronary heart disease. Arterioscler Thromb 1991;5:1245-1249.
9. Ridker PM, Stampfer MJ, Rifai N. Novel risk factors for systemic atherosclerosis: a comparison of C-reactive protein, fibrinogen, homocyteine, lipoprotein (a), and standard cholesterol screening as predictors of peripheral vascular disease. JAMA 2001;285:2481-2485.
10. Torzewski M, Rist C, Mortensen RF, Zwaka TP, Bienek M, Waltenberger J, Koenig W, Schmitz G, Hombach V, Torzewski J. C-reactive protein in the arterial intima: role of C-reactive protein receptor-dependent monocyte recruitment in atherogenesis. Arterioscler Thromb Vasc Biol 2000;20(9):2094-2099.
11. Cermak J, Key NS, Bach RR, Balla J, Jacob HS, Vercellotti GM. C-reactive protein induces human peripheral blood monocytes to synthesize tissue factor. Blood 1993;82(2):513-520.
12. Kohler P, Grant PJ. Plasminogen-activator inhibitor type 1 and coronary artery disease. N Engl J Med 2000;342:1792–1801.
13. Vassalli JD, Sappino AP, Belin D. The plasminogen activator/plasmin system. J Clin Invest 1991;88;1067–1072.
14. van Meijer M, Pannekoek H. Structure of plasminogen activator inhibitor 1 (PAI-1) and its function in fibrinolysis: an update. Fibrinolysis 1995;9:263–276.
15. Böhm T, Geiger M, Binder BR. Isolation and characterization of tissue-type plasminogen activator–binding proteoglycans from human umbilical vein endothelial cells. Arterioscler Thromb Vasc Biol 1996;16:665-672.
16. Aronson D, Bartha P, Zinder O, Kerner A, Shitman E, Markiewicz W, Brook GJ, Levy Y. Association between fasting glucose and C-reactive protein in middle-aged subjects. Diabet Med 2004;21(1):39-44.
17. Vague J, Alessi MC. PAI-1 and atherothrombosis. Thromb Hemost 1993;70:138–153.
18. Lijnen HR, Collen D. Mechanism of physiological fibrinolysis. Baillieres Clin Hematol 1995;8:277–290.
19. Vaughan DE, Declerck PJ, Van Houtte E, De Mol M, Collen D. Reactivated recombinant plasminogen activator inhibitor-1 (rPAI-1) effectively prevents thrombolysis *in vivo*. Thromb Haemost 1992;68(1):60-63.
20. Levi M, Biemond BJ, van Zonneveld AJ, ten Cate JW, Pannekoek H. Inhibition of plasminogen activator inhibitor-1 activity results in promotion of endogenous thrombolysis and inhibition of thrombus extension in models of experimental thrombosis. Circulation 1992;85(1):305-312.
21. Friederich PW, Levi M, Biemond BJ, Charlton P, Templeton D, van Zonneveld AJ, Bevan P, Pannekoek H, ten Cate JW. Novel low-molecular-weight inhibitor of PAI-1 (XR5118) promotes endogenous fibrinolysis and reduces postthrombolysis thrombus growth in rabbits. Circulation 1997;96(3):916-921.
22. Eren M, Painter CA, Atkinson JB, Declerck PJ, Vaughan DE. Age-dependent spontaneous coronary arterial thrombosis in transgenic mice that express a stable form of human plasminogen activator inhibitor-1. Circulation 2002;106:491–496.
23. van Kooten C, Banchereau J. CD40-CD40 ligand. J Leukoc Biol 2000;67:2–17.
24. Mach F, Schonbeck U, Sukhova GK, Bourcier T, Bonnefoy JY, Pober JS, Libby P. Functional CD40 ligand is expressed on human vascular endothelial cells, smooth muscle cells, and macrophages: implications for CD40-CD40 ligand signaling in atherosclerosis. Proc Natl Acad Sci USA 1997;94:1931–1936.
25. Henn V, Slupsky JR, Grafe M, Anagnostopoulos I, Forster R, Muller-Berghaus G, Kroczek RA. CD40 ligand on activated platelets triggers an inflammatory reaction of endothelial cells. Nature 1998;391:591–594.

26. Slupsky JR, Kalbas M, Willuweit A, Henn V, Kroczek RA, Muller-Berghaus G. Activated platelets induce tissue factor expression on human umbilical vein endothelial cells by ligation of CD40. Thromb Haemost 1998;80:1008–1014.
27. Lindmark E, Tenno T, Siegbahn A. Role of platelet P-selectin and CD40 ligand in the induction of monocytic tissue factor expression. Arterioscler Thromb Vasc Biol 2000;20(1):2322-2328.
28. Aukrust P, Muller F, Ueland T, Berget T, Aaser E, Brunsvig A, Solum NO, Forfang K, Froland SS, Gullestad L. Enhanced levels of soluble and membrane-bound CD40 ligand in patients with unstable angina. Possible reflection of T lymphocyte and platelet involvement in the pathogenesis of acute coronary syndromes. Circulation 1999;100(6):614-620.
29. Misumi K, Ogawa H, Yasue H, Soejima H, Suefuji H, Nishiyama K, Takazoe K, Kugiyama K, Tsuji I, Kumeda K, Nakamura S. Comparison of plasma tissue factor levels in unstable and stable angina pectoris. Am J Cardiol 1998;81:22–26.
30. Annex BH, Denning SM, Channon KM, Sketch MH Jr, Stack RS, Morrissey JH, Peters KG. Differential expression of tissue factor protein in directional atherectomy specimens from patients with stable and unstable coronary syndromes. Circulation 1995;91:619–622.
31. Tracy R. Atherosclerosis, thrombosis and inflammation: a question of linkage. Fibrinolysis Proteolysis. 1997;11(supplement 1):137–142.
32. Nakagomi A, Freedman SB, Geczy CL. Interferon-gamma and lipopolysaccharide potentiate monocyte tissue factor induction by C-reactive protein: relationship with age, sex, and hormone replacement treatment. Circulation 2000;101(15):1785-1791.
33. Casscells W, Hathorn B, David M, Krabach T, Vaughn WK, McAllister HA, Bearman G, Willerson JT. Thermal detection of cellular infiltrates in living atherosclerotic plaques: possible implic thermal detection of cellular infiltrates in living atherosclerotic plaques: possible implications for plaque rupture and thrombosis. Lancet 1996 25;347(9013):1422-1423.
34. Stefanadis C, Diamantopoulos L, Vlachopoulos C, Tsiamis E, Dernellis J, Toutouzas K, Stefanadi E, Toutouzas P. Thermal heterogeneity within human atherosclerotic coronary arteries detected *in vivo*: A new method of detection by application of a special thermography catheter. Circulation 1999;99(15):1965-1971.
35. Anderson, Valvanao J. Small artery heat transfer model for self-heated thermistor measurements of perfusion on the kidney cortex. Journal of Biomechanical Engineering (ASME) 1994;116(1):71-78.
36. Roemer R. Conditions for equivalency of countercurrent vessel heat transfer formulations. Journal of Biomechanical Engineering (ASME) 1999;121(5):514-520.
37. Zhu L, Weinbaum S. Model for heat transfer from embedded blood vessels in two-dimensional tissue preparations. Journal of Biomechanical Engineering (ASME) 1995;117:64-73.
38. Klemick SG, Jog MA, Ayyaswamy PS. Numerical evaluation of heat clearance properties of a radiatively heated biological tissue by adaptive grid scheme. Numerical Heat Transfer (Part A): Applications 1997;31(5):451-467.
39. Chan C. Boundary element method analysis for the bioheat transfer equation. Journal of Biomechanical Engineering (ASME) 1992;114(3):358-365.
40. Ma H, Huang R, Hage-Korban E, Maheshwari A, Qiao X, Dickinson MG, Abela GS. Arterial Wall Tissue Content of Cholesterol Directly Correlates with the Extent of Arterial Thrombosis After an Acute Vascular Event. FASEB Experimental Biology 2003;8(LB38).
41. Ma H, Claycombe K, Huang R, Abela GS. C-reactive protein rise is associated with the development of acute events in a model of plaque rupture and thrombosis. FASEB Journal 2004;18(8):C193-194.
42. Ma H, Huang R, Prieto AR, Abela GS. Pravastatin preserves vasomotor response in atherosclerotic arteries after balloon angioplasty. FASEB Experimental Biology 2002;48(LB244).
43. Hage-Korban EE, Ma H, Prieto AR, Qiao X, Akhrass F, Huang R, Abela GS. Beta-carotene preserves endothelium dependent relaxation in an atherosclerotic model of plaque disruption and thrombosis. Am Coll Phys 1999.
44. Abela GS, Huang R, Ma H, Prieto AR, Lei M, Schmaier AH, Schwartz KA, Davis JM. Laser-light scattering, a new method for continuous monitoring of platelet activation in circulating fluid. J Lab Clin Med 2003;141(1):50-57.
45. Prieto AR, Ma H, Huang R, Khan G, Schwartz KA, Hage-Korban EE, Schmaier AH, Hasan AAK, Abela GS. Thrombostatin, a bradykinin metabolite, reduces platelet activation in a model of arterial wall injury. Cardiovascular Research 2002;53(4):984-992.

46. Ma H, Huang R, Abela GS. Heat shock protein 70 expression is reduced in rat myocardium following transmyocardial laser revascularization. Journal of Investigative Medicine 2004;52:36.
47. Beck J, Blackwell B, St Clair C. Inverse Heat Conduction - Ill Posed Problems, Wiley, New York, 1985.
48. Papaioannou T, Levinsman J, Sorocoumov O, Taylor K, Pitzer Shane, Grundfest WS. Particulate debris analysis during excimer laser thrombolysis: An *in vitro* study. Lasers in Surgery: SPIE 2002;4609:404-411.
49. Papaioannou T, Sorocoumov O, Taylor K, Grundfest WS. Excimer laser assisted thrombolysis: The effect of fluence, repetition rate and catheter size. Lasers in Medicine: Proc SPIE 2002;4609:413-418.

Growth studies of *Pseudomonas fluorescens* implicated in soft rot of purple variety of Onions in Southern Nigeria

O.O. Aboaba
Dept. of Botany and Microbiology
University of Lagos,
Lagos, Nigeria
simboaboaba@yahoo.com

Abstract: This is the growth studies of *Pseudomonas fluorescens* implicated in soft rot of purple variety of Onions in Southern Nigeria. As the conclusion, the initiation and development of rot can be prevented by controlling the temperature and relative humidity of the storage environment as well as reducing general inoculation level through adequate sanitary practices during storage and handling. [Nature and Science. 2007;5(4):75-80].

Keywords: *Pseudomonas fluorescens;* onions; Southern Nigeria; storage

INTRODUCTION

Many economic plant produce are highly prone to microbial diseases especially in storage. Bacteria and fungi are well known plant pathogens and therefore pose serious problems to farmers. Bacterial pathogens include *Pseudomonas syringae* on a variety of plants (Scortichini *et al*., 2005). *Buckholderia gladioli* on Orchids and Onion slices (Keith *et al*., 2005) and *Xanthomonas campestris* pv *raphani* causing leaf spot disease of *Brassicas* (Vicente *et al*., 2006).

Earlier work had revealed the role of *Pseudomonas* species in soft rot development of Onions (Buckholder, 1950; Cother *et al*., 1976; Oguntuyo, 1981).

It is well known that establishment of a pathogen in its host must be determined by factors such as presence of nutrients, pH, water activity, presence of antimicrobials, competing microorganisms, and external factors in the storage environment. Plant tissues contain food substances that enable the support and growth of microorganisms. Onions in particular contain soluble sugars 6.600%/g, amino acids 0.019%/g, lipids 0.530%/g and 91% water (Aboaba and Ekundayo, 2000).

They found that there was appreciable loss in the sugar content during spoilage by *P. fluorescens*. Starr (1959) found that the gross nutritive requirement for the growth of practically any bacterial phytopathogen could be met by organic substances present in the suitable host.

It has been established that the atmosphere of storage at the post harvest stage contributes to onset and rate of spoilage of farm produce. The extrinsic factors needed for rapid proliferation of microbial cells are usually temperature, relative humidity and accessibility of air. Robinson *et al*. (1975) suggested that commodities resistant to evaporation such as onions may be stored at lower humidities thus reducing microbial hazards. The warm humid tropical environment poses a lot of hazards to plant produce. In Nigeria, the bulbs are grown mainly in the northern part of the country from where they are packed in jute bags and transported to various parts of the country. The period from harvest to availability in the market may take several months.

The aim of this study was to investigate the physiological requirements of this organism (*P. fluorescens*) as a means of producing information for control strategies against extensive post harvest deterioration of Onions in Nigeria.

MATERIALS AND METHODS

Collection of Samples

The Onion bulbs were obtained from different markets in Lagos area in Southern Nigeria. The lyophilized cultures of the pathogen was obtained from Microbiology Research Laboratory of the University of Lagos.

Requirement for Carbon and Nitrogen Sources

The ability of the organism to use different carbon sources for growth was determined by culturing the 24 hr old culture on minimal salt medium containing galactose, lactose, maltose, mannitol, sucrose, sorbose, fructose and glucose. All the sugars had equal weight (0.4 g) of carbon. Growth was assessed using the turbidimetric method. The best carbon source was later used at different concentration for optimal

growth requirement. The above procedure was used with Alanine, Glycine, Tyrosine, Sodium Nitrate, Ammonium Sulphate and Asparagine, each with 0.15g of nitrogen. The best nitrogen source was also used at different concentrations. The optical density values were plotted against log number of cells.

Growth in vitro

A known aliquot of the 24hr old bacterial suspension (9.2×10^7 cfu) was inoculated on a variety of commercially produced nutrient medium for bacteria and Onion extract agar (Oguntuyo, 1981). The plates were incubated at 4°C, 29 ± °C and 37°C for maximum of three (3) days. The media were also prepared in the broth form and inoculated in the same manner. The cultures were placed in a rotary shaker at 4°C, 29 ± 2°C and 37°C for 30hrs. The bacterial number was determined every 2hrs using the turbidimetric method. Duplicate Optical Density readings were obtained for each analysis using the Photoelectric Colorimeter Model AE-11.

pH Effect in Onion Broth

Onion broth was prepared according to Oguntuyo (1981), 50ml each was placed in 250ml conical flask. The content each of the duplicate flasks was adjusted to pH2 with 6 N HCl. The same procedure was done to obtain pH 4, 6 and 8 using HCl and 2N NaOH The flasks were inoculated with 24hr old culture (10^7) , incubated in a rotary shaker at 29 ± 2°C for 30 hours. The flasks containing sterile onion broth served as the control. The optical density readings were obtained every 2 hours.

T-test analysis was used to find the level of significance in the growth of the organisms in different t media, at different temperatures and pH values of growth medium.

Growth of Pathogen in Onion Bulb

Healthy onion bulbs were surface sterilized according to method of Booths, 1971. The bulbs were artificially inoculated into previously made openings (0.5cm diameter) with varying inoculum concentration of a 24hr old bacterial culture (10^3 x 10^9 cells). The bulbs were placed into sterile glass jars, incubated for seven (7) days at room temperature (29 ± 2°C). The tissue at the point of inoculation showing soft rot was removed with a sterile cork borer, weighed and homogenized with 100mls of sterile distilled water. The number of recovered cells per gramme was estimated using the dilution plate technique.

The diameter of rot tissue showing necrotic tissue at least 2mm beyond point of inoculation was measured in cm as this is considered evidence of infection for pathogenicity test. Control bulbs were inoculated with 1ml of sterile distilled water.

Environmental Conditions and Rot Development

The healthy onion bulbs were treated as above placed in sterile glass jars inoculated with 10^9 cfu and incubated at different temperature regimes of 4°C, 29 ± 2C, 37°C and 44°C for 4 weeks. The extent of rot was determined by measuring the diameter of rot tissue around the point of inoculation every 24 hours.

The relative humidity effect was determined by incubating the inoculated bulbs in R.H Chamber adjusted to different relative humidity values. The relative humidity values were obtained by placing 100mls of appropriate saturated salt solution corresponding to between 95% and 50% at 29°C (Winston and Bates, 1960). All control bulbs were inoculated with same amount of sterile distilled water.

RESULT

In Vitro Studies

The pathogen had optimal growth in the presence of 1.5% (w/v) glucose, 1.06% (w/v), glycine, and temperature of 29 ± 2°C. Nutrient agar and onion extract agar supported growth at 29 ± 2°C and 37°C with population counts of 10^7 cfu/m and 10^3 cfu/ml at 4°C. However, growth could not be achieved in onion broth at 4°C. (Figs. 1 and 2).

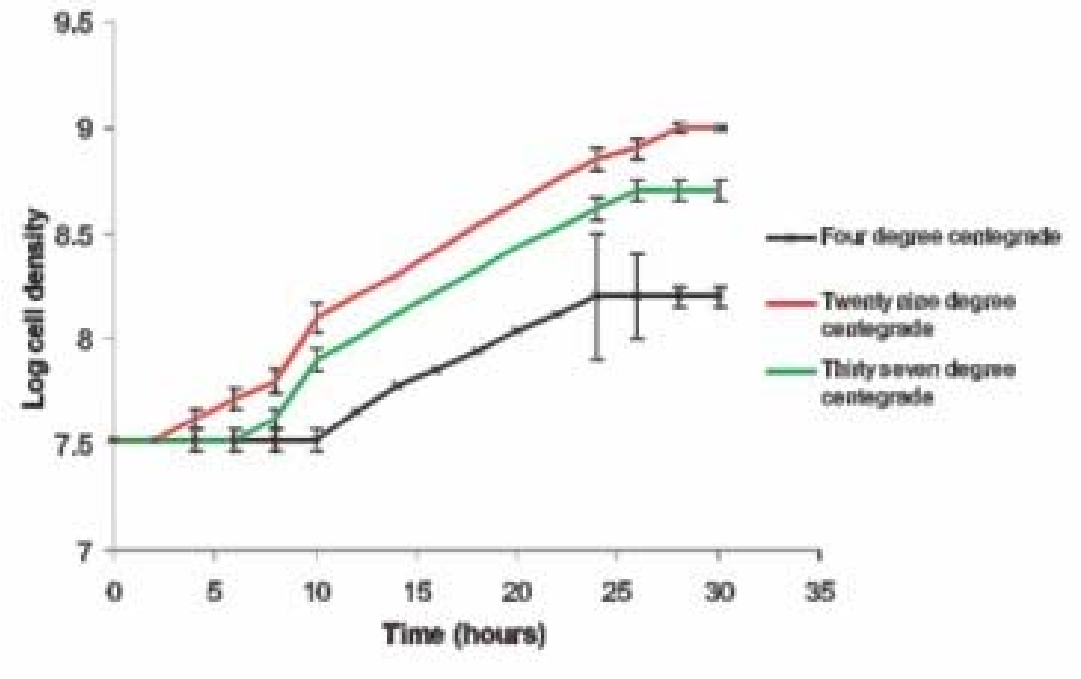

Fig. 1: Growth of *P..flourescens* in Nutrient broth at different temperature.

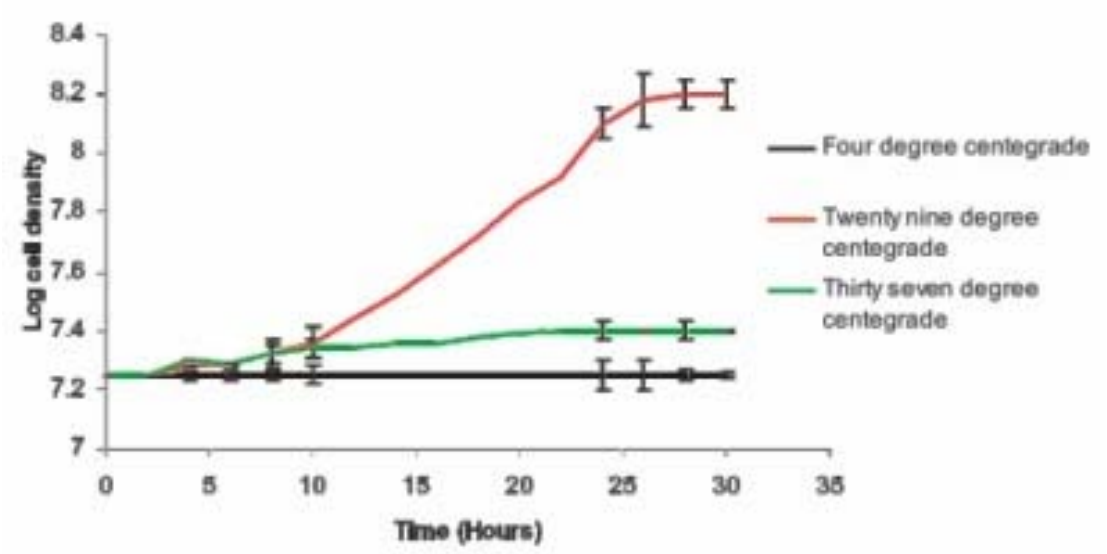

Fig. 2: Growth of *P. flourescens* on Onion broth at different temperatures.

In Vivo Studies

Soft rot development was initiated in the presence of the pathogen. The diameter of rot increased from as inoculated concentration increased and reached the peak 0.23cm on day 1 to 4.47 cm on day 7 at room temperature when inoculation concentration was 10^9 cfu/ml.

There was corresponding increase in number of viable cells recovered in the rot tissues till the 5^{th} day and then a slight decrease was observed by the 7^{th} day. (Fig. 3 and Plate 1).

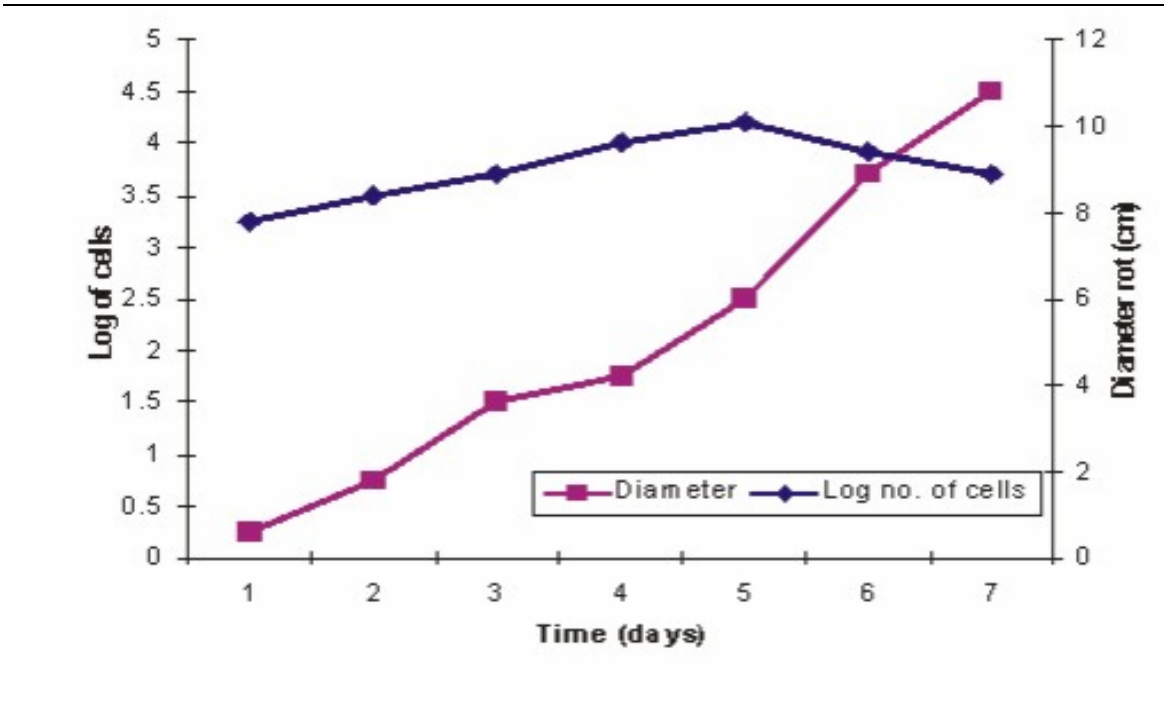

Fig. 3: Extent of rot development and growth of *P. flourescens* in the Onion bulbs

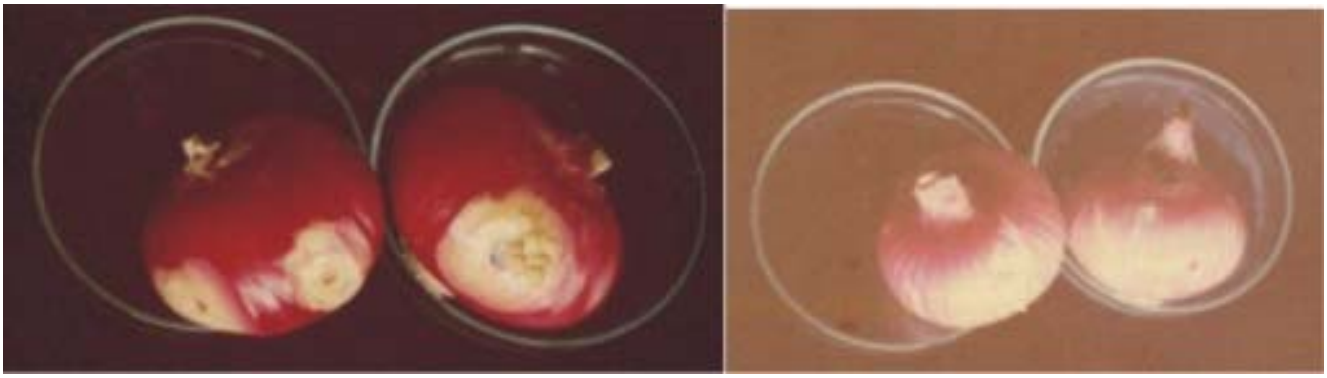

Plate 1: Artificially inoculated bulbs and control bulbs.

Environmental Effects and Rot Development

Diameter of rot tissue was optimal at 29 ± 2°C (4.36 cm) and at Relative Humidity 100% (4.53 cm) (Tables 1 and 2).

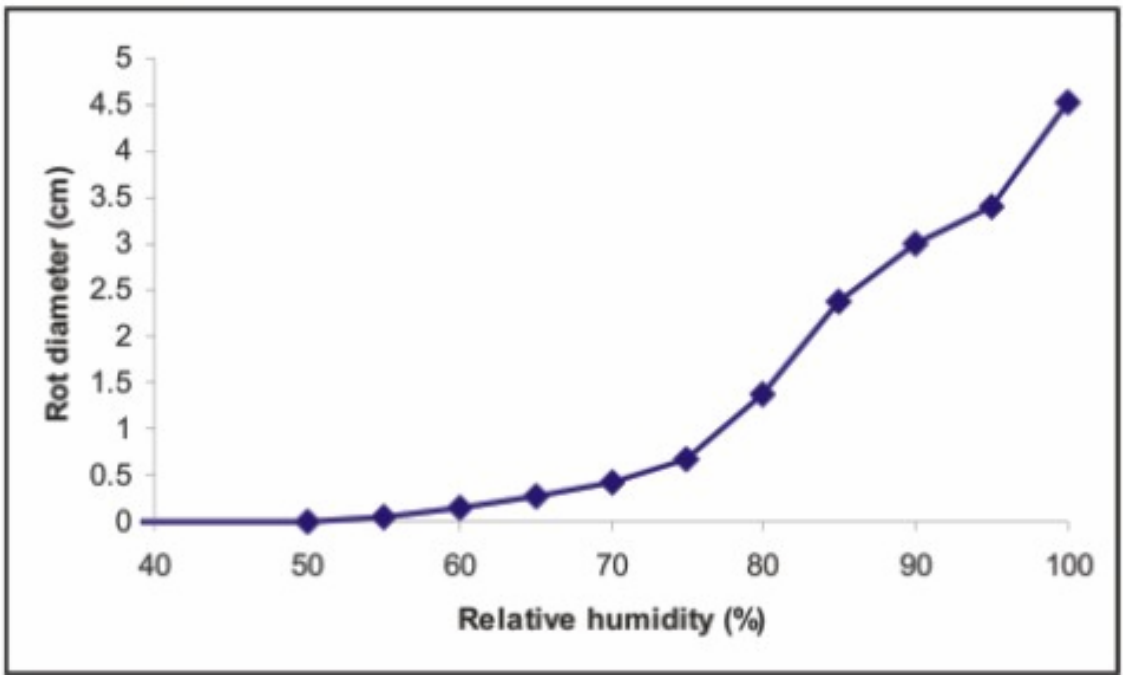

Fig. 4: Extent of rot development at different relative humidities

DISCUSSION

Pseudomonas fluorescens was implicated as a soft rot pathogen of onions as it conformed with Koch postulate (Aboaba and Ekundayo, 2000). In this study, the pathogen was able to utilize a wide variety of carbon and nitrogen sources when cultured in minimal salt medium. This is not surprising as *Pseudomonas* species are metabolically very active and excellent scavengers. Growth however was optimal with glucose and glycine. These simple forms of carbohydrate and protein were found to be present in healthy onion bulbs (Aboaba and Ekundayo, 2000). Microorganisms usually have preference for nutrients in their simple forms in any environment. It is also known that nutritive requirement for pathogens can be satisfied from the organic molecules present in the host tissue. This was confirmed by the in vivo studies.

The pathogen grew readily in all the commercial media used at room temperature. It was optimal in nutrient agar at all temperatures except 44°C and in onion extract agar at 29°C. *Pseudomonas* species generally grow on simple unenriched media such as Nutrient agar.

In vivo studies showed that the pathogen was able to initiate and proliferate in the onion tissue when healthy bulbs were artificially inoculated. The extent of rot development increased with increase in inoculum size as storage period increased at room temperature and 80 – 100% R.H. Buckholder (1948) had stated that optimal temperature requirement for most bacterial pathogen was 27°C. Cother *et al*. (1970) had also found that moist environment around onion bulbs after a heavy dew could be conducive to the maintenance and increase of bacterial population. This supports the fact that increase in rot development under these conditions was proportional to bacterial population recovered from affected tissue. The presence of readily available utilizable nutrients coupled with favourable environmental conditions favoured growth and proliferation of the pathogen. This made invasion of tissue easier manifesting in soft rot condition.

It is important therefore to store onion bulb under controlled environment. Robinson *et al.* (1975) had suggested that reduction in temperature should be complemented with the need to reduce evaporative losses. Onions however have minimal exposed surface per volume ratio as the dried scale leaves protect the fleshy succulent bulbs. It was suggested that the foliage especially in the neck region should be dried before storage as this shrivels and forms a seal which prevents ingress of pathogens (Jones, 1963).

In view of this, the bulbs should be stored at low relative humidity and temperature. It is important however that the bulbs must be used immediately after removal from the storage environment as they will

be prone from microbial attack because of the high ambient relative humidity and temperature in Southern Nigeria. Long term storage may be in form of pickles as the pathogen cannot survive acidic conditions. This however may have huge financial implications.

CONCLUSION

The initiation and development of rot can be prevented by controlling the temperature and relative humidity of the storage environment as well as reducing general inoculation level through adequate sanitary practices during storage and handling.

Correspondence to:
O.O. Aboaba
Dept. of Botany and Microbiology
University of Lagos,
Lagos, Nigeria
simboaboaba@yahoo.com

REFERENCES

1. Aboaba and Ekundayo. Microbial rotting of purple variety of Onions (*Allium cepa*. L.) in the Lagos area of Nigeria. *Journal of Sci. Res. Dev*, **5:** 2000, 159-169.
2. Cother, E.J; Derbyshire, B. and Brewer, J, *Pseudomonas aeruginosa*, cause of an internal brown rot of onion. *Phytopathology* **66**: 1976, 828-834.
3. Edens, D.G., Gitaitis, R.D., Sanders, F.H. and Nischwitz, C. First report of *Pantoea agglomerans* causing a leaf blight and bulb rot of onions in Georgia. *Plant Diseases* **90** (12): 2006, 1551.
4. Jones, H.A. and Mann, L.K. *In onions and their allies*. Leonard Hill. 1963. 143.
5. Keith, L.M.; Sewake, K.T. and Zee, F.T. Isolation and characterization of *Burkholderia gladioli* from orchids in Hawaii. *Plant Diseases* **89** (12): 2005,1273-1278.
6. Lee, Y.A and Chan, C.W. Molecular typing and presence of genetic markers among strains of banana finger-tip rot pathogen, *Buchholderia cenocepacia* in Taiwan. *Phytopathology* **97** (2): 2007, 195-201.
7. Molan, Y and Ibrahim, Y. First report of Tomato (*Lycopersicon esculentum*) pith necrosis caused by *Pseudomonas flourescens* and *P. corrugata* in the Kingdom of Saudi Arabia. Plant *diseases* **91** (1): 2007, 110.
8. Oguntuyo, O.O. Studies of microbial spoilage of onions (*Allium cepa* L). PhD thesis. University of Lagos. Lagos.1981.
9. Robinson, J.E.; Browne, K.M. and Burton, W.G. Storage characteristics of some vegetables and soft fruits. *Ann .Appl Biol*., **19**: 1975, 399-408.
10. Scortichini, M.; Rossi, M.P.; Loreti, S.; Bosco, A.; Fiori, M.; Jackson, R.W.; Stead, D.E..; Aspin, A.; Marchesi, U.; Zini, M. and Janse, J.D. *Pseudomonas syringae* pv. coryli, the causal agent of bacterial twig dieback of *Corylus avellana*. *Phytopathology* **95** (11): 2005,1316-1324.
11. Starr, M. P. Bacteria as plant pathogens. *Annual Review of Microbiology*, **13**: 1959, 211-238.
12. Vincente, J.G; Everett. B and Roberts, S.J. Identification of isolates that cause a leaf spot disease of Brassicas as *Xanthomonas carpestris* pv raphani, pathogenic and genetic comparison with related pathovars. *Phytophatology*, **96** (7):2006, 735-745.
13. Winston, P.W. and Bates, D.H. Saturated solutions for the control of humidity in biological research. *Ecology*, **41**: 1960, 232-237.

"Antibacterial and antifungal activity of leaf extracts of *Luffa operculata*, vs *Peltophorum Pterocarpum*, against *Candida albicans, Staphylococcus aureus and Escherichia coli*"

R. C. Jagessar*+, A. Mohamed®, G. Gomes+

*+Lecturer and Supervisor, Department of Chemistry, University of Guyana, Faculty of Natural Sciences, South America, raymondjagessar@yahoo.com

+Microbiologist, Department of Biology, John's Campus, University of Guyana, Faculty of Natural Sciences, South America

®Final Year Research student, Department of Biology

ABSTRACT: The antibacterial and antifungal activities of *Luffa operculata*, and *Peltophorum.pterocarpum* were investigated against *S. aureus* (gram+ve), *E. coli* (gram-ve) and *C. albicans* using the Stokes disc diffusion, the pour plate, well diffusion and streak plate method. These extracts were obtained by three extractions each with hexane, dichloromethane, ethyl acetate and ethanol. Solvents were removed in *vacuo* to yield viscous oils and paste which were made up to a concentration of 0.03g in 10 mL of the respective solvents. These were tested in varying volumes of 100-600 uL/plate (i.e. concentrations of 0.03-0.18 mg/10 mL agar). The solvents were used as control whereas ampicillin and nystatin were used as references for bacteria and fungal species respectively. The solvents had no effect on the microorganisms whereas ampicillin and nystatin inhibited microbial growth. All three plants showed antimicrobial inhibitory activity at 0.18 mg/10mL plate of medium. Activity was also most prominent with the ethanol extracts and least or negligible with the hexane. This study suggests that the ethanol and ethyl acetate extracts of *Luffa operculata* and *Peltophorum.pterocarpum* can be used as herbal medicines in the control of *E. coli* and *S. aureus* induced medical diseases, following clinical trials. [Nature and Science. 2007;5(4):81-93].

Keywords: Antimicrobial, *S.aureus*, *E.Coli*, *C.albicans*, Stokes Disc diffusion, Pour plate, Well diffusion, Streak plate, herbal medicines.

Introduction

This paper investigates the microbiological properties of leaves of two plants from the coastal plane of the Guyana flora, in an attempt to evaluate their future use as possible herbal medicines. Plants studied are *Luffa operculata*, and *Peltophorum.pterocarpum*. Their antimicrobial properties were investigated against S.aureus (gram+ve), E.coli (gram-ve) and C.albicans using the Stokes disc diffusion sensitivity technique, Pour plate, Well diffusion and Streak plate.

Guyana has a rich diverse flora whose crude extracts, both organic and aqueous can be investigated for antimicrobial activity. Also, the specified plants parts of the same species be screened for natural products whose antimicrobial activity can also be correlated. Following this, clinical trials can lead to the formulation of an herbal plant cream. Plants extracts have been used for their antimicrobial properties[1-14]. In Guyana, there are many folk remedies but most are without scientific research. Thus, there exist an urgent need to correlate folklore herbal practices with scientific evidence. With an increasing emphasis on scientific research, Guyana stands well in this area. Besides used as an herbal cream, following clinical trials, plant extracts can be subjected to chromatographic separation, leading to the isolation and purification of new and un known and known bioactive natural products/phytochemicals whose medicinal activity can also be investigated [2,4,14].

Research in herbal medicine and isolated drug discovery need to be continued, considering the threat of new emerging disease such as SARS, bird flu, not to mention AIDS. Plants are a good source of herbal medicine and natural products/ phytochemicals[1-14]. Guyana stands well for the establishment of a phytopharm, a farm set aside for the sole purpose of cultivating plants rich in natural products/phytochemicals[14]. Phytopharm has been established in the UK since 1990 and is the first botanical development company. The company is developing treatments for Alzhemeimer's disease, appetite suppression and inflammation. One advantage of botanicals is that a company can start immediately to evaluate plant extracts for clinical efficacy in diseases if there is a history of its use. USA based Phytoceutica uses assay, informatics and clinical trials to discover and develop botanicals drugs[14]. Guyana stands

well for the establishment of phytopharms. This would require though scientific evidences to confirm folklore practices. One such evidence is an investigation of antimicrobial activity of selected plants using contemporary antimicrobial tests. Thus, the antimicrobial activity of *Luffa operculata*, and *Peltophorum.pterocarpum* are presented here.

The luffas species are tropical and subtropical annual vines comprising the genus Luffa[15]. Luffa belongs to the family called Cucurbitaceae. *L. acutangula* (Angled luffa, Ridged Luffa), L. *aegyptiaca* (Smooth luffa, Egyptian luffa), *L. operculata* (Sponge cucumber), are some species. It is commonly called "nenwa". The fruit of at least two species, *L. acutangula* and L. *aegyptiaca*, is grown to be harvested before maturity and eaten as a vegetable, sometimes called jhingey or nenwa.. The fruit of L. aegyptiaca may also be allowed to mature and used as a bath or kitchen sponge after being processed to remove everything but the network of xylems. In this research, *luffa operculata* was studied.

Peltophorum pterocarpum is a deciduous tree growing up to 15–25 m (rarely up to 50 m) tall, with a trunk diameter of up to 1 m[16]. The leaves are bipinnate, 30-60 cm long, with 16-20 pinnae, each pinna with 20-40 oval leaflets 8-25 mm long and 4-10 mm broad. The flowers are yellow, 2.5-4 cm diameter, produced in large compound racemes up to 20 cm long. The fruit is a pod 5-10 cm long and 2.5 cm broad, red at first, ripening black, and containing one to four seeds. Trees begin to flower after about four years. The bark of plant is used for dysentery, tooth powder, eye lotion, embrocation for pains and sores. The bark also gives a dye of a yellow colour.

Fig. 1.0 *Peltophorum pterocarpum*

The above two plants extracts were tested against *E.Coli*, *S.aureus* and *C.albicans*. *Escherica*. *coli* can cause several intestinal and extra intestinal infections such as urinary tract infections, meningitis, peritonitis, mastitis, septicemia and gram-negative pneumonia[17]. Staphylococcus aureus can cause furuncles (boils), carbuncles (a collection of furuncles)[18]. In infants, *Staphylococcus aureus* can cause a severe disease Staphylococcal scalded skin syndrome (SSSS). *Staphylococcal endocarditis* (infection of the heart valves) and pneumonia may be fatal. *Candida Albicans* is a diploid fungus (a form of yeast) and is a casual agent of opportunistic oral and genital infections in humans[19-20].

Procedure:

2.1: **Collection of Plant materials**: The leaves of the above two mentioned plants were collected off the coastal plain of Guyana. The detached plant leaves were subjected to aerial drying for two weeks and crushed into very small pieces and placed in separate conical flasks. This increased the surface area for extraction.

Extraction: The leaves were first extracted in hexane thrice over a period of five days[4-11].Water was removed from the accumulated extract by stirring over anhydrous Na_2SO_4 and extract filtered.Solvents were removed in vacuo using rotary evaporation.The extracts were placed in vials and then in a dessicator. Extracts were stored in capped vials and were weighed. The above procedure was repeated with the same leaves but with different solvents of differing polarity such as dichloromethane, ethyl acetate, and then ethanol.

2.3. Antimicrobial activity tests

2.3.1. **Making up extract solution**

0.03 g of each dry crude extract was weighed and placed in a 10mL volumetric flask. The respective solvent was then added to make up the 10 mL solution.

2.3.2. Microorganisms:

Micro organisms were obtained from the Georgetown Public Hospital (GPH) microbiology laboratory. These were *Staphylococcus aureus*, *Escherichia coli* and *Candida albicans*. They were stored in a refrigerator at the Food and Drug microbiology lab.

2.3.3. **Potato dextrose agar (PDA)** [21]

The potato was peeled and 100 g was measured, finely chopped and boiled to a mash in distilled water. The dextrose was measured (12.5 g) and placed in a 1L measuring cylinder. Agar was measured (12.5 g) and added to the measuring cylinder (with the dextrose).The potato mash was stirred and strained into the cylinder. Hot distilled water was added to make up 500 mL.The contents was continuously poured and stirred until consistency was achieved. The content was then poured into a conical flask, plugged with cotton wool, over which aluminium foil was tightly wrapped. The flask was then autoclaved at 121 ^{0}C for 24 hrs.

2.3. 4. Reference and Control:

The references were antibiotic in nature. Ampicillin and Nyastatin. Ampicillin was choosen as the reference for all bacterial species used: *E.Coli* and *S.aureus*. Nyastatin was used as the reference for the fungus, *Candida.albicans*. The Control experiment consists of a plate of solidifying agar onto which was inoculated pure solvent with microorganism mixed in a 1:1 portion [21].

2.3.5. Aseptic conditions:

The aseptic chamber consists of a wooden box (1m x 1m x 0.5 m) with a door, was cleaned with 70% ethanol and irradiated with short wave UV light (from a lamp).

2.3.6. Mother plates:

These were made before by culturing *C. albicans* on PDA. A sterilized 6 mm cork borer was used to cut agar discs in the plate.

2.3. 7. Nutrient Agar:

500 ml of nutrient agar was made by placing 14g of the powdered mixture in a 1L flask, stirred, boiled and then autoclaved for 15 minutes at 121^{0}C. The plates were poured in a sterile environment and allowed to cool for 2 hours. Under aseptic conditions, the micro organisms were streaked onto separate plates and the discs were applied with a forceps.

They were labeled and placed in an incubator at 37 ^{0}C for 24 and 48 hours for bacteria and fungi respectively.

2.3.8. **Colonies Counting**: Colonies were estimated with the assistance of a colony counter. The number was estimated for 1 cm^2 and then calculated for the entire plate. The plate radius was determined.

2.3.9. Retention Factor: R_f = Distance moved by sample/Distance moved by solvent front. In general, the most polar compound has the lowest R_f value.

2.3.10. Disc diffusion: Stokes Disc diffusion sensitivity technique [21].

Using Stokes Disc diffusion sensitivity testing technique[21] , an inoculum containing bacterial or yeast cells was applied onto nutrient agar plates. On each plate, a reference antibiotic was also applied.The reference antibiotic disc contained 10mg of antibiotic/disc. The discs were made by cutting discs (5-6 mm) from a filter paper with a perforator, placing 5 of these discs in a vial and adding 0.2mL of each extract solution. These were left to dry. Discs were also made for the controls: ampicillin for the bacteria and nystatin for the fungus. Each disc was impregnated with the anticipated antimicrobial plant extract at appropriate concentration of 200 mg/ml using a microlitre syringe. This was then placed on a plate of sensitivity testing nutrient agar which was then incubated with the test organism:Bacteria/fungi. Incubation was done at 37ºC for 24 hr and 48 hr for the bacteria and Candida albicans species respectively. The antimicrobial compound diffuses from the disc into the medium. Following overnight incubation, the culture was examined for areas of no growth around the disc (zone of inhibition). The radius of the inhibition zone was measured from the edge of the disc to the edge of the zone. The end point of inhibition is where growth starts. Larger the inhibition zone diameter, greater is the antimicrobial activities. It is anticipated through the antimicrobial activity of plant extract, no area of growth will be induced around the disc. Bacteria or fungal strains sensitive to the antimicrobial are inhibited at a distance from the disc whereas resistant strains grow up to the edge of the disc. Discs applied to the plates already streaked with bacteria and the fungus.

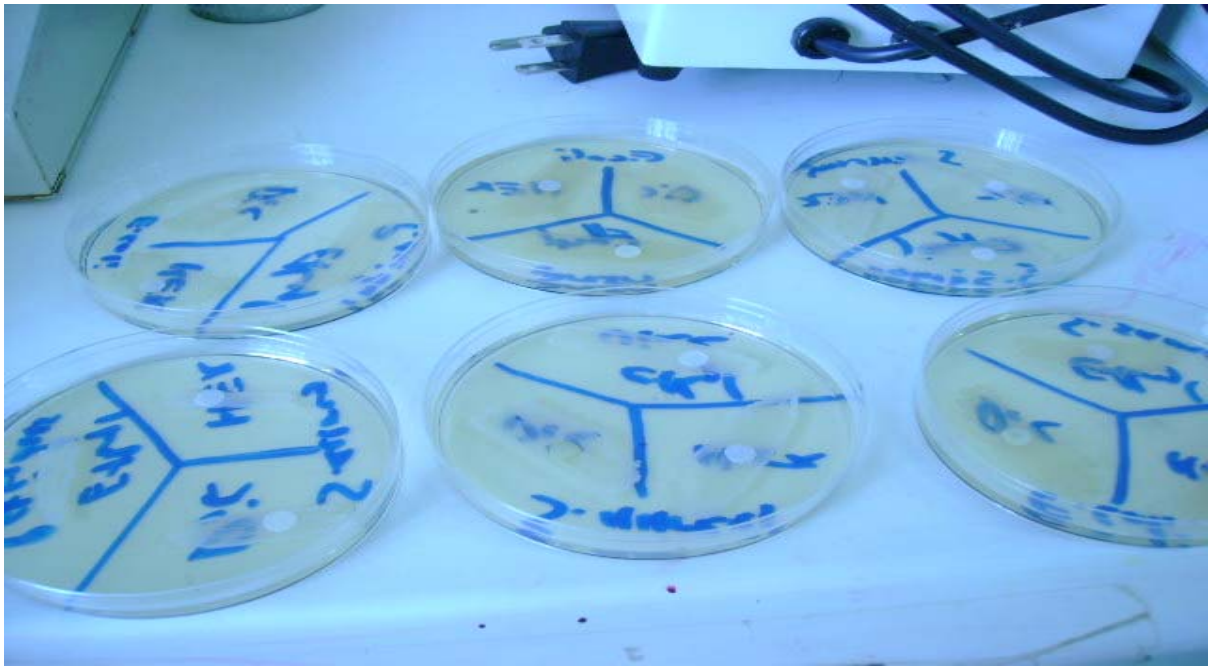

Fig. 2.0. Discs applied to the plates already streaked with bacteria and the fungus, Stokes disc diffusion method.

2.3.11. Pour Plate Method [21].

After the nutrient agar was placed in the autoclave at 120ºC for one and half hour, it was taken out and left to semi cool in a sterilized environment. 0.1mL of each solvent type extract and control were measured and placed

in separate sterile glass plates plates (100 mm diameter). 10 mL of nutrient agar was then poured into the 100 mm plate, with an even depth of 4 mm on a level surface shaken and allowed to cool. A sterile glass rod was used to uniformly stir the mixture into the nutrient agar which was left to solidify in the glass plate. The microorganisms were then streaked onto the plates and placed in an incubator at 37 ^{0}C for 24 and 48 hours for bacteria and fungi species respectively.

The inoculated plates were incubated in an inverted position (lid on bottom) to prevent collection of condensation on the agar surface. Unless the surface is dry, it will be difficult to obtain discrete surface colonies. The plates were examined for the appearance of individual colonies growing throughout the agar medium. The number of colonies were counted so as to determine how effective the plant extract were against bacterial and fungi.

2.3.12. Diffusion plate (well diffusion):

The fungus (Candida albicans) was mixed with the warm, melted, autoclaved PDA and poured into plates under aseptic conditions. The plates were covered and allowed to cool. As soon as the agar was partly solidified, the plates were inverted and left for 2 h. When cooled, a well was made at the centre of the plate. The well was made by using a 6mm cork borer that was sterilized with alcohol and flame. The extracts were applied to different wells in volumes of 100-600uL using a micro liter syringe. The four solvents (hexane, dichloromethane, ethyl acetate and ethanol) were used as control whereas nystatin was used as the reference.The plates were labelled, covered, inverted and placed in a fume hood (no incubator was available) for 48h.

2.3.13. Streak plate for bacteria:

Nutrient agar was prepared as described above and 10mL was poured into plates. The plates were treated with the extracts and reference compound ampicillin in varying volumes of 100-600 uL.The plates were allowed to cool and then the bacteria were streaked onto the surface.These plates were left for 24 hours. The plates with inhibition were used in further experiments.

2.3.14. Thin Layer Chromatography (TLC):

A baseline was drawn on the TLC plate. A spot of the plant extract was placed on the baseline with use of the pipette and allowed to dry.The plate was placed in the developing jar with the solvent. When taken out of the jar, the solvent front was drawn.They were examined under the UV/Vis lamp and the specks were circled with a pencil. The plates were then held in the iodine jar for a few seconds, shaken and taken out.The plate was further examined under UV lamp and any new specks were marked. The specks were labeled and their distances from the baseline were measured. The distance between the baseline and the solvent front was measured.The R_f values were determined.

2.3.15. **Results**:

Mass of dried leaves used for Luffa and P. pterocarpum were 4.38 g and 39.4 g respectively. The physical state of the dried extract are shown in Table 1.0.

Table 1.0 Shows physical properties of the dry extracts

Solvent	Plant	Dried extract
Hexane	*Luffa operculata* *Peltophorum.pterocarpum*	Opaque, oily. Hard, green, gummy.
Dichloromethane	*Luffa operculata* *Peltophorum.pterocarpum*	Rust brown, oily. Black, soft, gummy.
Ethyl acetate	*Luffa operculata* *Peltophorum.pterocarpum*	Rust brown, oily. Soft, black, gummy.
Ethanol	*Luffa operculata* *Peltophorum.pterocarpum*.	White flaky. Black, gummy.

These extracts were in the concentration of 0.03 g in 10 ml of solvent. This works out to 0.0003 mg/uL and 0.02 mg/uL of crude extract respectively. The ampicillin and nystatin controls were in concentration of 250 mg in 10 ml.

Disc diffusion:

Table 2.0. Antimicrobial activity of Plant extracts as shown by the inhibition zone diameter

Area of inhibition. (mm^2) using E.Coli	**Area of inhibition. (mm^2) using** S.aureus	**Area of inhibition. (mm^2) using** Candida albicans	**Plant Extracts**	**Reference compound (mm^2)**	**Control Experiment**
			Luffa operculata		No zone of inhibition
< 5	**<5**	**<5**	Hexane extract	**27**	No zone of inhibition
<5	**<5**	**<5**	Dichloromethane extract	**27**	No zone of inhibition
10	**6**	**5**	EtOAc extract	**28**	No zone of inhibition
22	**18**	**21**	Ethanol extract	**31**	No zone of inhibition
			Peltophorum.pterocarpum		
< 5	**< 5**	**< 5**	Hexane extract	**27**	No zone of inhibition
< 5	**< 5**	**< 5**	Dichloromethane extract	**29**	No zone of inhibition
22	**23**	**22**	EtOAc extract	**28**	No zone of inhibition
24	**27**	**25**	Ethanol extract	**30**	No zone of inhibition

Pour Plate:

Table 3.0 showing the number of visible colonies when viewed under a colony counter

Bacterium	**Extract**	**Volume**	**# of colonies**
E.coli	*Peltophorum.pterocarpum* with ethanol	600 uL	1
S. aureus	*Luffa operculata* with ethyl acetate	600 uL	0
E. coli	*Luffa operculata* with ethanol	600 uL	$18/cm^2$x $0.3(63.6cm^2)$= 381.
S.aureus	*Peltophorum.pterocarpum* with EtOAc	600 uL	
Controls:	solvents	600 uL	Excess growth observed.
S.aureus *E.coli*	Nutrient agar only Nutrient agar only	-------- ---------	$26/cm^2$x $63.6cm^2$=1653. $20/cm^2$x $63.6cm^2$=1272.
Ampicillin	Nutrient agar only	600 uL	0

These colonies were estimated with the assistance of a colony counter. The number was estimated for 1cm^2 and then calculated for the entire plate. The plate radius was 45mm, therefore the area was 63.6 cm^2.

Table 4.0. Results of the well diffusion for plant extracts against C.albicans

Zones of inhibition (mm^2)	**Extract**	**Volume**	**Observations**
0	*Luffa operculata* with hexane	600 uL	No zones of inhibition visible.
0	*Luffa operculata* with ethyl acetate	100-400 uL	No zones of inhibition visible.
25x30	*Luffa operculata* with ethyl acetate	500uL	Zones of inhibition visible.
30x40	*Luffa operculata* with ethyl acetate	600uL	Zones of inhibition visible.
0	*Peltophorum.pterocarpum* with hexane	100-600 uL	No zones of inhibition visible.
30x40	*Peltophorum.pterocarpum* with dichloromethane	600 uL	Zones of inhibition visible.
0	*Peltophorum.pterocarpum* with dichloromethane	100-400 uL	No zones of inhibition visible.
5x10	*Peltophorum.pterocarpum* with ethyl acetate	100 uL	Zones of inhibition visible.
20x20	*Peltophorum.pterocarpum* with ethyl acetate	200 uL	Zones of inhibition visible.
22x28	*Peltophorum.pterocarpum* with ethyl acetate	300 uL	Zones of inhibition visible.
30x40	*Peltophorum.pterocarpum* with ethyl acetate	400 uL	Zones of inhibition visible.
35x48	*Peltophorum.pterocarpum* with ethyl acetate	500 uL	Zones of inhibition visible.
40x70	*Peltophorum.pterocarpum* with ethyl acetate	600 uL	Zones of inhibition visible.
75x45	*Luffa operculata* with ethanol	600 uL	Complete zones of inhibition.
75x45	*Peltophorum.pterocarpum* with ethanol	600 uL	Complete zones of inhibition.
20x30 30x50 50x70	Nystatin	200 uL 400 uL 600 uL	Zones of inhibition
Controls	Diffusion well with four solvents		Scattered colonies
Reference	Nyastatin	600 uL	Complete zones of inhibition

Streak plate:

Table 5.0. showing the results of the streak plate method

Bacterium	Solvent Extract	Volume	Observations
S.aureus	*Luffa operculata* with ethyl acetate	600uL	Limited growth
	Peltophorum.pterocarpum with ethanol	600uL	Limited growth
E.coli	*Peltophorum.pterocarpum* with ethyl acetate	200-600uL	Limited growth
	Luffa operculata with ethanol	200-600uL	Limited growth
	Peltophorum.pterocarpum with ethanol	600uL	Limited growth
Controls	The four solvents: hexane,dichloromethane, ethyl acetate and ethanol	600uL	Growth of microorganism
Reference (Ampicillin)		200-600uL	Inhibition

Table 6.0. showing the results of the TLC for all the extracts

Solvents	**Plants**	**No of spots visible by UV**	**R_f value= d moved by sample / d moved by solvent**
Hexane/ dichloromethane, 50:50, v/v)	*Luffa operculata*	3	0.23 0.73 1.0
Hexane/ dichloromethane, 50:50, v/v)	*Peltophorum.pterocarpum*	3	0.33 0.67 0.94
Dichloromethane/hexane, 90: 10, v/v)	*Luffa operculata*	1	0.03
Dichloromethane/hexane, 90: 10, v/v)	*Peltophorum.pterocarpum*	5	0.08 0.17 0.22 0.40 0.97
Ethylacetate/dichloromethane, 90: 10, v/v)	*Luffa operculata*	1	0.5
Ethylacetate/dichloromethane, 90: 10, v/v)	*Peltophorum.pterocarpum*	3	0.18 0.53 0.92
Ethanol/hexane, 90: 10, v/v)	*Luffa operculata*	1	0.07
Ethanol/hexane, 90: 10, v/v)	*Peltophorum.pterocarpum*	6	0.09 0.17 0.38 0.57 0.64 0.95

Graphs: Bar graphs are shown in Fig. 3.0 (a) and (b) whereas the corresponding line graphs for (b) and (c) are shown in Fig. 4.0 (a) and (b).

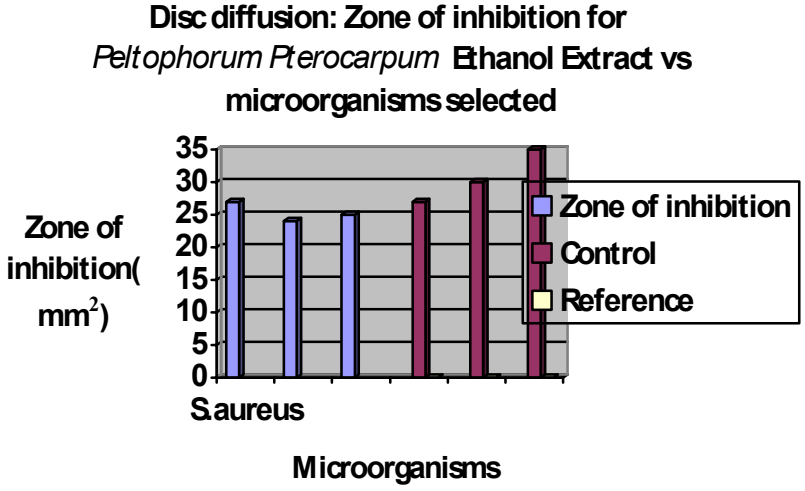

(a)

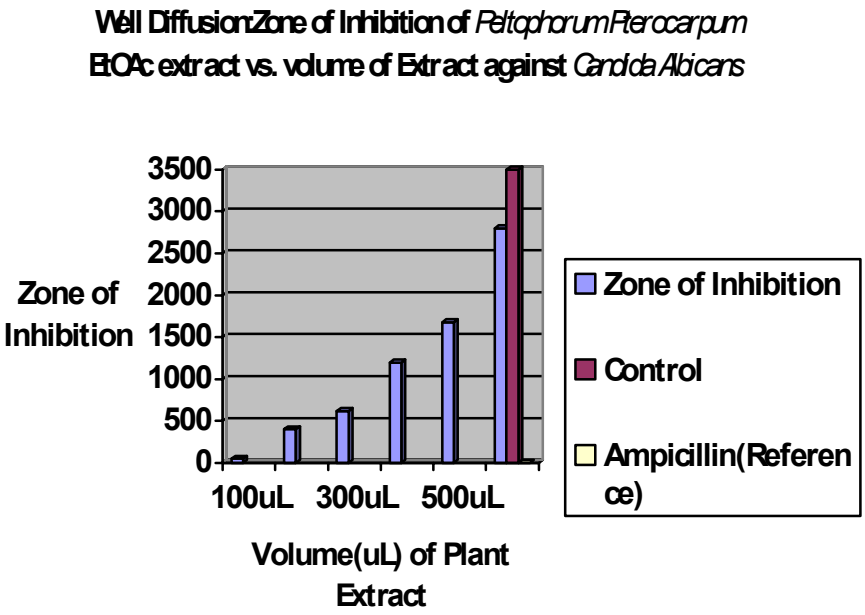

(b)

Fig. 3.0. (a) and (b)

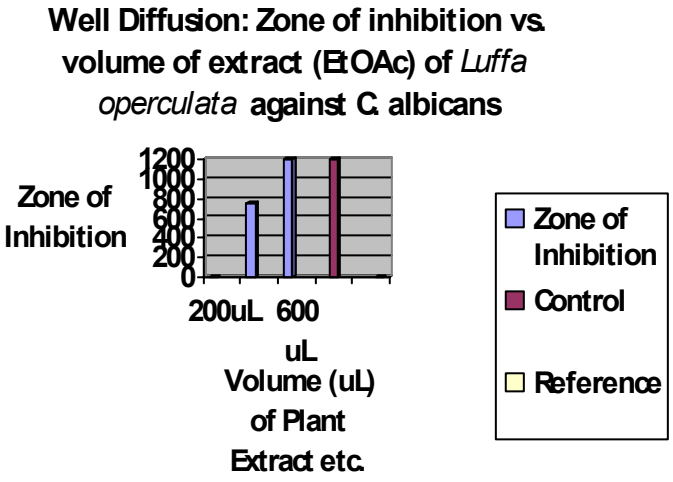

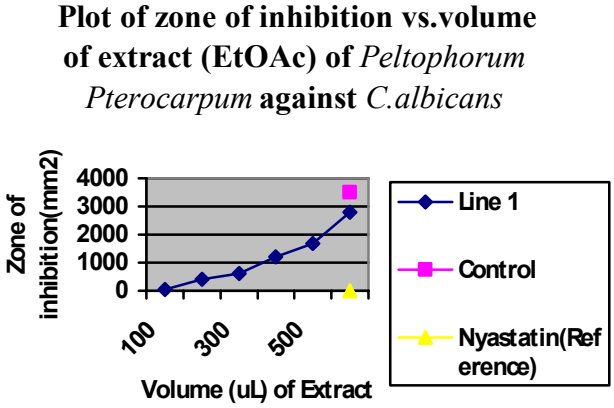

(a)

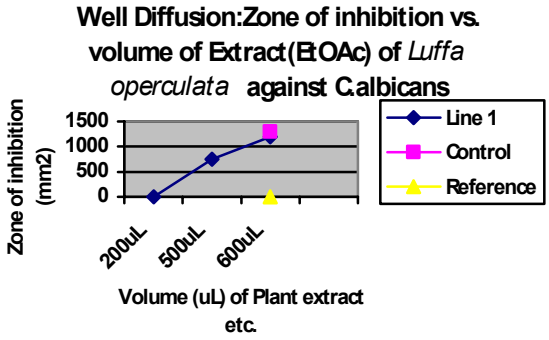

Fig. 4.0. (a) and (b).

2.3.17. Discussion:

All four methods: Stokes disc diffusion sensitivity techniques, pour plating, Well diffusion and Streak plate were successful in determining the two plants antimicrobial activities. In general antimicrobial activity follow the sequence: Ethanol extract > EtOAc extract > dichloromethane extract > hexane extract. Stokes disc diffusion indicates that the hexane and dichloromethane of *Luffa operculata* and *Peltophorum Pterocarpum* had neglible antimicrobial activity. Only a maximum zone of inhibition of 10mm^2 was observed against E.coli.However, in constrats, *Peltophorum Pterocarpum* EtOAc extract was effected against all microorganisms. For example, a maximum zone of inhibition of 23 mm^2 was noted against S.aureus. In all cases, all two plants ethanol extracts were effected against all three microorganisms studied. Significant zone of inhibition were observed. This range from 18 mm^2 to 27 mm^2. The former was obtained for Luffa operculata against *S.aureus* whereas the latter was obtained for *Peltophorum*. *Petrocarpum* against *S.aureus*.

The Well diffusion method was also used against *C. albicans*. The Well diffusion indicate that the ethyl acetate extract of *Luffa operculata* at volume of 100-400 uL respectively induce no zones of inhibition i.e microbial. Instead scattered colonies were observed.Also, both Luffa operculata and P. pterocarpum dichlormethane extract showed zero zone of inhibition at 100 uL. However, P. pterocarpum dichloromethane extract at 600uL showed zero zone of inhibition. However, Luffa operculata EtOAc extract at a volume of 500uL and 600 uL induce zone of inhibition of 750 mm^2 and 1200 mm^2 respectively. *Peltophorum*. *pterocarpum* ethylacetate extract at a volume of 500 and 600 uL induced zone of inhibition of respectively. Furthermore, as the volume of extract increased from 100uL to 600uL, zones of inhibition increased from 50 mm^2 to 280 mm^2 respectively. The ethanol extract of Luffa operculata and P.Pterocarpum showed complete zones of inhibition.Interestingly, the zone of inhibition was observed to be of the same magnitude: 75 x 45 mm^2. P.pterocarpum hexane extracts at 100-600 ul showed zero zone of inhibition. However, *Peltophorum*. *pterocarpum* dichloromethane extract against C. albicans showed zone of inhibition of 1200 mm^2 at 600 uL. The reference antibiotic: Nystatin showed zone of inhibition of 600 mm^2 to 3500 mm^2 as the volume of the extract increase from 200uL to 600 uL respectively. For the control experiment, the well with the four solvents induced scatterred colonies i.e negative inhibition

For the pour plate method, *Peltophorum*.*Pterocarpum* ethanolic extract at a volume of 600 uL was antimicrobial i.e zero colonies survived. In constrast, the ethanolic extract of Luffa operculata species at 600 uL against *E. coli* was microbial, inducing the growth of 381 colonies. Both ethyl acetate extract of *Luffa operculata* and *Peltophorum*. *Pterocarpum* at a volume of 600 uL showed 100% inhibition against *S. aureus*. Control experiments for pour plate indicate that the solvents induce growth of bacteria: S.aureus and E. coli, Table 2.0. However, the reference compound ampicillin completely inhibit the growth of microorganisms.

For the Streak plate method, both plant extracts were used against bacterial species: S.aureus and E.Coli. The EtOAc and ethanol extract of *Peltophorum*.*Pterocarpum* and *Luffa operculata* at a volume of 600 uL showed limited growth against S.aureus. and E. Coli. The control experiment indicate that all four solvents showed growth of the two bacterial species whereas the reference compound Ampicillin showed inhibition at 200-600 uL.

Fig. 3.0. (a) represents a disc diffusion plot of the zone of inhibition vs. volume (uL) of *Peltophorum*.*Pterocarpum* ethanol extract against all three microorganisms (b) represents a plot of the zone of inhibition vs. volume (uL) of *Peltophorum*.*Pterocarpum* EtOAc extract for well diffusion against *Candida albicans* whereas Fig. 4.0 (a) and (b) represent plots of the corresponding line graphs. As is evident, as the volume of plant extract increased so too is the zone of inhibition for the well diffusion method.

TLC analyses in various solvent system for each solvent type extract revealed the presence of spots that range from one to a maximum of six. Each spot is presumbably due to a pure natural product or phytochemical. Each also has a specific R_f value. The larger the R_f value, the lower the polarity of natural product/phytochemicals The number of spots and R_f value for each spot is recorded in Table 5.0. For example for the dichloromethane extract, P. pterocarpum has five spots with R_f values of 0.08, 0.17, 0.22, 0.40 and 0.97 in dichloromethane/hexane, 90: 10, v/v respectively. The largest number of spots of six was seen for the ethanol extract of P. Pterocarpum. These having R_f value of 0.09, 0.17, 0.38, 0.57, 0.64 and 0.95 respectively. The solvent system for elution been ethanol: hexane, 95:5)

Conclusions:

It is clearly seen that these two plants have antimicrobial properties.However, antimicrobial activity is solvent dependent with the ethanol extract, the most potent and hexane the least. In general the order of antimicrobial activity follow the sequence: Ethanol extract > EtOAc extract > dichlormethane extract > hexane extract. However, the other solvent extracts such as EtOAc were in some cases also very effective. Thus, the ethanol extract and in the case of *Peltophorum*.*Pterocarpum*, the EtOAc extract can be used as the active constituent of an antimicrobial cream. Future work such as isolation and purification of bioactive constituents should target the ethanol and ethylacetate extract of these plants.

Acknowledgements:

This research was carried out by a final year research student A.Mohamed under my constant supervision and also that of Dr. G. Gomes, microbiologist at John's campus, University of Guyana in the county of Berbice.We thank the University of Guyana, Faculty of Natural Sciences, Chemistry Department for the provision of laboratory space for the extraction process and equipment to carry out this research. Special thanks also extend to Food and drugs, Kingston, Georgetown for partial use of the microbiology laboratory there at the initial microbial stage of this project. Also, the Georgetown Public hospital (GPH) for the provision of microorganisms essential for research. This research was supported via a grant to Dr.R.C.Jagessar from the Research and Publication agency of the University of Guyana.

Correspondence to:
Dr. R. C. Jagessar, BSc, PhD, PDF
Lecturer and Supervisor,
Department of Chemistry,
University of Guyana, Faculty of Natural Sciences,
South America
raymondjagessar@yahoo.com

References:

1. Kandil, O; Redwan, N.M; Hassan, A.B., Amer, A.M.M., El-Banna, H.A., 1994. Extracts and fractions of Thymus capitatus exhibit antimicrobial activities. *Journal of Ethnopharmacology* 44, 19-24.
2. Barre, J.T, B.F. Bowden, J.C.Coll, J.Jesus, V.E. Fuente, G.C.Janairo, C.Y. Ragasa. 1997. "A bioactive triterpene from Lantana camara, *Phytochemistry* 45: 321-324.
3. Batista, O., A. Duarte, J.Nascimento and M.F.Simones. 1994. Structure and antimicrobial activity of diterpenes from the roots of Plectranthus her *J. Nat. Products*. 57: 858-861.
4. Rojas, A., L. Hernandez, R. Pereda-Miranda, R.Mata. 1992. "Screening for antimicrobial activity of crude drug extracts and pure natural products from Mexican medicinal plants". *Journal of. Ethnopharmacology*. 35: 275-283.
5. Silva, O., A. Duarte, J.Cabrita, M.Pimentel, A. Diniz and E. Gomes. 1996. "Antimicrobial activity of Guinea-Bissau traditional remedies". *Journal of.Ethnopharmacology*. 50: 55-59
6. "The isolation and structural elucidation of natural products from a marine organism and a plant species, a research project in collaboration with the University of the West Indies, St. Augustine campus", R.C.Jagessar*, University of Guyana library, 2004.
7. Research abstracts "Extractions and isolation of natural products from *Momordica Charantia*", R.C.Jagessar*, A.Mohamed, 15th Annual conference of the Caribbean Academy of Sciences, Guadeloupe, 2006.
8. Research abstracts "The making of perfumes from the essential oils of local flowers", R.C.Jagessar*, W.Narine, 14 th annual conference of the Caribbean Academy of Sciences, Mount Hope, Trinidad, 2004.
9. Research abstracts "Phytochemical screening of the stems, twigs, roots and bark of *Conacarpus erectus* L", R.C.Jagessar*, M. F. Cox , 14 annual conference of the Caribbean Academy of Sciences, Mount Hope, Trinidad, 2004.
10. Research abstracts "Antimicrobial activities of selected plants", R.C.Jagessar*, N.Mohamed, 1st International conference on the status of Biological Sciences in the Caribbean and Latin America Societies, Buddy's International hotel, Providence, Guyana, 2007

11. Research abstracts "Antimicrobial activities of selected tropical plants", R.C.Jagessar*, N.Mohamed, 1st International conference on the status of Biological Sciences in the Caribbean and Latin America Societies, Buddy's International hotel, Providence, Guyana, 2007.
12. Paper presentation "Antimicrobial activities of selected tropical plants", R.C.Jagessar*, N.Mohamed, 1st International conference on the status of Biological Sciences in the Caribbean and Latin America Societies, Buddy's International hotel, Providence, Guyana, 2007.
13. Research Proposal for funding from the Royal Society of Chemistry, England and the University of Guyana,"Extraction, Isolation and structural elucidation of Natural products from the Guyana flora", R.C.Jagessar*, 2006 and 2007.
14. Chemistry in Britain, December, 2003; pg 27-29.
15. http://en.wikipedia.org/wiki/Luffa
16. http://en.wikipedia.org/wiki/*Peltophorum_pterocarpum*
17. http://en.wikipedia.org/wiki/Escheria_coli.
18. http://en.wikipedia.org/wiki/*Staphylococcus_aureus*
19. http://en.wikipedia.org/wiki/*Candida_albicans*
20. http://hcd2.bupa.co.uk/fact_sheets/html/fungal_skin_infections.html
21. Murray,P.R.,Baron, E.J., Pfaller, M.A., Tenover, F.C., Yolke, R.H., 1995. Manual of Clinical Microbiology, 6th ed. Mosby Year Book, London.

Disinfection effect of chlorine dioxide on air quality control in Armed Forces General Hospital of Taiwan

Kuen Song Lin[1], Ming June Hsieh[1], Ming Jer Liou[2], Sheau Long Lee[2], Cheng-Kuo Lai[3]

[1]Department of Chemical Engineering & Materials Science/Fuel Cell Center, Yuan Ze University, Chungli City, Taoyuan, Taiwan 320, R.O.C.
[2]Department of Chemistry, ROC Military Academy, Fengshan, Taiwan 830, R.O.C.
[3]Army NBC Protection Research Center, Taoyuan, Taiwan 320, R.O.C.
leesheaulong@gmail.com

Abstract: Under the increasing threat of various global infectious diseases, the importance of epidemic prevention and air quality control in hospital is accented. Four disinfectants were prepared and tested to verify the disinfection effect of air environment in Taoyuan Armed Forces General Hospital (TAFGH). STB bleach powder (1417 ppm), Type 82 disinfectant (4877 ppm), NaOCl bleacher (1386 ppm) and chlorine dioxide disinfectant (193 ppm) were all capable to sterilize medical disposal of 3.2×10^5 CFU/mL with disinfection efficiency higher than 99.9% were observed from the environmental specimen and disinfection tests in the physician out-patient department. Before sterilization, the average residual colony was 180 per handset, which were higher than the value of 15 on door knob. After spraying 1 mL of 200 ppm chloride dioxide solution twice onto the surfaces of different objects using the hand-held sprayer, the comparison for average disinfection efficiencies of the samples was door knob (100%) = handset of telephone (100%) > chair cushion (90.3%) > floor (20.5%) in series. In addition, the background data of biological aerosols also revealed that the comparison of average space colony numbers was semi-closed out-patient area in the physician department (318 CFU/m^3) > semi-closed out-patient area in the surgical department (183 CFU/m^3) > open-space emergency ward (58 CFU/m^3) in series. After using ultrasonic aerosol and handheld sprayer ways to sprinkle the chlorine dioxide solution into hospital spaces for 30 minutes, the average colony number in the physician out-patient area decreased from 421 to 21 CFU/m^3, approaching to a disinfection efficiency of 95.0 %. The disinfection efficiency of chlorine dioxide in gas or solution phase is notably affirmative and available for the infection control of hospital. [Nature and Science. 2007;5(4):94-99].

Keywords: disinfectant; chlorine dioxide; air quality control; hospital; biological aerosol

1. Introduction

Chlorine dioxide is a disinfectant recommended by the World Health Organization (WHO) of the United Nations (UN) and the Food and Agriculture organization (FAO). It is also a disinfectant listed on the Guideline for Laboratory Biosafety of the WHO[1]. The disinfection efficacy of chlorine dioxide is not affected by the pH and its advantage of not generating carcinogen (THMs)[2], make Chlorine dioxide a green disinfectant highly praised by the european countries and the United States. As early as in 1946, Ridenour et al. reported that Chlorine dioxide is plausible to deactivate and even kill the virus that cause poliomyelituss[3]. And in 1973, Smith et al. found that Chlorine dioxide has a higher disinfection rate than Chloride against various viruses, like Echo viruses Type 7, Coxsackie virus B3 and Sendai virus [4]. In 1980, Roberts et al. reported thst after exposure of chlorine and chlorine dioxide for 2 minutes, the survival rates of Polioviruses type 1 are 63.1 % and 6.3 %, respectively[5].

As early as in 1967, the EPA of the US has cataloged the solution of Chlorine dioxide as a disinfectant or sanitizer. In 1988, the US EPA has further classified the Chlorine dioxide gas as a class 3 sterilant[6]. Besides, according to Hoehn's report, there are more than 700 waterworks worldwide that use Chlorine dioxide to replace Chloride in drinking water disinfection[7]. The number of waterworks that use Chlorine dioxide has grown to over 2000 up to date because of the advantage that Chlorine dioxide does not induce the generation of THMs. According to the reports concerning the disinfection efficency of Chlorine dioxide published by Huang et al. in 1997 and the US EPA at 1999, it has been shown that Chlorine dioxide has a higher disinfection rate than ozone and Chloride. Chlorine dioxide has a very prominent disinfection effect against Coxsackievirus, Echo viruses, Polioviruses, Herpes simplex virus (HSV), Hepatitis B virus, Newcastle disease virus, Bacteriophage, Vaccinia virus, Poliomyelitis virus and Sendai virus et al. in water[8,9].

In a series of anthrax attacks following the 911 terrorism attack, Chlorine dioxide was chosen for

disinfection because of its excellent disinfection efficiency. The US EPA, for the first time, successfully used Chlorine dioxide gas of 500ppm to disinfect Bacillus anthrax in the building where Senator Hart's office located in the Capitol Hill in the US. In the following year, the US EPA used Chlorine dioxide steam again to successfully disinfect a locker in the Brentwood mail process and delivery center at Washington DC[6]. During the SARS outbreak, the national troops of ROC also used Chlorine dioxide solution, with concentration ranging from 500 ppm to 1000 ppm fro the surveillance of the contamination control on the passage between the disinfection area and the clear area in Taipei Veterans General Hospital and Taipei City Hospital He-Ping and Yang-Ming branche. 5ppm of chlorine dioxide was also added to the water system of the personnel decontamination station.

The present report was based on the environment of Taoyuan Armed Forces General Hospital. We report this disinfection efficiency of Chlorine dioxide under different environments. The results can be of great value for reference use in hospitals.

2. Material and Methods

Instruments and chemicals in using were listed as follows:

Microbe incubation (autoclave, laminar flow, temperature-control incubator, colony counter).

Iodine titration.

Record the values from Chlorine dioxide spectrometer (ODYSSEY DR/2500) and analyze by the built-in CRP and DPD methods.

Handheld sprayer (1 liter)

EP606 ultrasonic aerosol (with frequency of 17000 times per second)

XMX/2AL Aerosol Concentrator (Dycor, Canada)

EP606 Two part system chlorine dioxide (Gosh corporation, ROC Taiwan)

2.1 Experiment procedure

1. This study was focused on the sampling and disinfection of the wastewater, out-patient area and the waiting area in Taoyuan Armed Forces General Hospital. The main disinfectant used was the EP606 two part system chlorine dioxide purchased from Gosh (ROC Taiwan). For the quality analysis of effective chlorine and Chlorine dioxide, we referred to the iodometric titration analysis and the spectrophotometry in the "Standard methods for the examination of water and wastewater" published by the American Public Health Association (APHA)[10].

ClO_2 content=(V-V0)xCx0.01349xD/(W)x100%

where V and V0 are the volume of sodium thiosulfate used to titrate the sample solution and the control solution, respectively. And W is the amount of sample in gram, while C is the equivalent concentration of sodium thiosulfate and D is the dilution fold.

2. Medical wastewater treatment: We first collect the wastewater and then used four biochemical disinfectants, namely super tropic bleaching powder (STB ; calcium hypochlorite), ROC Army disinfectant Type 82 (sodium dichloroisocyanurate), home-use bleacher (sodium hypochlorite) and EP606 disinfectant (Chlorine dioxide) to test the disinfection efficiency, followed by using mixing dilution method (NIEA E204.51).

3. The door knob, handset of telephone, chair cushion and the floor: soak sterilized cotton with dilution solution or distilled water to rub the surface of the door knob, handset of telephone, chair cushion and the floor, respectively to collect the background value of the bacteria in the environment. The samples were labeled sequentially. The same areas were disinfected by 200 ppm Chlorine dioxide and the concentration of bacteria were examined again by the same procedures describe above.

4. The space of the out-patient area: By using Aerosol concentrator, the bacteria concentration in the air were collected before and after the disinfection by using EP 606 containing 200 ppm of Chlorine dioxide.

3. Results and Discussion

3.1 Disinfection of wastewater

A series concentration of chlorine dioxide solution and NaOCl solution were added to the wastewater of hospital with a 9:1 ratio, 1 mL of samples were then incubated after a period of 10 minutes incubation time. The result was shown in Table 1. The total colony of the control was $3.2x10^5$ CFU/mL while the E. coli colony was $2.0x10^4$ CFU/mL. The disinfection rate of 10 ppm Chlorine dioxide and 30 ppm NaOCl solution were as good as 99.81 % and 99.93 %, respectively. It is similar to the results published by Huang *et al* at 1997, which demonstrate that 0.6 ppm Chlorine dioxide solution and 1.2 ppm NaOCl solution can disinfect 90 % of *Bacillus subtilis*.

The disinfection rate of Chlorine dioxide solution and NaOCl solution were still 63.41 % and 86.06 % if the concentration decreased to as low as 0.07 ppm and 0.173 ppm, respectively. According to the current medical wastewater disposal standard (coliform conc. < $2x10^5$ CFU/100 mL), the discharged wastewater can conform to the standard if even only treated by the lowest concentration of Chlorine dioxide and NaOCl in Table 1.

The disinfection ability of Chlorine dioxide to bacteria were proposed to initiated through changing the permeability of the bacteria membrane. Chlorine dioxide can then penetrate the membrane and oxidize the –SH group of glucose oxidase to an –S-S- group. Because the oxidizability of Chlorine dioxide is about 2.5 times high as that of liquid chlorine, Chlorine dioxide can efficiently inactivate the enzyme activity and cause the bacterium death. In the case of conventional treatment by liquid chlorine, the effect component of which is hypochlorate (HOCl). However, HOCl and OCl- coexist in water and the bacteriacidal efficiency of OCl- is only 1/80 of HOCl[11]. When the higher the pH is, the higher the ration of OCl- is and the weaker the disinfectability of liquid chlorine is. Hence, the disinfection efficiency of Chlorine dioxide under neutral condition is at least two to three times higher than sodium hypochlorate.

To compare the disinfection ability of various disinfectants, the disinfectant solutions were added to the un-pretreated wastewater, followed by incubation times of 2, 5 and 10 minutes. The results are shown in Table 2. It showes that various biochemical disinfectants can achieve disinfection rates of higher than 99.9 % when incubated for 10 minutes. And the efficiency of Chlorine dioxide is the best among these four disinfectants, which can achieve equivalent disinfection rate when the concentration is only 1/7 to 1/25 of other disinfectants.

3.2 Environmental disinfection test in physician out-patient area

Table 3 showes that the average bacteria number on each handset of telephone is 180, which is higher than the average bacteria number of 15 CFU/m^3 on the door knob. This is caused by the fact that telephones were placed at positions where doctors, nurses and patients can access. And further, various bacteria colonies can accumulate if the one who use telephone has bacteria on his/her hands or they didn't use a mask when use a telephone. In table 3, we also observed that the disinfection rate in order is door knob (100 %) = handset of telephone (100 %) > chair cushion (90.3 %) > floor (20.5 %). The disinfection rate is better when the surface of the subject is smooth and is not absorbent. It is not very suitable to use spray to disinfect floor which is very dirty, full of dust and very absorbent. The disinfection rate will increase if the floor was disinfected by wiping with a mop or sprinkling.

After spraying 1 mL of 200 ppm Chlorine dioxide solution twice on the surface of door knob, handset of telephone and chair cushion, the disinfection rates reaches 90 %. The point is that the surface of these objects is smooth and not absorbent plastic surface, which makes the Chlorine dioxide solution can soak the bacteria efficiently. The disinfection rate on the fllor is lower, which is only 20.5 %, might cause by the fact that surface of the floor is abrasive and absorbent. In 1967 Bernade[12] reported that main mechanism of microorganism inactivation is protein break down. And in 1986 Aieta and Berg[13] suggested the imbalance of osmosis can distroy the outer membrane of a cell, which causes final degradation of pathogens. In 2006 Ison *et al*. summarized the possible mechanisms of the disinfection effects of chlorine dioxide[14]. The bases mentioned above are only possible when an efficient contact exist. Therefore, when using chlorine dioxide spray to disinfect an object, the smoothness, toughness and absorbance are important determinant factors.

3.3 Disinfection of aerosols in the physician out-patient area

Aerosols is an important transfer media of bacteria and viruses in hospital. It is difficult to sample representative aerosols in a hospital because of the sampling process may disturbed by factors like time, space, temperature, humidity and circulation. We use random sampling first bu operating the XMX/2AL

aerosols collecting machine (1000 L/min) to gather background value to assess the bacteria content of different areas. The bacteria in the open-space emergency department is 58 CFU/m^3, 183 CFU/m^3 in the semi-closed out-patient area in the surgical department and 318 in the out-patient area in the physician department. We chose the out-patient area of the physician department as the target for Chlorine dioxide disinfection.

The spatial volume of the physician out-patient area is about 445.5 cubic meter. We released 1090 mL of Chlorine dioxide solution into the space, which corresponded to the efficient concentration of 200 ppm, to test the disinfection rate. EP 606 ultrasonic aerosol machine was used, together with handheld sprayer to spray on the walls and the air. Because the boiling point of Chlorine dioxide is 11^{o}C, which is lower than the room temperature of 24^{o}C, the Chlorine dioxide solution was nebulized immediately after which the Chlorine dioxide molecules were evaporized and were capable to destroy bacteria in the space. The maximum concentration of chlorine dioxide in the space after 30 minutes is 0.8 ppm which is lower than 0.10 ppm after 8 hours in the US OSHA bulletin. The results are summarized in Table 4.

The collection volume of the aerosols collecting machine is 15000 liters, which equals to 15 cubic meter. Therefore the background value of the physician out-patient area was 421 CFU/m^3, which was in accord with the normal distribution of the hospital aerosol which ranges between 370 CFU/m^3 and 740 CFU/m^3. The variation of the bacteria at a same smpling spot is correlated to the number of waiting patients in the out-patient area. When sampling for te first time, there were 20 patients in the waiting area, which resulted in 83 CFU/m^3. While sampling for the second time, there were around 70 patients in the waiting area, which resulted in 758 CFU/m^3. We therefore speculate that more patients in the waiting area will result in more bacteria in the aerosol and higher transmission rate. The background value drop from 421 CFU/m^3 to 21 CFU/m^3, reached a high disinfection rate of 94.9%, after treated by EP 606 Chlorine dioxide gas. The value is far lower than standard of high quality air in Singapore (500 CFU/m^3) or in Japan (300 CFU/m^3).

According to the reports published by Guo et al.[15], the possible pathogens in aerosol in hospital include Acinetobacter spp., Burkholderia, E. coli, Enterococcus, Klebsiella spp., Ps. Aeruginosa, S. aureus and Sta. epidermidis. Infection through aerosol can be very remarkable. Other potential pathogens in the aerosol can cause an even larger threat to medical staff and patients. Influenza virus, Enteroviruses and SARS virus can also be transmitted through aerosol. Thus, monitoring and disinfection of aerosol cannot be overlooked in infection control.

Table 1. Disinfection rate of chloride dioxide and bleacher solution

EP 606 Chlorine dioxide solution				NaOCl bleacher solution			
Conc. (ppm)	Total colony (CFU/mL)	Coliform (CFU/100mL)	Disinfect. rate (%)	Concentration (ppm)	Total colony (CFU/mL)	Coliform (CFU/100mL)	Disinfect. rate (%)
Control	3.2 x 10^5	2.0 x 10^4	-	Control	3.2 x 10^5	2.0 x 10^4	-
100	0	0	100	200	0	0	100
51	150	0	99.95	139	0	0	100
10	600	80	99.81	30	216	20	99.93

Table 2. Time effect on the disinfection rate of four disinfectants

Disinfectant	STB		Type 82		NaOCl bleacher		EP 606 ClO_2 disinfectant	
Conc.	1417 ppm		4877 ppm		1386 ppm		193 ppm	
microbe	Total※	Coliform※	Total	Coliform	Total	Coliform	Total	Coliform
Control	3.2 x 10^5	2.0 x 10^4	3.2 x 10^5	2.0 x 10^4	3.2 x 10^5	2.0 x 10^4	3.2 x 10^5	2.0 x 10^4
2 min.	500	0	250	0	150	0	500	0
5 min.	300	0	250	0	0	0	400	0
10 min	250	0	200	0	0	0	300	0

Disinfection rate (10 min.)	99.92 %	100 %	99.94 %	100 %	100 %	100 %	99.91 %	100 %

※ Unit for total colony is CFU/mL; Unit for coliform is CFU/100mL

Table 3. Disinfection rate of chlorine dioxide (200ppm) in the physician department

Room no. Test against		7	8	9	10	11	12	13	Average	Disinfection rate (%)
Knob (m^2)	Background (CFU)	2	50	4	50	0	2	0	15	100
	Disinfected (CFU)	0	0	0	0	0	0	0	0	
Handset (m^2)	Background (CFU)	360	264	38	300	98	150	50	180	100
	Disinfected (CFU)	0	0	0	0	0	0	0	0	

Out-patient area		Sampling spot A	Sampling spot B	Average	Disinfection rate
Cushion (m^2)	Background (CFU)	40	82	62	90.3
	Disinfected (CFU)	2	10	6	
Floor (m^2)	Background (CFU)	306	16	161	20.5
	Disinfected (CFU)	245	11	128	

Table 4. Disinfection rate of chlorine dioxide (200ppm) of the aerosol in physician department

Physician out-patient	Sampling spot A		Sampling spot B		Average	Averaged disinfection rate
Background (CFU/m^3)	50	581	117	936	421	94.9 %
Disinfected (CFU/m^3)	23	6	50	5	21	

4. Conclusion

The chlorous disinfectants investigated in this study revealed disinfection rates higher than 99.9 % for highly contaminated medical wastewater. To reach the same disinfection rate, the concentration of Chlorine dioxide is only 1/7 to 1/25 of other chlorous disinfectants. In different surfaces in the physicina department, we observed the disinfection rate of door knob of 100 %. At handset of telephone was also 100 % in comparison to chair cushion of 90.3 % and floor of 20.5 %. Disinfection by spraying has better effect on smooth and non-absorbant surface. Meanwhile, sprinkling or wiping with mop provides a better effect on surfaces which is dirty, full of dust and absorbant.

The background values of bacteria in aerosol are semi-closed out-patient area in the physician department (318 CFU/m^3) > semi-closed out-patient area in the surgical department (183 CFU/m^3) > open-space emergency department (58 CFU/m^3). The air quality of above areas all conformed to the standard bacteria number in the aerosol. After distribution of 1090 mL of 200 ppm Chlorine dioxide solution into the air by using ultrasonic aerosol and handheld sprayer for thirty minutes, the average number of bacteria drop from 421 CFU/m^3 to 21 CFU/m^3. Chlorine dioxide is very efficient to disinfect bacteria in aerosol and can be used as a refernce.

Correspondence to:
Sheau Long Lee, Ph.D.
Associate Professor, ROC Military Academy
Fengshan, 830 Taiwan, R.O.C.
886-7742-9442
leesheaulong@gmail.com

6. References

1. World Health Organization: Laboratory Biosafety Manual: Disinfection and sterilization, 2nd ed. Geneva: WHO. 2003; Chapter 14:59-66.
2. Li, J.W., Yu, Z., Cai, X., et al, "Trihalomethanes Formation In Water Treated With Chlorine dioxide." Wat. Res. 30(10), pp. 2371-2376 (1996)
3. Ridenour, G.M., Ingols, R., "Inactivation of Poliomyelitis Virus by Free Chlorine." Amer Public Health. 36:639 (1946)
4. Smith, J.E., McVey, J.L., "Virus Inactivation by Chlorine dioxide and Its Application to Storm Water Overflow." Proceeding, ACS Annual Meeting. 13(2), pp. 177 (1973)
5. Roberts, P.V., Aieta, E.M., Berg, J.D., et al, "Chlorine dioxide for Wastewater Disinfection: A Feasibility Evaluation. Stanford University Technical Report." 1980, October: 251.
6. USEPA, "Guidance Manual Alternative Disinfectants and Oxidants: 4. Chlorine dioxide.", US EPA 815-R-99-014, (April 1999).
7. Hoehn, R.C., Rosenblatt, A.A., Gates, D.J., "Considerations for Chlorine dioxide Treatment of Drinking Water." Conference proceedings, AWWA Water Quality Technology Conference, 1996,Boston, MA.US
8. Huang, J., Wang, L., Ren, N., Ma, F., Juli., "Disinfection effect of chlorine dioxide on Viruses, Algae and Animal Plankton in Water." Wat. Res., 31(3), pp. 455-460 (1997)
9. US EPA (1999, April). Guidance Manual Alteration Disinfectants and Oxidants: 4. Chlorine dioxide. US EPA(815-R-99-014) http://www.epa.gov/safewater/mdbp/mdbptg.html
10. APHA, AWWA, WEA: Standard Methods for the Examination of Water and Wastewater. 1998; Chapter 4: 73-8.
11. Huang, J., Wang, L., Ren, N., Ma, F., Juli., "Disinfection effect of chlorine dioxide bacteria in water." Wat. Res., 33(3), pp. 607-613 (1997)
12. Bernade, M.A., Snow, W.B., Olivieri, V.P., "Chlorine Dioxide Disinfection Temperature Effects" Jour. Appl. Bacteriol., 30, pp. 159-165 (1967)
13. Aieta, E.M., Berg, J.D., "Review of Chlorine Dioxide in Drinking Water Treatment" Jour. Amer. Wat. Works. Assoc. (AWWA), 78(6), pp. 62-72 (1986)
14. Ison, A., Odeh, I.N., Margerum, D.W., "Kinetics and Mechanisms of Chloride Dioxide and Chlorite Oxidations of Cysteine and Glutathione." Inorg. Chem., 45(21), pp. 8768-8775 (2006
15. Guo, C.I., Liang, C.S., Chen, Y.J., "Research of Biological Aerosol in Hospitals" Conference proceedings, US Safety and Health Conference, 2003,Taipei, Taiwan ROC

Nature and Science

Call for Papers

The international academic journal, ***"Nature and Science"*** (ISSN: 1545-0740)**,** is registered in the United States, and invites you to publish your papers.

Any valuable papers that describe natural phenomena and existence and reports that convey scientific research and pursuit are welcome, including both natural and social sciences. Papers submitted could be reviews, objective descriptions, research reports, opinions/debates, news, letters, and other types of writings that are nature and science related.

Here is a new avenue to publish your outstanding reports and ideas. Please also help spread this to your colleagues and friends and invite them to contribute papers to the journal. Let's make efforts to disseminate our research results and our opinions in the worldwide for the benefit of the whole human community.

Papers in all fields are welcome.

Please send your manuscript to editor@sciencepub.net; naturesciencej@gmail.com

For more information, please visit: http://www.sciencepub.org

Marsland Press
P.O. Box 21126
Lansing, Michigan 48909
The United States
Telephone: (517) 349-2362
Email: editor@sciencepub.net; naturesciencej@gmail.com
Website: http://www.sciencepub.org

Nature and Science

ISSN 1545-0740

The ***Nature and Science*** is an international journal with a purpose to enhance our natural and scientific knowledge dissemination in the world under the free publication principle. Any valuable papers that describe natural phenomena and existence or any reports that convey scientific research and pursuit are welcome, including both natural and social sciences. Papers submitted could be reviews, objective descriptions, research reports, opinions/debates, news, letters, and other types of writings that are nature and science related.

1. General Information

(1) Goals: As an international journal published both in print and on internet, *Nature and Science* is dedicated to the dissemination of fundamental knowledge in all areas of nature and science. The main purpose of *Nature and Science* is to enhance our knowledge spreading in the world under the free publication principle. It publishes full-length papers (original contributions), reviews, rapid communications, and any debates and opinions in all the fields of nature and science.
(2) What to Do: *Nature and Science* provides a place for discussion of scientific news, research, theory, philosophy, profession and technology - that will drive scientific progress. Research reports and regular manuscripts that contain new and significant information of general interest are welcome.
(3) Who: All people are welcome to submit manuscripts in any fields of nature and science.
(4) Distributions: Web version of the journal is freely opened to the world, without any payment or registration. The journal will be distributed to the selected libraries and institutions for free. For the subscription of other readers please contact with: editor@americanscience.org or americansciencej@gmail.com or editor@sciencepub.net.
(5) Advertisements: The price will be calculated as US$400/page, i.e. US$200/a half page, US$100/a quarter page, etc. Any size of the advertisement is welcome.

2. Manuscripts Submission

(1) Submission Methods: Electronic submission through email is encouraged and hard copies plus an IBM formatted computer diskette would also be accepted.
(2) Software: The Microsoft Word file will be preferred.
(3) Font: Normal, Times New Roman, 10 pt, single space.
(5) Manuscript: Don't use "Footnote" or "Header and Footer".
(6) Cover Page: Put detail information of authors and a short title in the cover page.
(7) Title: Use Title Case in the title and subtitles, e.g. "**Debt and Agency Costs".**
(8) Figures and Tables: Use full word of figure and table, e.g. **"Figure 1.** Annul Income of Different Groups**", Table 1. Annual Increase of Investment".**
(9) References: Cite references by "last name, year", e.g. "(Smith, 2003)". References should include all the authors' last names and initials, title, journal, year, volume, issue, and pages etc.

Reference Examples:

Journal Article: Hacker J, Hentschel U, Dobrindt U. Prokaryotic chromosomes and disease. Science 2003;301(34):790-3.
Book: Berkowitz BA, Katzung BG. Basic and clinical evaluation of new drugs. In: Katzung BG, ed. Basic and clinical pharmacology. Appleton & Lance Publisher. Norwalk, Connecticut, USA. 1995:60-9.

(10) Submission Address: editor@sciencepub.net, Marsland Company, P.O. Box 21126, Lansing, Michigan 48909, The United States.
(11) Reviewers: Authors are encouraged to suggest 2-8 competent reviewers with their name and email.

2. Manuscript Preparation

Each manuscript is suggested to include the following components but authors can do their own ways:
(1) Title page: including the complete article title; each author's full name; institution(s) with which each author is affiliated, with city, state/province, zip code, and country; and the name, complete mailing address, telephone number, facsimile number (if available), and e-mail address for all correspondence.
(2) Abstract: including Background, Materials and Methods, Results, and Discussions.
(3) Keywords.
(4) Introduction.
(**5) Materials and Methods**.
(**6) Results**.
(**7) Discussions**.
(8) Acknowledgments.
(9) References.

Journal Address:

Marsland Company
P.O. Box 21126
Lansing, Michigan 48909
The United States
Telephone:(517) 349-2362
E-mail: editor@sciencepub.net;
naturesciencej@gmail.com
Websites: http://www.sciencepub.org

ISSN 1545-0740

9 771545 074108

Marsland Press